Molecular Structure Engineering of Semiconducting Perylene Monoanhydride Diesters

by

Hao Zhang

A dissertation submitted to the Graduate Faculty in Chemistry in partial fulfillment of the requirements for the degree of Doctor of Philosophy

The City University of New York.

2013

This manuscript has been read and accepted for the Graduate Faculty in Chemistry in satisfaction of the dissertation requirement for the degree of Doctor of Philosophy.

Professor Shi Jin

Date

Chair of Examining Committee

Professor Maria C. Tamargo

Date

Executive Officer

Professor Michael Mirkin

Professor Krishnaswami Raja

Supervisory Committee

The City University of New York

Abstract

Molecular Structure Engineering of Semiconducting Perylene Monoanhydride Diesters

by

Hao Zhang

Advisor: Professor Shi Jin

The last decade has witnessed a significant progress in the field of organic electronic materials and devices. Inspired by organic electronics' promising potential and wide applications, intensive research effort has been made to discover and design organic molecules which can give good performance in organic electronic devices. In this thesis, my research effort focused on two important fields of organic electronics: polyethylene oxide (PEO)-based conducting polymers and perylene monoanhydride diester (PEA)-based discotic columnar liquid crystalline (DCLC) materials. In Chapter 1, general background of PEO-based polymer electrolytes is introduced in part I. Different strategies to improve the polymer's conductivity, including block copolymers, graft copolymers and cross-linked polymers, are summarized. In part II of Chapter 1, it is the general background of DCLC materials. Representative DCLC materials based on a broad class of π-conjugated materials such as hexabenzocoronenes (HBCs), porphyrins and perylene diimides (PDIs) are briefly reviewed. In Chapter 2, a new, efficient chemical modification method of poly (epichlorohydrin-*co*-ethylene oxide) (PECH-PEO) was proposed and executed. The PECH-PEO copolymer was successfully modified by oligo ethylene glycol (OEG)

side chains via click chemistry. The high degree of modification and minimum chain degradation were achieved. The resulted PEO-based polymer demonstrated high room temperature (RT) ionic conductivity upon forming a lithium complex, which makes it useful as a solid electrolyte in lithium batteries. In Chapter 3, a mild, one-pot synthesis strategy to prepare PEAs containing labile functional groups is presented. Currently this is the only approach towards PEAs containing labile functional groups. Furthermore, using an asymmetrically substituted PEA as the intermediate, a tetraphilic perylene monoimide diester (PEI) that contains acid-labile functionalities was synthesized in good yield for the first time. And the fluorine-containing PEI showed highly interesting structure properties. In Chapter 4, a *tert*-butyl-based PEA was designed as the intermediate towards unsymmetric perylene derivatives. Unlike previous reported PEA intermediate, the *tert*-butyl-based PEA can be easily cyclized in an appreciably milder condition. This unique property makes it an ideal candidate for the synthesis of PEIs with acid-labile functional groups. In Chapter 5, a series of PEAs with bundled-stack discotic columnar liquid crystalline (BSDCLC) phase were synthesized and characterized. Compared to conventional DCLC materials, BSDCLC materials are structurally more robust to the occurrence of defects and therefore are expected to exhibit enhanced charge carrier characteristics. More importantly, perylene-based BSDCLC phase with single stacking mode is realized for the first time. Furthermore, our experimental data show that the self-assembly of a PEA can be effectively tuned not only by changing the branching unit, but also by changing the nature of flexible chains. Compared to alkyl chains, OEG chains can induce the

BSDCLC phase of PEAs with much higher atom efficiency.

Apart from synthesis and molecular design, characterization is critical to my dissertation research. A full scope of instrumentation techniques including Fourier transform infrared spectroscopy (FTIR), nuclear magnetic resonance (NMR), differential scanning calorimetry (DSC), polarized light microscopy (PLM), gel permeation chromatography (GPC), small-angle and wide-angle X-ray diffraction (XRD) have been employed. Additionally, molecular simulation has also been applied to predict and obtain details in molecular packing.

To sum up, the achievements in this research contribute an advance in the field of developing perylene-based BSDCLC materials which can be potentially used for organic electronics; and PECH-PEO based polymer electrolytes have reasonable good dimensional stability and conductivity, which are important properties for the application in lithium battery industry.

Dedication

This thesis is dedicated to my daughter, Margaret Sandy Li, with a hope that she would one day realize that education is a magical key to open doors of success.

Acknowledgements

I would like to have the pleasure to express my deep gratitude to my advisor, Professor Shi Jin for his guidance and understanding throughout the courses of my research. I have learned a tremendous amount from him during my study at the City University of New York, both scientifically and personally.

I am greatly appreciative to my research committee members, Professor Krishnaswami Raja from College of Staten Island, Professor Michael Mirkin from Queens College for their valuable time and insight regarding my dissertation. I have been benefiting from their guidance and advisements.

Thanks to my colleagues in Professor Jin's group, Dr. Runkun Sun, Dr. Bin Wang, Dr. Guolin Lu, Dr. MinZhi Chen and Dr. Chenming Xue.

Special thanks go to Dr. Nan-Loh Yang for letting me get into this chemistry PhD program in CUNY and the financial support through these years. I have been inspired by his professional ethics and diligence.

Finally I would like to sincerely thank my wife, Li Li, and my parents Zhao Zhang and Lijuan Zhu for their endless devotion and understanding.

Table of Contents

List of Figures

List of Tables

List of Schemes

CHAPTER 1. INTRODUCTION

Part I: PEO-based ionically conducting polymer electrolytes

Polymer electrolytes, which were first discovered by Wright in 1973[1, 2], usually consist of a salt, e.g. LiI, dissolved in polymers, e.g. PEO. Specifically, PEO-based solid polymer electrolytes (SPEs) have wide application in the rechargeable lithium battery industry. The major goals of all-solid-state rechargeable lithium batteries are high energy storage capacity, safety and the ability to release the stored energy at a high rate. [3] The progress in SPEs technology has enabled the lithium battery's large-scale application on personal electronic devices such as cell phones, tablets and laptop computers. Motivated by SPEs' promising potential, intensive research effort has been made to enhance the polymer electrolytes' conductivity performance.

For an electrolyte to be valuable in industry applications, it should satisfy several requirements such as: a Li^+ ion conductivity $\sigma>10^{-4}$ S/cm over the temperature range of battery operation; chemical stability over operation temperature; materials safety, preferably nonflammable and nonexplosive if short-circuited; low toxicity and low cost. To achieve the best conducting performance, different materials have been used as the electrolyte in lithium batteries. They include inorganic solid electrolytes, ionic liquids, organic liquid electrolytes, inorganic liquid electrolytes and SPEs. SPEs, especially the PEO-based electrolytes, have attracted increasing research effort because their special advantages when used in a lithium battery. A SPE can retain the contact at the electrode/electrolyte interface during a modest change of the electrode

volume that is associated with the operation of a battery. PEO-lithium complex electrolyte is low-cost, nontoxic, and has good chemical stability. Furthermore, PEO-lithium complexes offer good lithium ion conductivity above their melting point (~ 60 °C). However, the SPEs' Li^+ ion conductivities are usually less than 10^{-5} S/cm at RT. Since most lithium batteries are expected to be used at or near RT, enhancing the conductivity at or near RT is a key part for PEO-based SPE's industry applications.

It is generally agreed that, in the PEO-lithium complex electrolyte system, the ion transport, which determines the conductivity performance of electrolyte, is dependent on the segmental motion of polymer chains. [4-7] Polymer chain segmental motion, especially the short-range motion promotes the coordination bonds' form-and-break between PEO chains and Li^+ ions. In addition, the motion provides the necessary free volume for the Li^+ ions' transportation. A PEO-based SPE usually consists three phases: PEO crystalline phase; PEO/Li^+ crystalline phase; PEO amorphous phase, which contains some solvated lithium salt. However, the polymer chain's segmental motion mainly happens in the amorphous phase, which means that the amorphous phase contributes the most (if not all) to the ionic conductivity of the polymer electrolyte.

For this reason, many research efforts have been devoted in incorporate PEO segments (or their oligomers) into polymers in an amorphous and highly mobile state. Since the glass transition temperature (T_g) of PEO is ~ -65 °C, if the crystallization of PEO (which occurs readily below its melting point ~60 °C for a high molecular weight PEO) can be hindered, the molecular mobility of PEO segments should be

sufficient high to provide a respectful lithium ion conductivity, as long as the temperature is above the T_g of PEO. The following approaches have been implemented to reduce the crystallinity of PEO and its oligomers.

1. Block copolymers

In this approach, the microphase separation between two chemically incompatible blocks is exploited to reduce the crystallinity of PEO segments and enhance the dimensional stability of the resulted polymer electrolytes. [8] Typically, such an approach involves a block copolymer that consists of a PEO block and another rigid block which is chemically incompatible with the PEO block. The self-assembly of such a block copolymer leads to the formation of a microphase separated structure. [9] While the PEO phase will be able to dissolve lithium ions and provide the needed ionic conductivity, the resulted SPE can offer enhanced shape stability, thanks to the rigid phase. Moreover, the crystallization of PEO phase in the polymer is expected to be more difficult than conventional unrestricted PEO chains, due to the combination of shorter PEO chains and the restriction imposed on the PEO chains by the rigid phase. Such a block copolymer could be of di-block, tri-block or multi-block type.

For example, PEUU, a block copolymer of 4, 4'-methylenebis-(cyclohexyl isocyanate), ethylenediamine and low molecular weight PEO has been synthesized and investigated by impedance measurement. The linear segmented polyurethanes are $(A\text{-}B)_n$ type multi-block copolymers comprised of alternating sequences of a glassy or hard (A) material and a rubbery or soft (B) material. The unfavorable interaction

between the hard and soft segments leads to the microphase-separated structure. After adding a lithium salt, the resulting SPE demonstrated good dimensional stability and a good conductivity of 10^{-4} S/cm at 80 °C. [10]

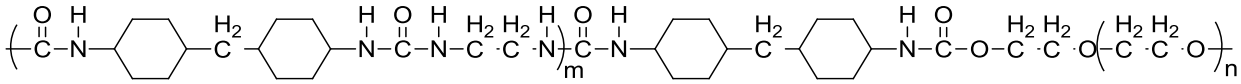

Scheme 1.1 Molecule structure of PEUU

2. Graft copolymers

When the molecular weight is relatively low, the melting point of PEO decreases substantially upon decreasing chain length. For instance, all polyethylene glycol monomethyl ethers (can be considered as oligomeric PEOs with methyl ether and OH as the two end groups of each chain) remain liquid at RT when their molecular weights are below 750 g/mol. Thus a straightforward approach toward high conductivity polymer electrolytes (especially at RT) is to incorporate OEG into a polymer as the side chains. With an appropriate OEG chain length, the side chain crystallization can be completely avoided while still offering excellent ability to form complexes with lithium ions and resulting polymer electrolyte is expected to offer high conductivity at or near RT. Furthermore, with a highly flexible polymer backbone, the segment motion of OEG chains can be enhanced and also contributes to a higher ionic conductivity. One of the highest RT conductivity values (for a dry polymer electrolyte) was reported for a double-comb siloxane polymer carrying OEG chains. [11]

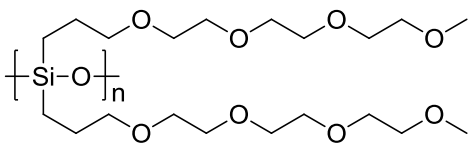

Scheme 1.2 Molecule structure of comb-like polysiloxanes with OEG chains

In this polymer electrolyte, a lithium salt is very easy to dissolve and disperse in polymer chains because the main chain (polysiloxane) and OEG side chain provide ample oxygen atoms which can effectively catch and transport lithium ions. Furthermore, the double-comb structure makes the polymer chain very hard to form an ordered, efficiently packed structure, which makes it hard to crystallize. When blended with $LiN(SO_2CF_3)_2$, the electrolyte's conductivity can reach 3.9×10^{-4} S/cm at RT with [O]/[Li] ratio 48:1. Nevertheless, the dimensional stability of this polymer is very poor, probably due to its low molecular weight.

Another successful strategy is using star-structure OEGs to lower the polymer's crystallinity. [12] This kind of highly branched polyether is intrinsically resistant to crystallization because of their inability to pack efficiently.

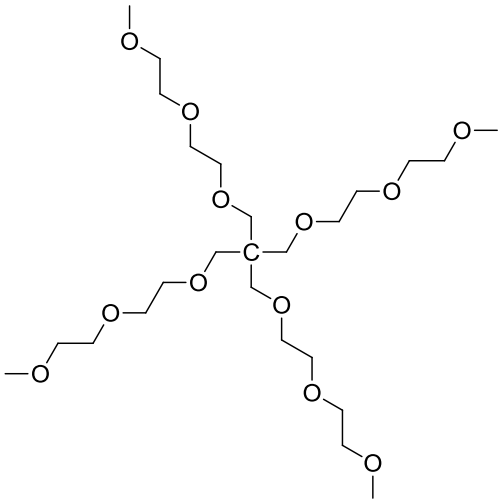

Scheme 1.3 Molecule structure of star OEG (2, 2, 2, 2)

Actually, this electrolyte is not solid because star-OEG (2, 2, 2, 2)'s low

molecular weight. However, OEG (2, 2, 2, 2) is hard to crystallize due to its unique molecular structure. The star-OEG (2, 2, 2, 2)-$LiClO_4$ complex has conductivity of 6×10^{-5} S/cm at 0 °C. Even at -40 °C, it still gives a conductivity of 3.7×10^{-7} S/cm.

3. Cross-linked polymers

Although the introduction of OEG side chains can generate polymer electrolytes with highly mobile OEG chain segments (even at RT) which usually manifests as high ionic conductivity, sometimes it negatively affects the polymer's mechanical properties which is an important factor in practical applications of SPEs. Crosslinking is a known strategy to improve mechanic properties of a polymer. Such an approach has also been applied to OEG-based polymer electrolytes. For example, the lithium complex of a siloxane-based network polymer containing OEG chains exhibited an ionic conductivity of 1×10^{-4} S/cm at 30 °C and significantly improved mechanical properties in the comparison with the linear-chain counterparts. [13]

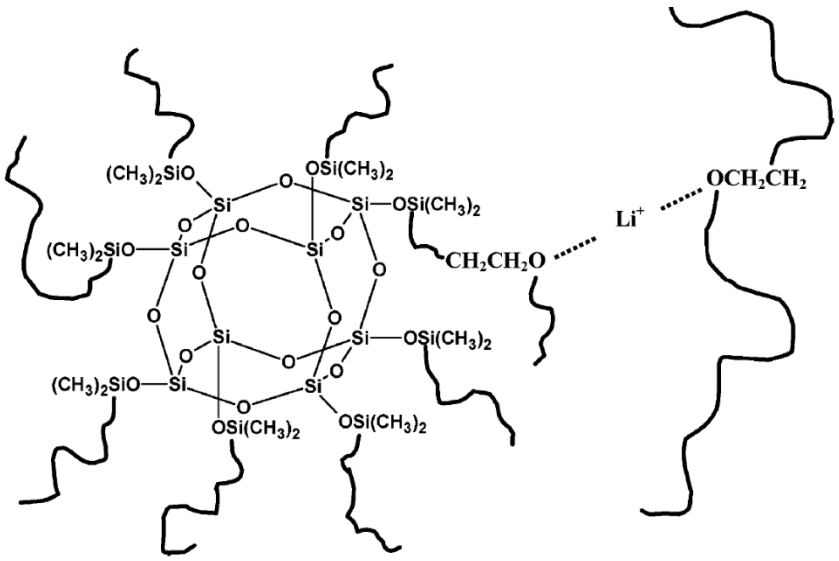

Scheme 1.4 OEG containing polymer network [13]

However, there is always a trade-off between the high conductivity and good

mechanical properties, as a highly cross-link density can improve mechanical properties and inhibit crystallization, but it also restricts polymer chain motions, which reduces ionic conductivity. Moreover, there are very limited way to process a covalently bonded network polymer. Therefore the application of cross linking strategy is relatively limited.

4. The anions in lithium salts

The anions in lithium salts (F^-, ClO_4^-, $[N(SO_2CF_3)_2]^-$ etc.) play very important roles in SPE's conductivity performance. Whether a lithium salt can form complex with polymer chains is one of the crucial factors which determine the electrolyte's ion conductivity. The lattice energy of a salt can strongly affect its capability of form complexes with a polymer. Lithium salts with lower lattice energy can form polymer-lithium salt complex more easily. The lattice energy of a lithium salt itself strongly depends on the nature of the anion in the following order [14]:

$$F^->Cl^->Br^->I^->SCN^->ClO_4^->BF_4^->AsF_6^->[N(SO_2CF_3)_2]^-$$

It has been suggested that if the anion in a lithium salt has a larger volume, and the anion's electric charge delocalizes more extensively, the lithium salt will have a better performance in polymer electrolytes.

Peter Bruce's group [15] replaces XF_6^- (X= P, As or Sb) anion by another of the same shape and charge and similar size, that is, by forming the solid solution: PEO_6: $Li(AsF_6)_{1-x}(SbF_6)_x$, the electrolyte's conductivity can increase more than 1 order of magnitude compared to PEO_6: $Li(AsF_6)_n$. An alternative method is replacing a few mol% of XF_6^- ions with different shape and size, such as $[N(SO_2CF_3)_2]^-$, or ions with

different charge, such as SiF_6^{2-}, the new PEO-lithium salt complex's conductivity can increase 1.5-2 order of magnitude compared to the original stoichiometric complexes.

Part II: DCLC materials and application in organic electronic devices

Discotic columnar liquid crystals, which were discovered by Chandrasekhar in 1977 [1, 2], have attracted intensive research effort due to their wide applications in organic electronic devices. [3-8] A typical discotic mesogen includes a central aromatic core functionalized with flexible peripheral chains. The self-organization of disc-like molecules into the DCLC phases is driven by the anisotropy in the intermolecular interactions between the neighboring molecules. The disk-like mesogens can pile up into extended one-dimensional (1D) columns which align with their column axis parallel to each other. Specifically, DCLC phase are generally considered most useful for organic electronics applications. [9-15] DCLC materials can form efficient π-π columnar stacks that produce high charge-carrier mobilities, the magnitude of which is fundamentally determined by the degree of order and π-π orbital overlap within the columnar stacks. Furthermore, because of their thermotropic properties DCLC materials possess the capacity to self-heal structural defects such as grain boundaries which act typically as traps of charge carriers and limit the performance of the semiconductor. [16-20] Moreover, DCLC materials can reorganize and modify their physical properties as a response to an external stimulus, such as temperature changes, and an electrical or magnetic field, which is extremely valuable for technological applications. [21-25]

Besides the unique structure characters, DCLC materials generally can be

processed from solution. This offers them good adaptability, simplicity and processability. More importantly, solution-processability makes the simple roll-to-toll printing process, which is inexpensive and suitable for large-scale production, feasible for the large-scale manufacture. [26, 27]

Although their charge carrier mobilities do not reach the levels seen in single crystalline organics, liquid crystals circumvent many the difficult issues of controlling crystal growth and morphology. More importantly, liquid crystals can self-organize and can be aligned by surface force and fields. When liquid crystals are annealed at elevated temperatures, self-healing occurs improving molecular packing and diminishing the number of local defects and macroscopic grain boundaries which impede the charge carrier transport. [28]

Figure 1.1 Molecular order and columnar stacks of a DCLC phase [16]

Generally, large aromatic cores are more likely to form DCLC phase with good columnar stability and high superstructure order. [16] The most intensively investigated large aromatic cores include phthalocyanines (Pcs) [29-32], perylenes [33, 34] and hexabenzocoronenes (HBCs) [35-37], etc.

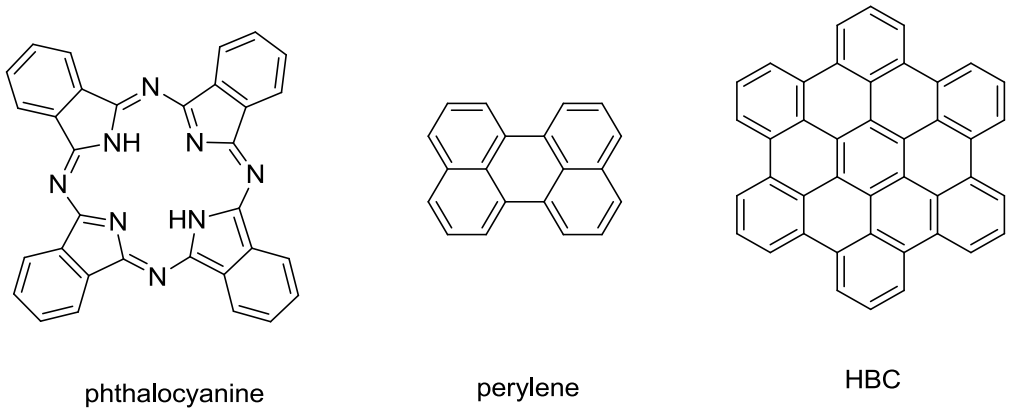

Scheme1.5 Chemical structure of phthalocyanine, perylene and hexa-*peri*-hexabenzocoronene (HBC)

Phthalocyanines bearing flexible peripheral chains can serve as typical discotic mesogens. As shown in **Scheme 1.6**, Pc1 was designed and synthesized in 1995. [38] Crown ether and alkyl chains were selected to ensure the compound's good solubility in organic solvents. Furthermore, the substituents' electron donating feature effectively increased the electron density of the aromatic system, which is important for its semiconductor performance as a *p*-type material.

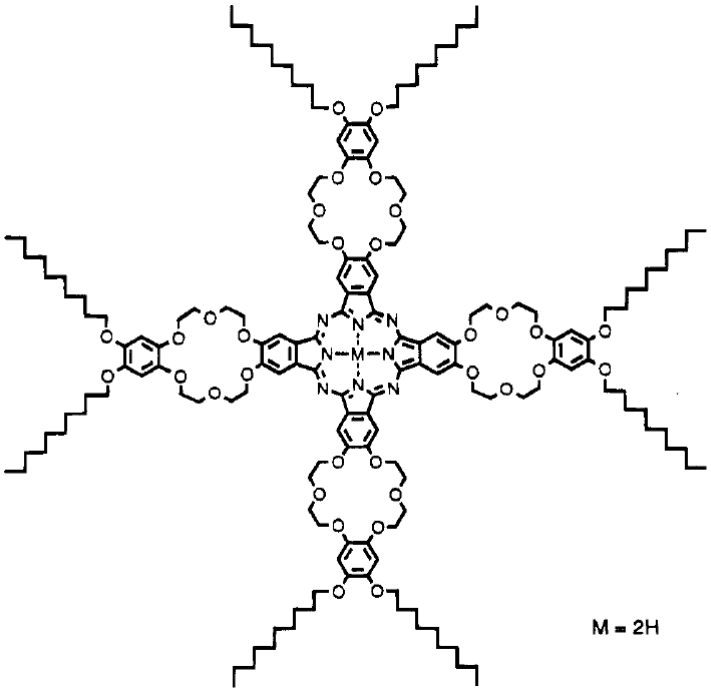

Scheme 1.6 Chemical structure of Pc1, a crown ether-substituted Pc [38]

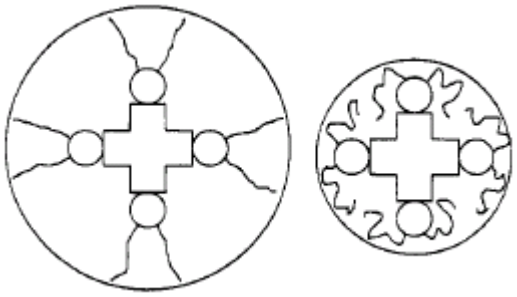

RT 170 °C

Scheme 1.7 Schematic representation of the disk-like molecules showing different molecule diameters at different temperatures [38]

The materials showed different phases with different molecule diameters at RT and 170 °C respectively. As shown in **Scheme 1.7**, at RT, the fully elongated decoxy chains gave the molecule larger molecule diameter, while at 170 °C, decoxy chains' bending back resulted from the chain flexibility at higher temperature. Pc1 showed a highly ordered crystalline phase at RT. The disk-like molecules piled up to form the columnar phase and the inter-Pc distance very close to 0.34 nm, while the crown ether

rings and the flexible alkyl chains were oriented perpendicular to the column axis. It is worth noticing that some empty space may be present in Pc1's crystalline structure. This space was probably occupied by solvent molecules, since elemental analysis reveals that chloroform could be tightly bound in the solid material. At 170 °C, the materials showed a DCLC phase which was confirmed by the small-angle XRD results. The column packing matched a hexagonal packing mode with intra-column distance of 4.05 nm. Compared to the molecule size, this distance suggests that the decoxy chains were folded backward. However, Pc1's DCLC phase can only present in narrow temperature range.

PDIs are the most intensively researched organic semiconducting materials among perylene derivatives owning to their broad electronic absorption spectrums, good chemical stability and large driving force to form π-stacks. [39-41] And PDIs have been incorporated into self-assembling building blocks employed in the design of complex systems and supra- and macromolecular assemblies that impact fields such as semiconductors, transistors and solar cells. [42-45] By chemical modification, PDI molecules can self-assembly into discotic columnar structures with two- and three-dimensional (2D and 3D) periodic orders.

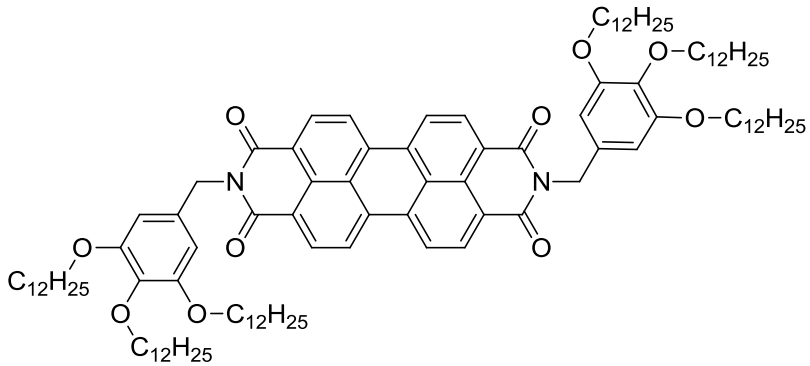

Scheme 1.8 Chemical structure of PDI X

The PDI X was synthesized and characterized in Dr. Marder's group in 2005. [46] It showed DCLC phase in wide temperature range (from -10 °C to 226 °C). According to the detailed XRD analysis made by Dr. Virgil Percec's group [48], the compound presents a 2D lattice with short range order along the column axis. Beyond the intra-column stacking, PDI X showed a highly ordered liquid crystalline columnar hexagonal phase. The supramolecular columns forming the hexagonal phase were constructed by a statistical mixture of the two kinds of arrangements resulting in an all up/all down, and up−down alternation. The alternative up−down conformation acts as structural defects that disrupt the helical packing and generate the weak 0.7 nm diffraction along the meridian direction which can be seen in **Figure 1.2**. The π−π stacking space between PDI layers was 0.35 nm. Along the column axis, PDI molecules piled up to form a unique helical structure.

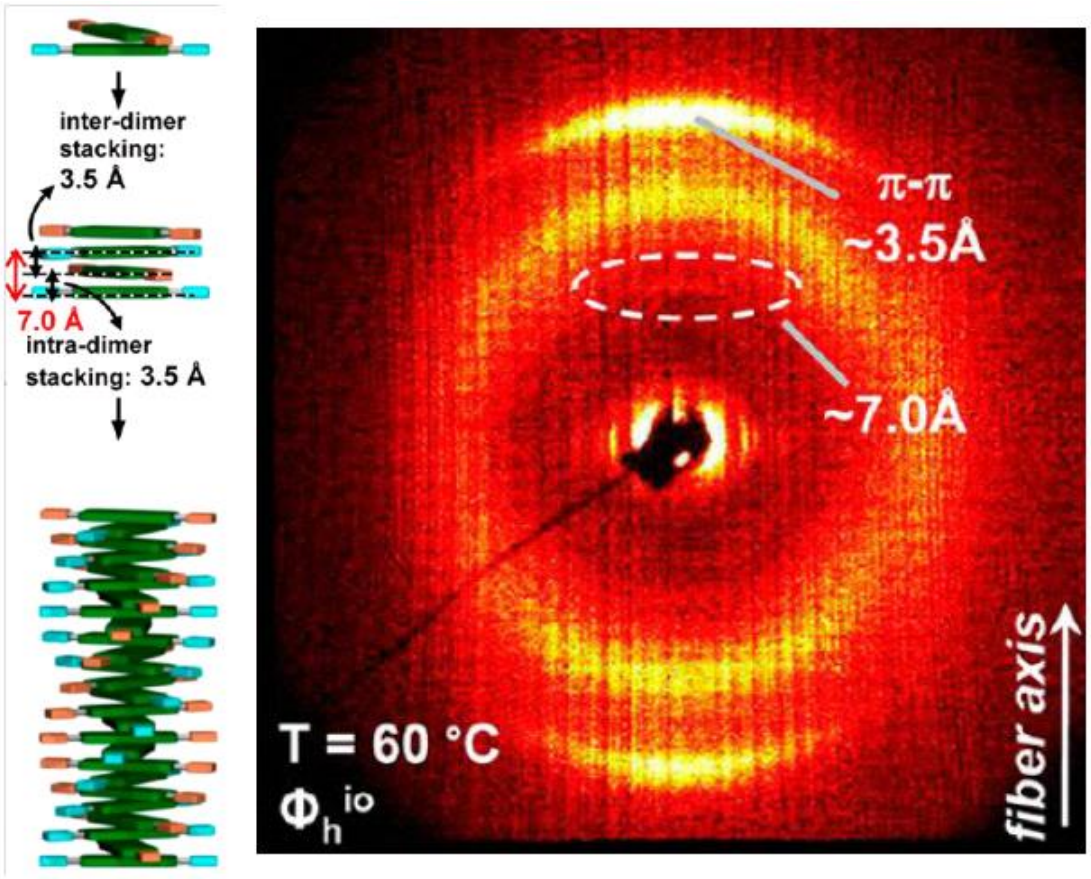

Figure 1.2 Schematic of the Self-Assembly of PDI X and wide-angle XRD pattern [47]

Compared to phthalocyanines and perylene derivatives, HBCs have more promising potential to form a stable DCLC phase. A HBC core consists of 42 carbon atoms bound together in 13 adjoining six carbon-membered rings to form the disc-shaped aromatic core. This large aromatic planar with high degree of symmetry has promising capability to form DCLC phase with enhanced columnar stability and high supramolecular order. HBC has reasonable good reactivity, which makes the aromatic core's chemical decoration feasible. Through the introduction of different side-chains, HBC derivatives' thermal behavior, solubility, and thus the processability can be controlled and tuned. More importantly, once form the DCLC phase, HBCs' large aromatic cores make the disk overlap fairly stable. The electronic charge

transport in such 1D column is expected to be mediated by the overlap between the aromatic π-orbitals of adjacent disks. The extensive π-system of HBC would therefore suggest that HBC-based DCLC materials have the promising potential to offer high charge carrier mobility.

As shown in **Scheme 1.9**, HBC X was reported by Dr. Müllen's group in 2008. [48] The compounds showed a crystalline phase at RT and transformed to a DCLC phase when heated to 145 °C. The distinct meridian diffractions related to a π-stacking distance of 0.36 nm were observed. And HBC molecular planes were arranged perpendicular to the column axis. The positions of equatorial diffractions suggested a hexagonal arrangement of columnar structures with a packing parameter of 2.51 nm.

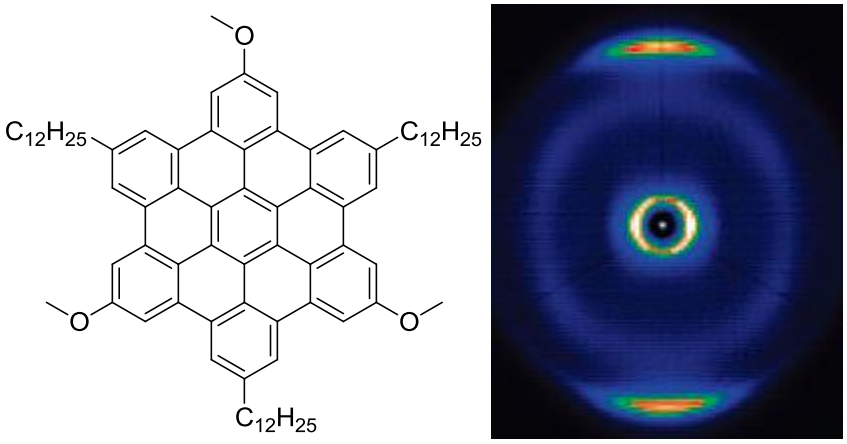

Scheme 1.9 Chemical structures of HBC X and 2D wide-angle XRD pattern [48]

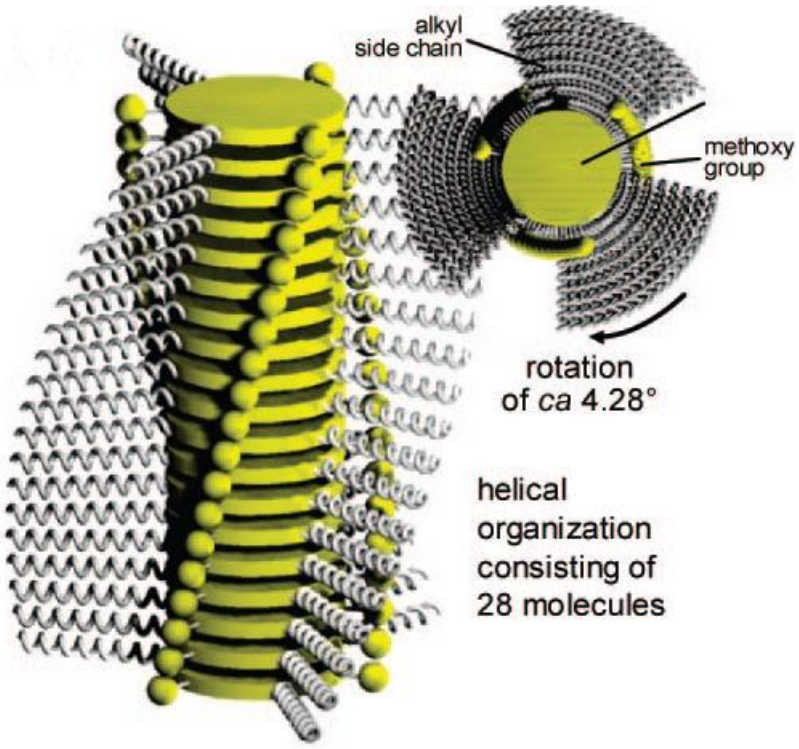

Figure 1.3 Schematic illustration of the intra-columnar arrangement of HBC X [48]

Interestingly, after annealing thoroughly at 30 °C, HBC X presented a columnar structure with helical properties. The molecules were slightly rotated by an angle of 4.28 ° to each other resulting in an intra-column helical packing. The helical arrangement of HBC X can be attributed to local dipole moments between carbon-oxygen bonds, as both π-stacking and dipole interactions could play important roles for the self-assembly leading to complex superstructures.

In 2002, a multi-stack intra-column self-assembly model was realized by Dr. Percec and co-workers. [49] Subsequently, a novel "dendron-wedge concept" was introduced and systematically studied in Percec's article in 2004. [50] According to the Dendron-wedge theory, asymmetrically substituted molecules with "wedge" shape are more likely to behave the multi-stack supramolecular assemblies. As shown in **Figure 1.4**, the naphthalene ring, which is not a large aromatic core, is fairly difficult to form

a stable discotic columnar phase. However, when functionalized by the semifluorinated tapered dendron, the molecule self-assemblied into a multi-stack super-column structure, and a highly ordered hexagonal column packing was observed. One of the possible driving forces of this self-assembly is molecule's wedge-shaped property provided by the unique dendron. And the charge carrier migration along columns is different from the traditional 1D migration. An intra-column inter-stack charge hopping process may be involved. [51, 52]

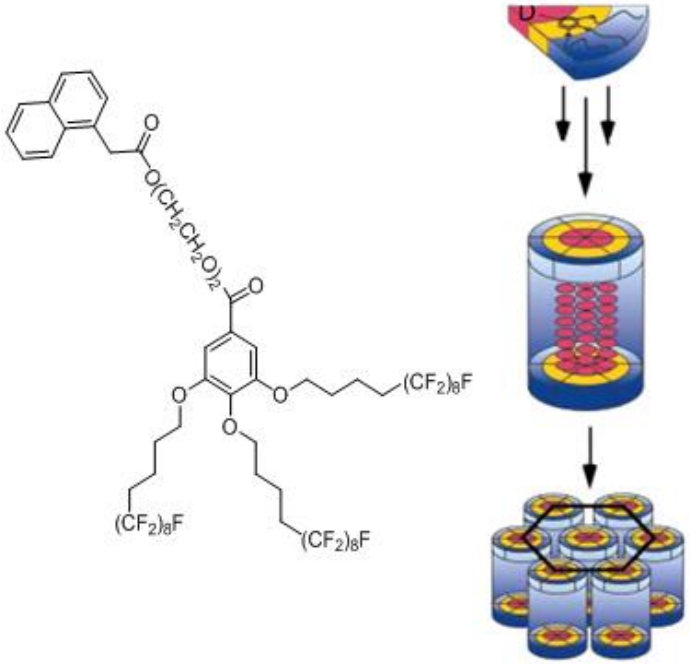

Figure 1.4 Schematic illustration of the liquid crystal assembly processes and wedge-shaped molecule structure [50]

Also in 2004, a partly "unwrapped" HBC Y was synthesized in Dr. Müllen's group [53] to enhance the compound's charge carrier migration via decreasing molecular substitution symmetry. As shown in **Scheme 1.10**, the HBC core of Y was asymmetrically substituted, leaving residual flexible chains to ensure solution processability and phase-forming properties. Generally, stable columnar phases

require more than 3 alkyl substituents on the mesogenic core and the exposure of edges can lead to other arrangements such as face-to-face interaction. When forming the DCLC phase, HBC Y has the potential to allow charge carriers hopping between columns avoiding the influence of the intra-column packing defects, which can substantially improve the charge transport robustness of a DCLC phase. However, this 2D charge migration was not realized based on HBC Y's characterization.

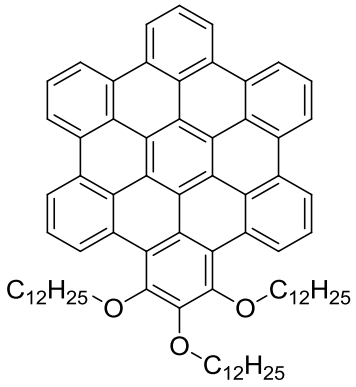

Scheme 1.10 Chemical structure of HBC

Inspired by Dr. Müllen's 2D charge migration model, we used PEA as the base molecule to pursue the novel BSDCLC phase. As presented in **Scheme 1.11**, the PEA molecule is intrinsically asymmetric and has promising potential to realize the self-assembly process resulting a multi-stack intra-column structure. The details will be thoroughly discussed in Chapter 5.

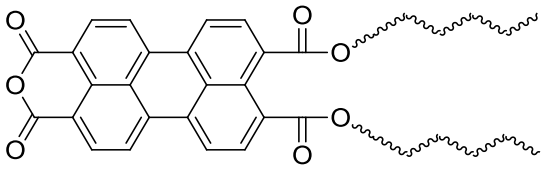

Scheme 1.11 A typical molecule structure of PEA

CHAPTER 2. PREPARATION AND CHARACTERIZATION OF A HIGHLY CONDUCTING POLYMER WITH COMB STRUCTURE FROM A COMMERCIAL-AVAILABLE POLYMER

2.1 Introduction

It has been shown that a grafted polymer with a highly flexible main chain bearing OEG side chains can be an excellent candidate for SPEs as far as the ionic conductivity is concerned. The conductivity as high as 4.5×10^{-4} S/cm has been reported for siloxane-based double comb polymer carrying OEG side chains. [1] However, the mechanical property of the polymer is very poor, likely due to the very low degree of polymerization. [2,3] Although cross-link (physically or chemically) is the most straightforward way to improve mechanical properties, increasing the molecular weight (MW) of a polymer is also an effective approach as the entanglement of polymer chains occurs very rapidly with the increase of MW. A polymer with a very high MW can offer excellent short-term dimensional stability even in its rubbery state due to extensive chain entanglement. Such a high MW polymer with OEG as the side chain would be able to provide both good dimensional stability (short-term) and high RT ionic conductivity. Taking the main-chain flexibility (for high lithium ion conductivity) and the preparation of the polymer into consideration, we set a high MW PEO-based polymer as the main-chain and OEG as the side chain. The PEO main chain is not only highly flexible, but also can directly contribute to the lithium ion conductivity of the polymer. Moreover, such a polymer can be potentially synthesized by functionalizing PECH-PEO, a polymer that is

commercially available with different MWs, including very high MWs. For the purpose of minimizing possible crystallization, a PECH-PEO random copolymer consists of 50 % ethylene oxide monomeric units was chosen.

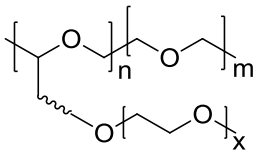

Scheme 2.1 Target comb-like polymer: PECH-PEO main chain with OEG side chains

Poly (epichlorohydrin) (PECH) and PECH–PEO have been considered as suitable starting materials for synthesizing new functional polymers with a wide range of applications because their chlorine atoms can be nucleophilically substituted. [4-9] More importantly, since the chlorine atoms are attached to primary carbon atoms instead of the PECH or PECH-PEO's main chain, incoming nucleophiles will experience smaller steric hindrance. PECH's main chain modification has been reported by several authors using a large number of nucleophiles such as azide [4], carbazole [5], carboxylates [6], sulfur compounds [7, 8] and phenolates [9-11] with the help of phase-transfer catalysis. However, main-chain cleavage problem, cross-linking side-reactions or a low degree of substitution have been reported in most cases. [7-11] For instance, knowing that PECH main chain is vulnerable to strong bases, Nishikubo and colleagues chose azide ion, a good nucleophile and weak base, to modify PECH. [4] However, the overall substitution percentage is only 18%.

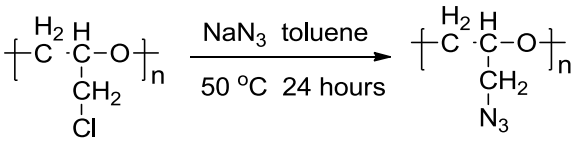

Scheme 2.2 Chemical modification of PECH using sodium azide

A more efficient azide modification of PECH was achieved by Frankel, M. B. and Flanagan, J. E. in dimethylformamide (DMF) at 100 °C. [12] The overall yield was as high as 73% and substitution percentage was nearly 100%. However, they only used low MW PECH (MW~1000 Da) as the starting material and polymer product obtained was a viscous amber liquid.

Higher degrees of PECH's substitution have been reported using different nucleophiles and the use of a phase transfer catalyst, such as tetra-n-butylammonium bromide. Ronda and colleagues [13] used sodium phenolate and phase transfer catalyst to carry out the following modification of PECH.

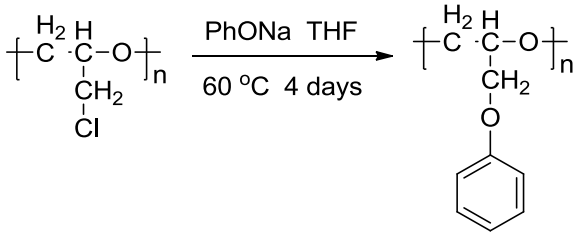

Scheme 2.3 Chemical modification of PECH using PhONa

Under this strategy, they found that a higher concentration of sodium phenolate can improve the substitution. When double amount of phenolate was used, the substitution percentage was successfully increased to 60%, however, the degree of elimination was as high as 25%. The following degradation mechanisms were proposed by Ronda.

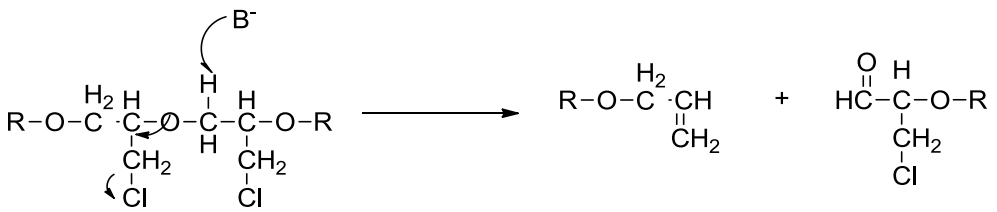

Scheme 2.4 PECH main chain degradation mechanism 1

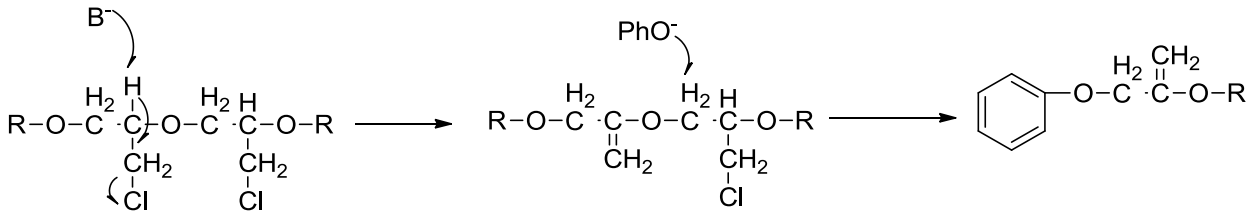

Scheme 2.5 PECH main chain degradation mechanism 2

According to these mechanisms, it is easy to understand that a higher nucleophile concentration and/or a more basic nucleophile in the reaction medium will lead to more extensive main-chain degradation.

Considerable research effort has also been applied to the modification of PECH-PEO copolymers. [14-16] The studies on the modification of PECH and PECH–PEO with sodium phenolate concluded that the PECH–PEO main chain did not degrade as much as the PECH main chain. This could be attributed to the more compact random coil PECH–PEO chains, which contains the more flexible ethylene oxide units. [14] It is worth mentioning that the use of a phase transfer catalyst, such as tetrabutylammonium bromide, could effectively increase the substitution reaction yield and substitution percentage, especially when the PECH-PEO copolymer was with high MW (MW>900000 Da). [16]

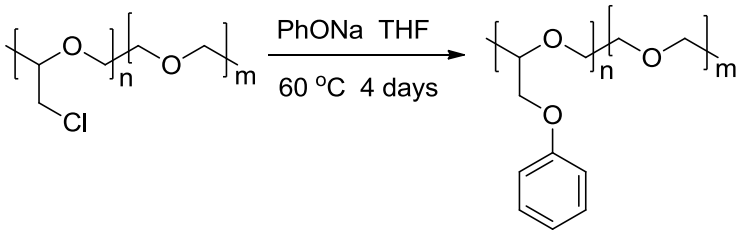

Scheme 2.6 Chemical modification of PECH-PEO using PhONa

Generally, no reported PECH and PECH-PEO modification methods achieved a high degree of substitution, a low degree of elimination, minimum chain

degradation on a high MW polymer. For instance, 100% degree of substitution and minimum elimination were achieved using Frankel's method [12], however, this method only work well on low MW polymers. On the other hand, high MW PECH-PEO and PECH were successfully modified by Ronda and coworkers [15, 16], and degree of substitution was as high as 78%, but substantial degree of elimination (20%) and severe main chain degradation were observed. Here we attempt to develop a facile method to modify the high MW PECH-PEO with high degree of substation, high yield and minimum main chain degradation.

The simplest synthetical route to our targeted high molecular weight polymer would be a one-step nucleophilic substitution of the chlorine atoms by an OEG alkoxide nucleophile in a high MW PECH-PEO random copolymer. However, this approach is very unlikely to be successful owing to the expected extensive elimination-based main-chain degradation whose mechanism was introduced before. The main-chain degradation in the hypothetic one-step functionalization would be significantly more extensive than what have been observed for cases where phenoxides were used as the nucleophile, since an OEG alkoxide (pKa of the conjugate acid is ~ 16) is much more basic than phenoxide (pKa of the conjugate acid is ~ 10).

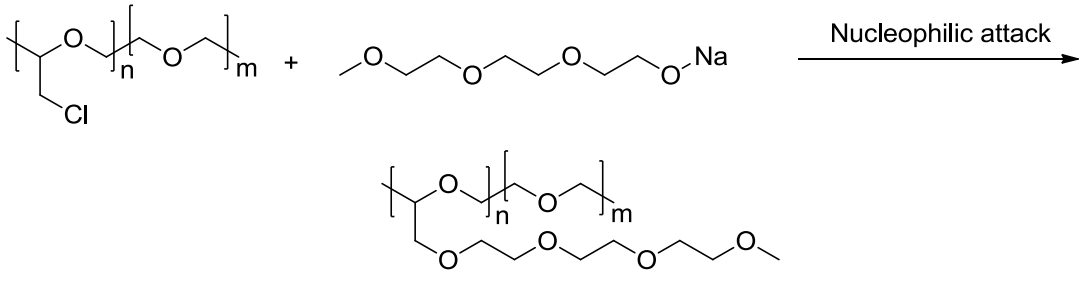

Scheme 2.7 Direct nucleophilic substitution of PECH-PEO main chain: an unrealistic approach

To achieve a high degree of functionalization while avoiding the main-chain degradation, we designed a two-step functionalization approach. In the first step, azide ion, a highly nucleophilic and weakly basic (pKa of the conjugate acid is ~ 4) nucleophile, will be applied to perform the initial functionalization of PECH-PEO. The reaction condition will be optimized to achieve a high degree of functionalization with little degradation. In the second step, the final functionalization will be carried out at a nearly neutral condition using a highly efficient and mild click chemistry.

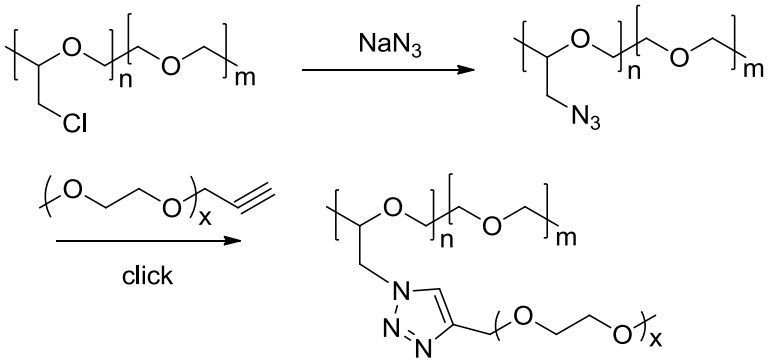

Scheme 2.8 Synthesis routine of OEG-modified PECH-PEO via click chemistry

2.2 Results and discussion

2.2.1 The substitution percentage and degree of degradation

FTIR spectroscopy provides the key evidence showing the complete replacement of chlorine atoms, yielding poly (ethylene oxide-*co*-glycidylazide) (PEOGA). As shown in **Figure 2.1**, C-H bending vibration of -CH_2Cl groups generates a sharp peak at 738 cm^{-1}. This peak completely disappeared after the

substitution reaction. While a sharp and intense peak at 2095 cm^{-1}, which is the characteristic peak of azide group, was observed after the substitution. [18] The degree of substitution was also more quantitatively assessed based on the elemental analysis result as shown in **Table 2.1**. As calculated from mass percentage of nitrogen, the degree of substitution is greater than 99%. Considering the error limit of elemental analysis (± 0.3%), it can be concluded that the complete substitution of chlorine atoms by azide groups has been successfully achieved

	C	N	H
Theoretically calculated	41.95	29.36	6.34
Experimentally determined	41.59	29.12	6.30

Table 2.1 Elemental Analysis Results of PEOGA (Wt %)

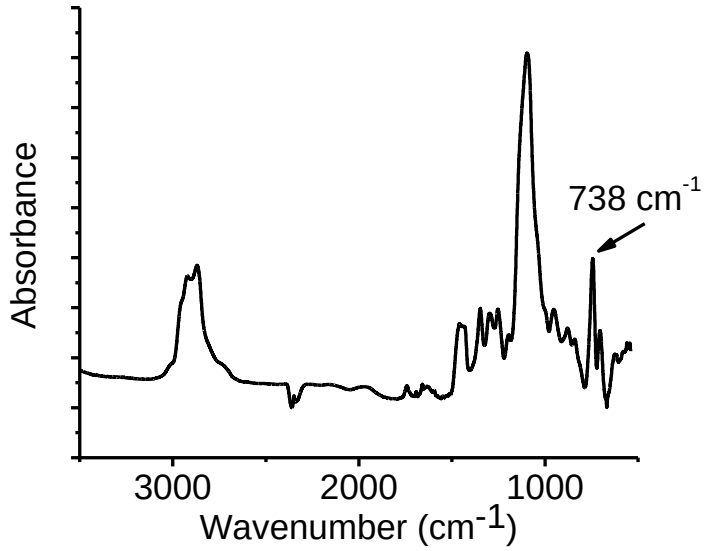

Figure 2.1 IR spectrum of PECH-PEO

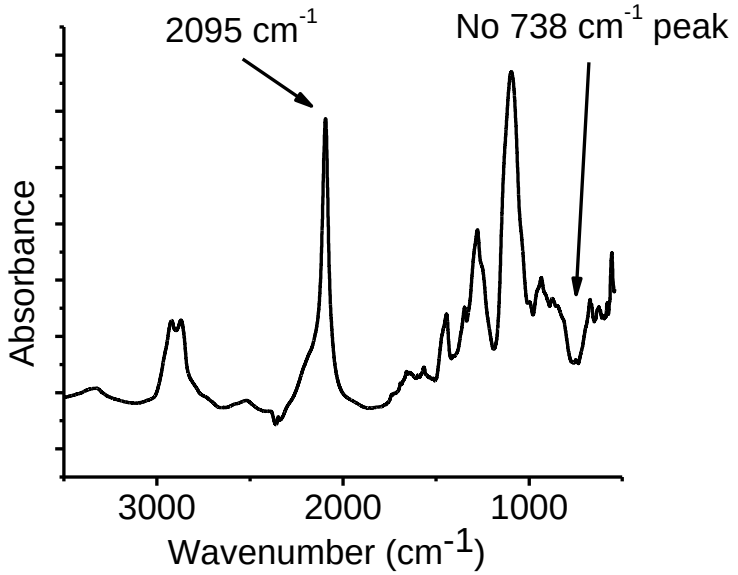

Figure 2.2 IR spectrum of PEOGA

The minimum main chain degradation was supported by the viscosity measurement. An Ubbelohde viscometer was used and polymer concentrations were varied between 0.25 and 2 g/L. At 25 °C, the intrinsic viscosity of original PECH-PEO in DMF is 0.979 g/dL, while the value of PEOGA in DMF is 0.986 g/dL. The slight higher intrinsic viscosity suggests that there was no any appreciable main degradation involved during the chemical modification.

The use of highly nucleophilic and weakly basic azide as the nucleophile is likely an important factor that leads to the successful substitution without any significant main-chain degradation. The weakly basic nucleophile minimized the possible elimination-based chain degradation. The use of DMF, a highly polar and nonprotic solvent, promoted S_N2 reaction. In addition, we used tetrabutylammonium iodide as the catalyst, which serves two roles: First, I^- can catalyze the nucleophilic replacement of chlorine atoms and second, the quaternary ammonium ion can serve as

the phase transfer catalyst. Finally, it is intrinsically easier to achieve a high degree of substitution on a PECH-PEO than a PECH, due to the lower steric hindrance, especially when a significant number of chlorine atoms already have been nucleophilically substituted.

2.2.2 The advantages of main chain modification via click chemistry

Compared to the traditional PECH-PEO main chain modification through nucleophilic substitution, we choose a more sophisticated method which introduces side chains to PECH-PEO backbone using a triazole ring. It is well known that click reaction can be carried out in a very mild chemical atmosphere and can give high yield. This, plus the azide substitution reaction's high modification degree and minimum main chain degradation, makes our main chain modification strategy successful and flexible. Theoretically, as long as an alkyne group can be introduced to the side chain molecule, any side chain can be connected to the PEOGA main chain in high yield and minimum chain scission. In addition, unlike many nucleophilic reactions, the click chemistry reaction does not have high requirements of operation and experimental conditions. It is not sensitive to water or oxygen, and many click reactions even use water as the reaction media. [19, 20]

2.2.3 The characteristics of OEG modified PECH-PEO

This PEO-based polymer is found to be a good candidate for polymer electrolyte with excellent processability. It is soluble in water and most of commonly used organic solvents, such as chloroform, tetrahydrofuran (THF), DMF, methanol

and hexane. When blended with certain ratio of lithium salt, the electrolyte showed reasonable good conductivity at RT. Its good conducting performance as polymer electrolyte results from the following reasons: 1. The PECH-PEO backbone, which can be considered as the random copolymer of 1,2-epoxy-3-chloropropane and ethylene oxide, has significant structure irregular character. This comb-structure polymer is very difficult to form a relatively ordered structure and crystallize. In other words, this polymer almost always remains in amorphous phase. This property was confirmed by the results from DSC and XRD analysis. As shown in **Figure 2.3**, no endothermic or exothermic peaks were observed during heating and cooling process, and the polymer's T_g was around -40 °C. The material's degree of crystallinity was too low to be observed. In **Figure 2.4**, the broad peak in 1D XRD pattern suggested that amorphous phase was the dominant phase. It is generally agreed that the polymer chain's segmental motion in amorphous phase is extremely important for polymer's conducting performance. 2. The polymer contains large amount of ethylene oxide units, which play important role of catching and transporting lithium ions. 3. The polymer's high MW is well maintained by successful main chain modification with high degree of substitution and minimum chain scission. According to GPC analysis results, this comb-like polymer's number average MW (Mn) reached 270,000 Da. High MW is crucial for polymer material's mechanical properties, which is important for polymer electrolyte's industrial application. The good dimensional stability is illustrated by **Figure 2.5**. A piece of rubber-like polymer was put on a clean glass

slide, which was placed upside down for three weeks. The material could perfectly maintain the dimensional stability for at least three weeks.

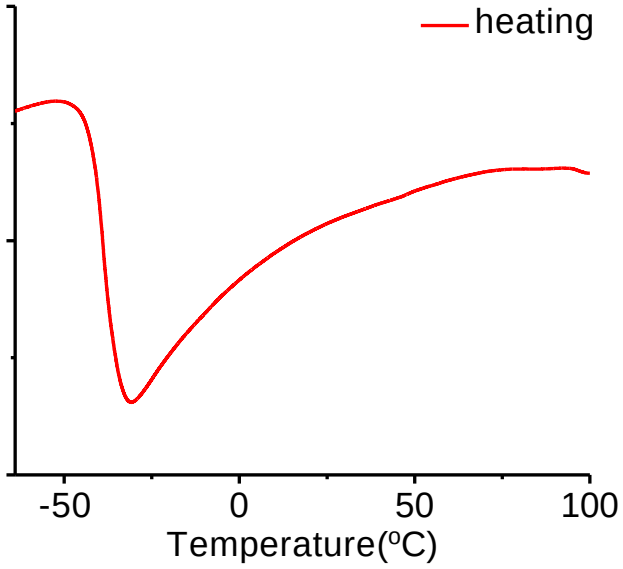

Figure 2.3 DSC result of OEG modified PECH-PEO polymer

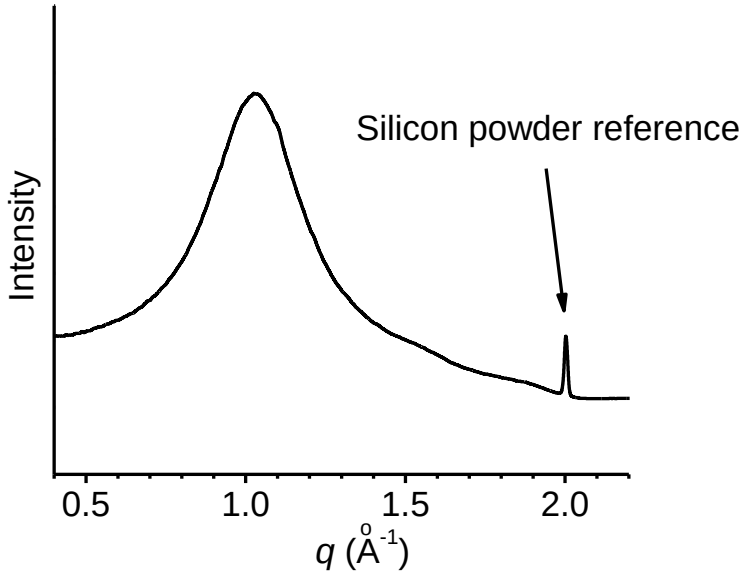

Figure 2.4 1D XRD pattern of OEG modified PECH-PEO polymer at RT

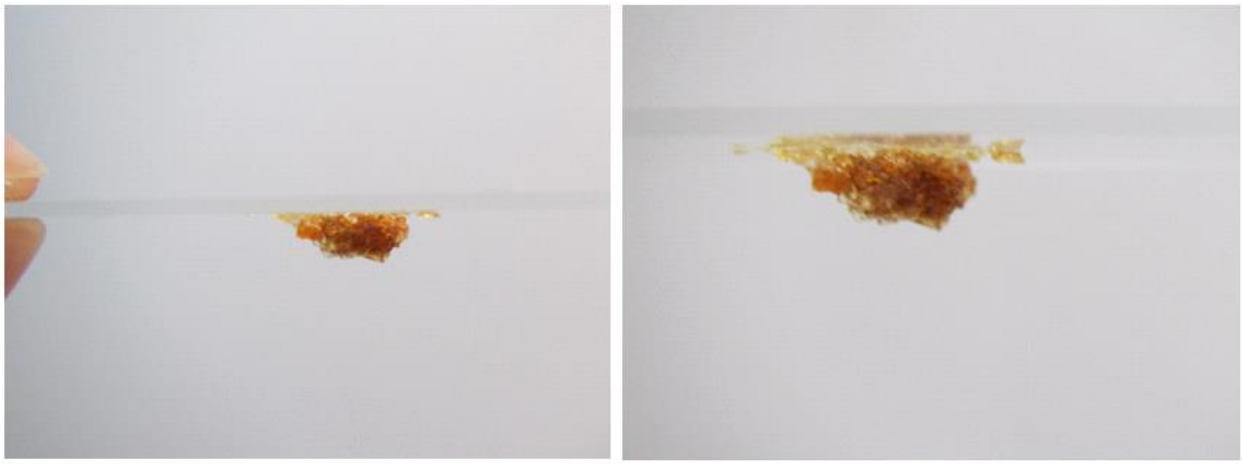

Original **Three weeks later**

Figure 2.5 Dimensional Stability of comb-like polymer at RT

2.2.4 The impedance measurement of polymer electrolytes

1. Preparation of polymer-lithium salt complex

Five complexes with different [O]/[Li] ratios (50:1, 40:1, 30:1, 20:1and 10:1) were prepared. The [O]/ [Li] ratio is defined as the number of polymer chain's oxygen atoms divided by the number of lithium ions in electrolyte.

[O]/[Li] ratio	Weight ratio (polymer/Li salt)	Polymer weight	$LiN(SO_2CF_3)_2$ weight
50:1	10:1	53.60 mg	5.40 mg
40:1	8:1	56.27 mg	7.06 mg
30:1	6:1	50.36 mg	8.35 mg
20:1	4:1	62.88 mg	15.69 mg
10:1	2:1	60.06 mg	30.01 mg

Table 2.2 The weight of samples with different [O]/ [Li] ratio

SPEs were prepared by carefully mixing a appropriate amount of $LiN(SO_2CF_3)_2$ with the comb-structure polymer in THF. The lithium salt and polymer

were precisely weighted. The majority of solvent was removed by nitrogen blow. Then the electrolytes were dried at 60 °C under vacuum for 3 days. Samples with a diameter of 2.38 mm and a thickness of 0.07 mm are sandwiched between two conducting stainless steel plates spaced by a plastic spacer.

2. Impedance measurement

The impedance measurements were carried out in glove box at RT using a computer-controlled advanced electrochemical system from Princeton Applied Research, frequency range was 20 k-1M Hz at 10 mV AC amplitude. [21] The "electrolyte sandwich" was connected to the electrochemical instrument as external cell. The data were analyzed by Princeton Applied Research Company's software: PowerSuite. Taking the electrolyte with [O]/ [Li] =40 as the example, the calculation of conductivity is described below:

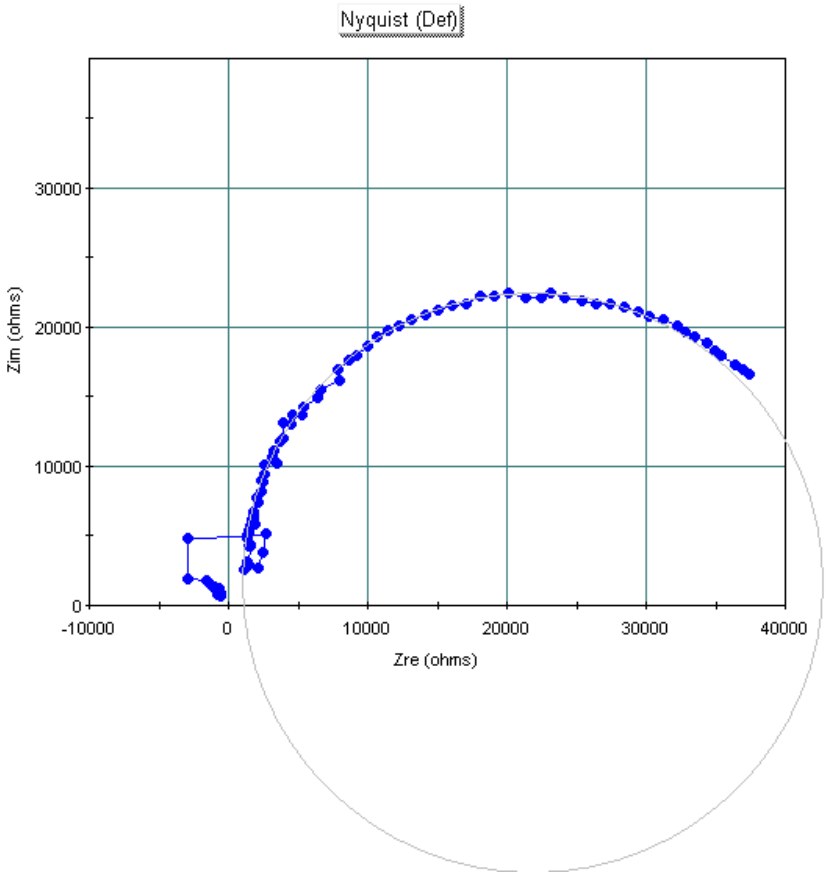

Figure 2.6 Impedance measurement spectrum of electrolyte ([O]/ [Li]: 40)

As shown in the graph, the trend of impedance points at different frequency (with blue color) is part of a circle, the intersection of the circle arc and the x-axis is the resistance value of this electrolyte. Here we used the circle fit method to calculate the resistance. A circle, which matched the arc most perfectly, was simulated by PowerSuite software. The information of this circle was given by coordinates. For this electrolyte, the parameters of circle fit are listed: center point's coordinate: X: 2.187×10^4, Y: 1527; diameter: 4.176×10^4. Based on these data, we calculated the resistance of this electrolyte is 1046 ohms. Using the classic formula $\sigma=A/ L\times R$(A is the conducting area of sample, L is the sample's thickness, R is resistance, the units of A and L are centimeter), we got the conductivity of this electrolyte was 1.5×10^{-4}

S/cm. Using this method, the conductivity values of different electrolytes are summarized in **Table 2.3**.

[O]/[Li] ratio	50:1	40:1	30:1	20:1	10:1
Conductivity	0.88×10^{-4} S/cm	1.5×10^{-4} S/cm	1.68×10^{-4} S/cm	1.16×10^{-4} S/cm	0.5×10^{-4} S/cm

Table 2.3 Conductivities of electrolytes with different [O]/[Li] ratio

Based on the data in **Table 2.3**, the electrolyte with [O]/[Li] ratio of 30 gave the best conducting performance, which illustrate that the concentration of Li^+ in electrolytes plays important role regarding electrolyte's conducting capability.

2.2.5 Further molecule engineering for the improvement of conductivity

Motivated by the good conductivity performance of tri-EG-modified PECH-PEO, we used the same synthesis strategy to modify the PECH-PEO backbone using tetra-EG side chains to further improve the material's conductivity. With the longer OEG side chains, the lithium ions' transportation in the electrolyte will be more efficient due to the polymer's higher component of ethylene glycol. The tetra-EG-modified polymer's chemical structure is shown in **Scheme 2.9**.

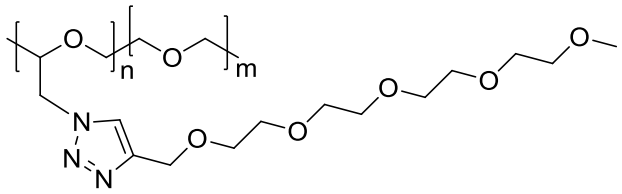

Scheme 2.9 Chemical structure of tetra-EG-modified PECH-PEO

Similarly, five complexes with different [O]/[Li] ratios (50:1, 40:1, 30:1, 20:1and 10:1) were prepared using tetra-EG-modified PECH-PEO. And the weights

of samples are presented in **Table 2.4** and the conductivity measurement results are shown in **Table 2.5**.

[O]/[Li] ratio	Weight ratio (polymer/Li salt)	Polymer weight	$LiN(SO_2CF_3)_2$ weight
50:1	9.7:1	46.60 mg	4.80 mg
40:1	7.8:1	50.66 mg	6.51 mg
30:1	5.8:1	48.60 mg	8.38 mg
20:1	3.9:1	45.73 mg	11.72 mg
10:1	1.95:1	50.08 mg	25.68 mg

Table 2.4 The preparation of complexes with various [O]/ [Li] ratios using tetra-EG-modified PECH-PEO

[O]/[Li] ratio	50:1	40:1	30:1	20:1	10:1
Conductivity	0.846×10^{-4} S/cm	0.885×10^{-4} S/cm	0.98×10^{-4} S/cm	1.26×10^{-4} S/cm	0.788×10^{-4} S/cm

Table 2.5 Conductivities of tetra-EG-modified PECH-PEO-based electrolytes

Due to the equipment limit, the impedance measurement of tetra-EG-based electrolytes were carried out in air. All the polymer-lithium salt complexes were pre-dried in vacumm oven for 24 hours at 50 °C. Subsequently the sticky complex was carefully loaded to sample holder made from a small piece of transparency, then the sample was dried in vacumm oven for another 12 hours at 50 °C. After the thorough drying process the sample was quickly sandwiched by two stainless plates and the impedance measurement was carried out in the air in two minutes at RT. As shown in **Table 2.5**, compared to those of tri-EG-based electrolytes, the conductivity performance of tetra-EG-based electrolytes is not impressive. Further measurement

will be carried out in glovebox to make more convincing comparison.

2.3 Experimental

2.3.1 Materials

THF (Aldrich) was dried and stored in a solvent purification system from Innovative Technology. DMF (EM Science) was used without previous purification. Tetra-*n*-butylammonium iodide (synthesis grade, Aldrich), was used as the catalyst. Sodium hydride (60% dispersion in mineral oil, Aldrich), triethylene glycol monomethyl ether (Fluka) and 3-bromoprop-1-yne (80% solution in toluene, Apollo Scientific) were used without previous purification. PECH–PEO (Zeon Chemicals Inc.) was used as the starting polymer. The weight average MW (M_w) = 334,000 Da and polydispersity is 2.2. The snakeskin pleated dialysis tubing (7,000 MWCO) from Thermo Scientific was used to purify the polymer product.

2.3.2 Synthesis of PEOGA

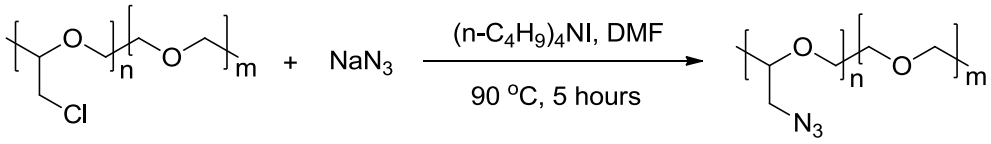

Scheme 2.10 Substitution reaction of PECH-PEO with sodium azide

2 g PECH-PEO copolymer (14.6 mmol, MW of repeating unit is 136.5) was dissolved in 20 ml DMF, then 1.3 g (20 mmol) sodium azide were carefully dispersed in the solution, and 0.1 g tetra-*n*-butylammonium iodide was added under inert atmosphere as the catalyst. The mixture was slowly heated to 90 °C and stirred vigorously for 5 hours; substitution was completed based on the IR spectrum information, (As shown in **Figure 2.1** and **Figure 2.2**, the absorption at 738 cm^{-1},

which is the peak of carbon-hydrogen bond -CH_2-Cl, disappeared completely). The product was precipitated in water, after centrifugation, the PEOGA was collected and dried in vacuum oven at 50 °C for 48 hours. The yield is 90%.

2.3.3 Synthesis of 2,5,8,11-tetraoxatetradec-13-yne

0.5 g NaH (21 mmol) was carefully dispersed in 15 ml dry THF in ice bath, then 1.6 g triethylene glycol monomethyl ether (10 mmol) was dropwise added to the solution in 30 minutes. The mixture was stirred at RT for another 30 minutes. Subsequently 1.78 g 3-bromoprop-1-yne (15 mmol) was added to the solution. The mixture was stirred at 45 °C for 4 hours then 10ml deionized water was added to quench the reaction. The crude reaction mixture was extracted by dichloromethane (5 ml each time) three times and purified by column chromatography with 100/3 (v/v) chloroform/methanol as the eluent to afford 1.74 g (86%) product as a light yellow liquid.

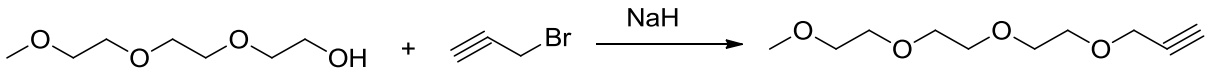

Scheme 2.11 Synthesis of 2,5,8,11-tetraoxatetradec-13-yne

2.3.4 Synthesis of 2,5,8,11,14-pentaoxaheptadec-16-yne

0.5 g NaH (21 mmol) was carefully dispersed in 15 ml dry THF in ice bath, then 2.1 g tetraethylene glycol monomethyl ether (10 mmol) was dropwise added to the solution in 30 minutes. The mixture was stirred at RT for another 30 minutes. Subsequently 1.78 g 3-bromoprop-1-yne (15 mmol) was added to the solution. The mixture was stirred at 45 °C for 4 hours then 10ml deionized water was added to

quench the reaction. The crude reaction mixture was extracted by dichloromethane (5 ml each time) three times and purified by column chromatography with 100/3 (v/v) chloroform/methanol as the eluent to afford 2.21 g (90%) product as a light yellow liquid.

2.3.5 Main chain modification via click chemistry (Tri-EG side chain)

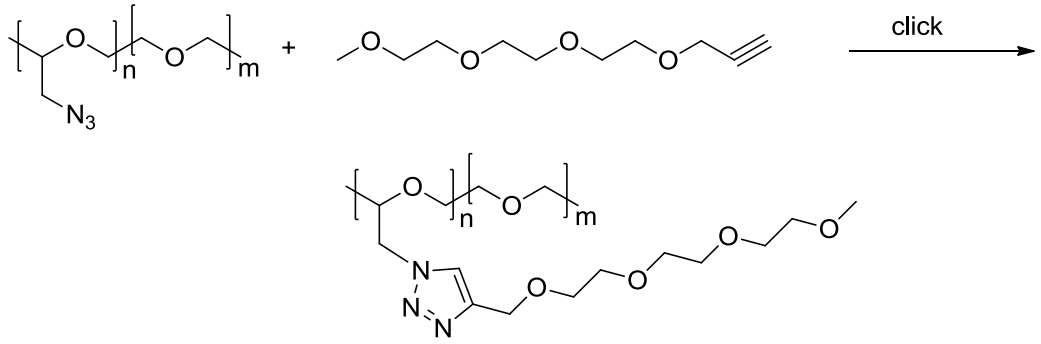

Scheme 2.12 Main chain modification via click chemistry

0.3 g PEOGA (2.1 mmol, MW of the statistic repeating unit is 143) and 0.9 g 2, 5, 8, 11-tetraoxatetradec-13-yne (4.2 mmol) were dissolved in 5 ml DMF and the mixture was bubbled with nitrogen for 1 hour. Then 0.05 g CuBr (0.35 mmol) and 0.05 g 1, 1, 4, 7, 7-penta-methyldiethylenetri-amine (0.3 mmol) were added to the mixture. The solution was bubbled with nitrogen for 1 hour and sealed well, then stirred at RT for 12 hours. [17] The reaction was monitored by IR until the peak of azide (2095 cm^{-1}) completely disappeared. Then the polymer was purified through dialyses for four weeks.

To perform the dialysis, the solution was first transferred into a snakeskin pleated dialysis tube; the two ends were tightly sealed by clips. Then the tube was dipped into 500 ml 20% ammonia water to remove the copper salts; the fresh

ammonia water was changed every 4 hours. After the complete removal of copper salts (it usually takes about 12 hours), as confirmed by UV spectroscopy, the tube was dipped into 1000 ml distilled water to remove all the ligand, residual 2,5,8,11-tetraoxatetradec-13-yne and DMF. The fresh water was changed every 12 hours. The dialyses continued for 10 days and the purity of the polymer product was monitored by proton NMR. After the dialyses, the water of polymer aqueous solution was removed by air blow. The polymer was dried in vacuum oven at 50 °C for 24 hours. The yield is 90%.

2.3.6 Main chain modification via click chemistry (Tetra-EG side chain)

0.3 g PEOGA (2.1 mmol, MW of the statistic repeating unit is 143) and 1.03 g 2, 5, 8, 11-tetraoxatetradec-13-yne (4.2 mmol) were dissolved in 5 ml DMF and the mixture was bubbled with nitrogen for 1 hour. Then 0.05 g CuBr (0.35 mmol) and 0.05 g 1, 1, 4, 7, 7-penta-methyldiethylenetri-amine (0.3 mmol) were added to the mixture. The solution was bubbled with nitrogen for 1 hour and sealed well, then stirred at RT for 12 hours. The reaction was monitored by IR until the peak of azide (2095 cm^{-1}) completely disappeared. Then the polymer was purified through dialyses for four weeks. The yield is 88% after dialysis and drying.

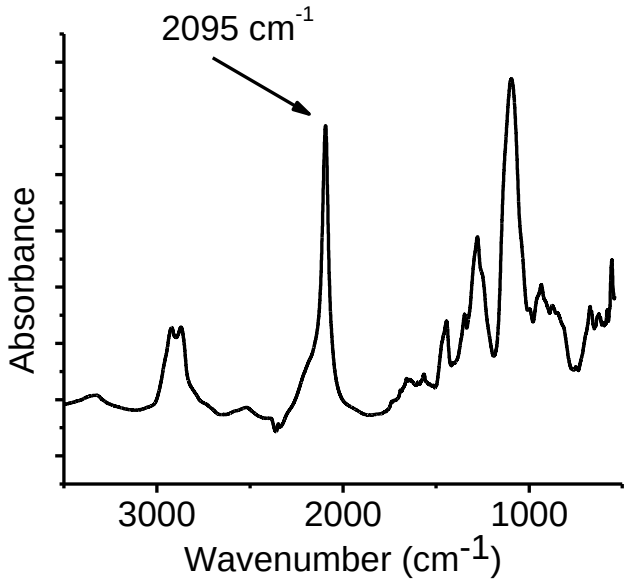

Figure 2.7 IR spectrum of PEOGA before click reaction

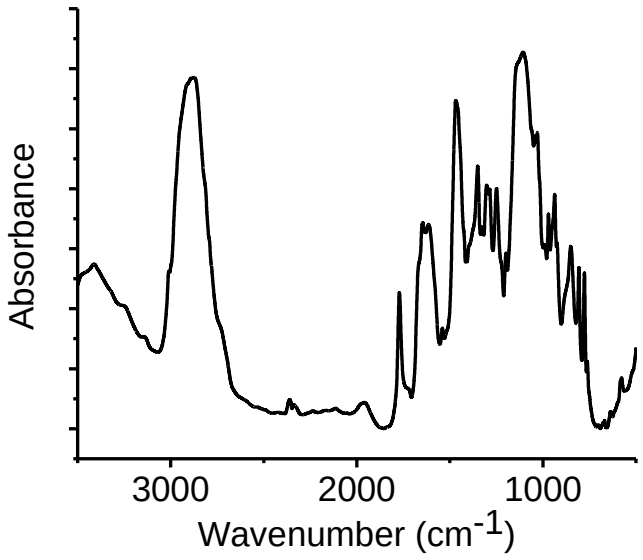

Figure 2.8 IR spectrum of PECH-PEO-based polymer after click reaction

2.4 Conclusion

A novel main chain chemical modification strategy of PECH-PEO was proposed and confirmed by experimental data. First, the chlorines of PECH-PEO main chain were successfully substituted by azide groups with high degree of substation and minimum chain degradation. Second, the PEO-based side chains are

introduced to the main chain via click chemistry. The click reaction's high efficiency and mild reaction atmosphere enhance the modification method's feasibility and universality. A PEO-based polymer with comb structure and high MW was successfully synthesized via click chemistry. With unique structure characteristics, this polymer was found to be a good candidate for solid electrolytes used in lithium batteries. When blended with lithium salts in certain ratios, the polymer can form solid electrolytes with good conductivity at RT. Furthermore, the polymer can easily dissolve in water and most of the commonly used organic solvents. The good processability is valuable for the material's industry application. Then electrolyte is a transparent solid with light yellow color, proving that it has potential in application of optical electrochemistry devices.

CHAPTER 3. SYNTHESIS OF PERYLENE MONOHANHYDRIDE DIESTERS VIA INTRAMOLECULAR CYCLIZATION

3.1 Introduction

Perylene tetracarboxylic derivatives based dyes are very interesting molecules that have a set of appealing physical and chemical properties that have attracted considerable amount of interests recently. Thanks to the rigid, planar perylene rings, many perylene tetracarboxylic derivatives exhibit high fluorescent quantum efficiency in their monomeric state and show an appreciate tendency to from π-stacks. Moreover, the direct attachment of four electron-withdrawing carbonyl groups to a perylene ring renders a perylene tetracarboxylic derivative molecule electron-deficient, which makes perylene tetracarboxylic derivatives good *n*-type semi-conductors. Generally speaking, symmetrically substituted perylene derivatives, such as symmetrically substituted perylene diimides (PDIs) and perylene tetraesters (PTEs), are straightforwardly accessible synthetically and have been applied in photovoltaic and other organic electronics. [1-5] In contrast, the preparation of unsymmetrically substituted perylene derivatives, such as unsymmetrically substituted PDIs, PTEs and perylene diester monoimides (PEIs) is much more challenging. To facilitate the synthesis of unsymmetrically substituted perylene derivatives, perylene-3,4-anhydride-9,10-di-(decyloxycarbonyl) (PEA-diC10) was designed and successfully synthesized in our group. [6]

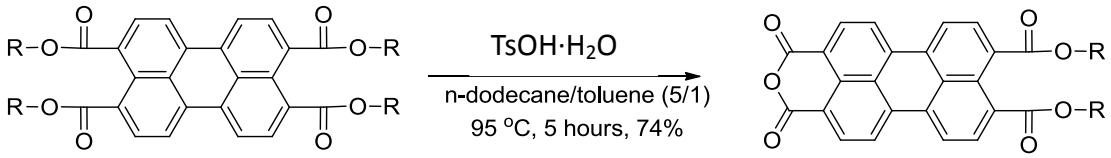

Scheme 3.1 Synthesis of PEA-diC10

Being an unsymmetrically perylene derivative itself, the large reactivity difference between the anhydride and ester groups ensured that reactions can occur highly selectively at the anhydride side. Moreover, the moderate reactivity of the ester groups enables their transformation to an anhydride group for further reactions via an acid-catalyzed hydrolysis reaction when the need comes up. Since then, PEAs have been utilized in the preparation of an array of unsymmetrically substituted perylene derivatives. Although designed with synthetic applications in mind, the applications of PEAs in the field of liquid crystals are extremely promising. As the anhydride group is completely planar with the perylene ring and free of any substituent atoms (even hydrogen atoms!), PEA is an ideal mesogen for the generation of materials that are capable of self-assembling into a BSDCLC phase, a phase that has been predicted to possess superior charge transport characteristics than a conventional DCLC phase but has yet to be experimentally observed. To encourage the formation of such a promising phase, PEA-10/14 was designed and synthesized according to our original synthetic route. The phase transition and structure characterization results indicate that PEA-10/14 indeed self-assembles into a RT BSDCLC phase. The charge carrier mobility result also confirmed the structural advantage of this unique phase. This is the first time that perylene-based BSDCLC phase has been experimentally observed.

The unique bundled-stack columnar structure and the strong electron deficiency (nearly the same as PDIs, the best *n*-type organic semiconductors) make PEA-10/14 an exceptionally attractive semi-conducting liquid crystalline material. However, the current preparation of PEA-10/14 is of very low yield.

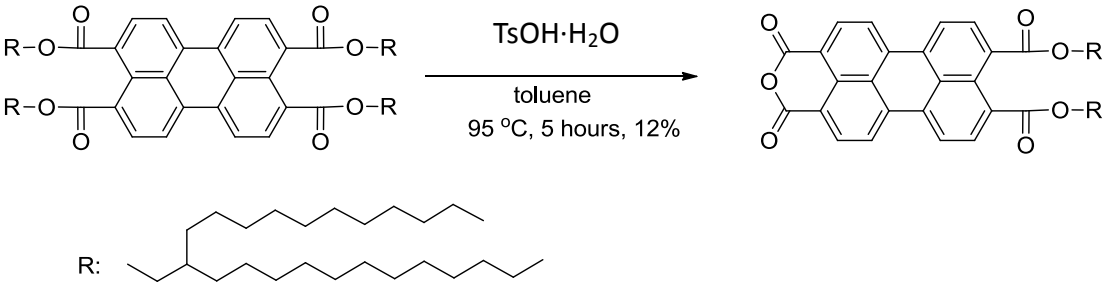

Scheme 3.2 Synthesis of PEA-10/14

As the only current available method, an acid-catalyzed partial hydrolysis/cyclization of a perylene tetraester was applied to prepare PEA-10/14. Two conditions must be met for such a reaction to generate a PEA at a high yield. First, the hydrolysis of ester groups must be fast enough. Second, a mechanism must exist to prevent the formed PEA further hydrolyzed into perylene dianhydride (PDA) which is the most stable product under the acid-catalyzed hydrolysis condition. It has been found that ~ 1 molar equivalent $TsOH \cdot H_2O$ at ~ 100 °C is necessary for ester groups to hydrolyze at a reasonable rate. To minimize the formation of PDA, the reaction condition must be tuned in such a way that the tetraester is available in the solution for the hydrolysis reaction while the PEA is removed from the reaction system, which was done by the precipitation of the PEA. This approach worked well for perylene tetraesters with relatively short alkyl chains (the yield of PEAs can be higher than 90% [6]), as the solubility difference between the PEA and the corresponding PTE is large

enough so that the solvent composition can be tuned that the PEA is insoluble while the PTE is highly soluble under the reaction condition. In this way, the PEA precipitates from the solution upon its formation therefore its conversion to PDA is minimized. However, the solubility of PEA-10/14 (or any PEA with similarly long, branched flexible peripheral chains) is very high even in the weakest solvent that can dissolve the corresponding PTE. Consequently, the removal of PEA-10/14 by precipitation from the reaction media does not occur, and it can readily further hydrolyze/cyclize into PDA. The result is a substantially lower yield (~30% from PTE to PEA). Moreover, the yield of the corresponding PTE from PDA is also of low yield, resulting in an overall yield of only 12%.

Besides the low yield, the current methodology imposes a significant limitation on functional groups that the flexible peripheral chains can bear. With the strong, hydrated acid ($TsOH \cdot H_2O$) and a moderately high temperature (~ 100 °C), this procedure works best only on alkyl peripheral chains. An ester group in the peripheral chain would undergo an acid-catalyzed hydrolysis reaction, therefore is not compatible with the current method. Even the existence of ether or olefin groups could potentially complicate the reaction. Such a limitation may severely impede the phase structure optimization of BSDCLC PEAs. As revealed by our structure analysis, the BSDCLC phase of PEA-10/14 is still far from being perfect. There are two stacking modes in the phase, which unavoidably induce systematically occurring packing defects that reduce the charge carrier mobility. In addition, the π-stack spacing is appreciably larger than what is typically found in tightly packed

perylene-based DCLC materials. To further improve the BSDCLC structure, it is important for us to be able to tune the peripheral chains systematically. In many case, such tuning may involve functional groups that are potentially incompatible with the current approach. Therefore an improved approach toward PEAs is highly desired, especially if it can provide PEA-10/14 at a higher yield and tolerate more labile functional groups. Here we report a one-pot approach toward PEAs. In this synthetic route, the functional groups in a peripheral chain are only exposed to either a weakly basic (carboxylate) or a weakly acidic (acetic acid) environment at ~ 60 °C, therefore many more functional groups can be incorporated into a PEA, which greatly improves the structural versatility of PEAs as well as PEIs and PTEs that can be prepared from a PEA. Moreover, the new approach can produce PEA-10/14 at an appreciably higher yield in a convenient one-pot fashion.

The new approach is designed on the basis of our recent finding that when a carboxyl group and an ester group are attached to the same side of a perylene ring, a spontaneously cyclization occurs giving an anhydride group, as shown in **Scheme 3.3**. Even at room temperature, such transformation completes in several hours.

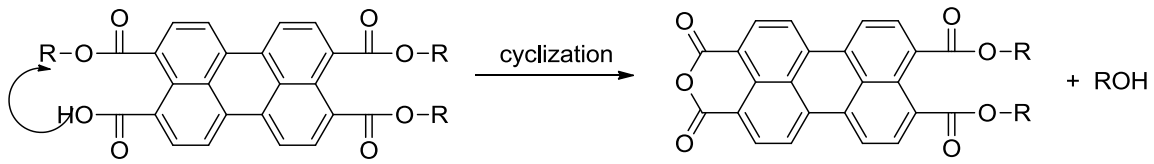

Scheme 3.3 Formation of anhydride via intra-molecular cyclization

Apparently, the breaking of the ester C-O bond is assisted by the formation of the six-membered anhydride ring so that it can occur at very mild condition. This observation implies that it may be possible to prepare a PEA according to **Scheme 3.4**.

Note in this case, only a weakly acidic environment is needed, just for the sake of protonating the carboxylate group. Although the synthesis of the triester carboxylate has not been reported, a three-fold ester formation from perylene tetracarboxylate appears to be a feasible route.

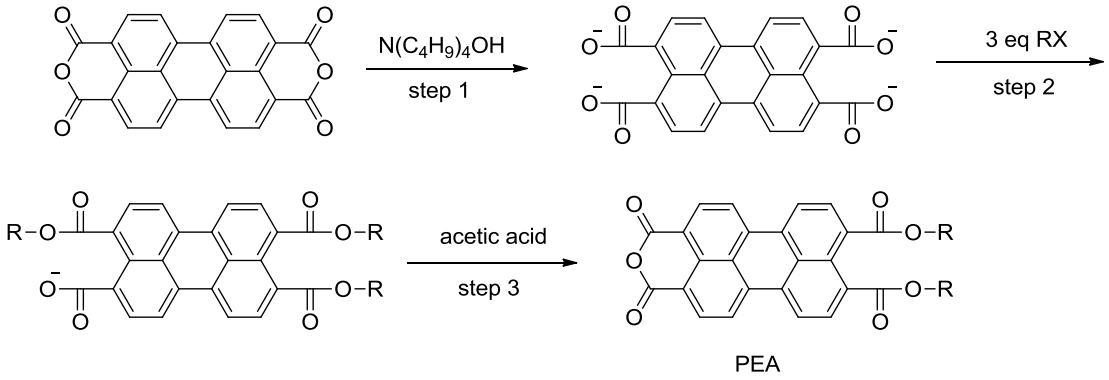

Scheme 3.4 Synthesis of PEA via a three-fold ester formation route

As one can expect that a number of substitution products (with different degree and/or patterns of substitution, as shown in **Scheme 3.5**) could form in such a three-fold ester formation. Care must be taken to maintain a proper nucleophile/electrophile molar ratio throughout the reaction in the phase where the nucleophilic substitution reaction takes place to maximize the yield of the desired tri-substitution product.

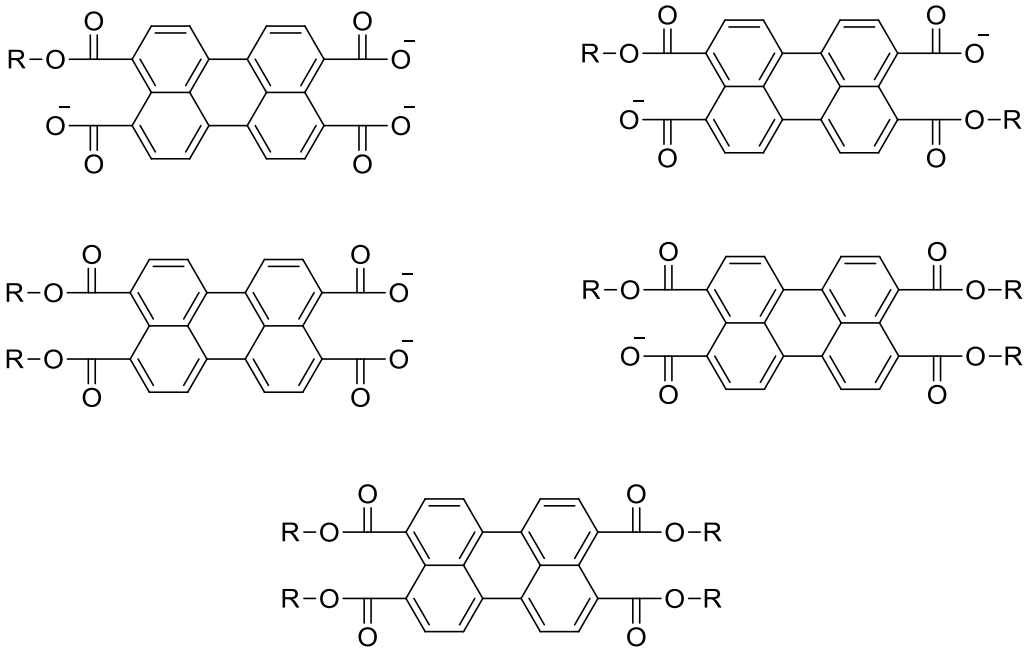

Scheme 3.5 Different degrees/patterns of substitution during the three-fold ester formation

If a sodium or potassium salt of perylene tetracarboxylate is used in an organic solvent which is necessary to dissolve an electrophile, the tetraester would be the only major product, because the electrophile/nucleophile molar ratio in the organic phase (the active medium) will be much greater than the feed ratio, due to the very low solubility of sodium or potassium perylene tetracarboxylate in typically aprotic polar solvents for a S_N2 reaction such as DMF and dimethyl sulfoxide (DMSO). For this reason, tetra-*n*-butylammonium perylene tetracarboxylate was used with DMSO as the solvent to make it possible to fully dissolve both the nucleophile and electrophile in the same phase. In this way, the nucleophile/electrophile mole ratio can be reliably controlled by tuning the feed ratio so that the yield of the desired tri-substituted product can be maximized. Note that to obtain the PEA in an analytically pure form, there is no need to isolate the perylene triester monocarboxylate. Instead, upon the completion of the nucleophilic substitution step, the cyclization step can be directly

carried out by adding acetic acid to the reaction mixture to establish a weakly acidic environment, making this preparation route a convenient one-pot procedure. To speed up the cyclization reaction, the temperature is set at about 60 °C. This one-pot three-step procedure is expected to generate only two soluble perylene derivatives, the desired PEA and the tetraester, that are soluble in organic solvents. All other substitution products shown in **Scheme 3.5** will transform into PDA which is not soluble in any common organic solvent.

3.2 Results and discussion

The new approach was first applied to synthesize PEA-10/14. Tetra-*n*-butylammonium perylene tetracarboxylate was prepared by adding four molar equivalent of tetra-*n*-butylammonium hydroxide into a suspension of PDA in DMSO. Upon the completion of the reaction as indicated by the formation of a clear solution, three molar equivalent of electrophile (based on PDA) was added into the solution. After the electrophile was fully consumed (according to TLC), eight equivalent of acetic acid was added to the reaction mixture and the temperature was kept at 60 °C for about three hours.

To our disappointment, this procedure did not produce PEA-10/14 in any noticeable amount. The vast majority of soluble perylene product is the tetraester. A careful inspection of the procedure revealed that the electrophile (a tosylate with a long, branched alkyl chains) is so hydrophobic that it does not dissolve well in DMSO. Instead, it mainly disperses in DMSO in the form of small droplets. As the result, the nucleophile (perylene tetracarboxylate) was gradually transferred into the

hydrophobic tosylate phase in the form of tetra-*n*-butylammonium salt and alkylated under a very large local electrophile/nucleophile molar ratio, leading to the tetraester as the only major soluble perylene product.

To improve the electrophile's solubility in the solvent, the tosylate was first dissolved in acetone, and then added dropwisely to the perylene tetracarboxylate DMSO solution. The final volume ratio of acetone and DMSO is 2:3. With the added acetone in the solvent mixture, its polarity is reduced to a point that both the highly hydrophobic tosylate and the ionic nucleophile can be dispersed molecularly so that the feed ratio truly reflects the local nucleophile/electrophile molar. With this method, the yield of PEA-10/14 increased sharply to 28%. Only trace amount of tetraester was observed. The fact that PEA-10/14 was the only major soluble perylene product confirmed the previous phase-transfer hypothesis. Although the yield is still low, it is more than twice of the yield of the original method. Moreover, in this convenient one-pot procedure, the functional groups in the flexible peripheral chains are only exposed to either a weakly basic (carboxylate ions during the formation of triester monocarboxylate) or weakly acidic (acetic acid in the cyclization step) environment at a mild temperature (~ 60 °C). As the result, the new procedure should accommodate many labile functional groups in the final PEA, which will greatly increase the structural versatility of PEAs.

The successful incorporation of ether groups in the peripheral chains was demonstrated by the synthesis of PEA-3EG and PEA-2EG as shown in the **Table 3.1**. Note that in these cases the tosylate is molecularly dissolved in DMSO therefore no

acetone is needed. This is the first time ether-bond containing PEAs have been synthesized. If the original method is applied, the use of $TsOH \cdot H_2O$ at ~100 °C may complicate the reaction due to the possible acid-catalyzed cleavage of either linkages.

PEA Name	Chemical Structure	Yield
PEA-10/14	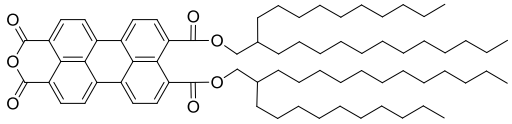	28%
PEA-BZ-D10	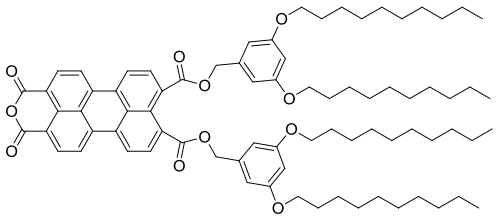	22%
PEA-di-(*Z*)-C10	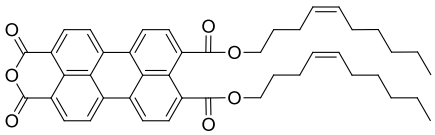	45%
PEA-4-BZ-D10	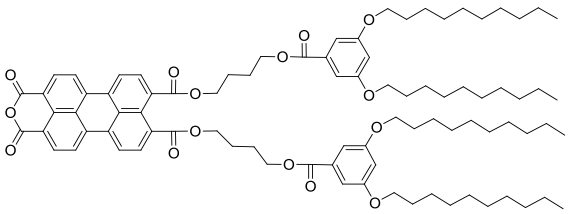	26%
PEA-3EG	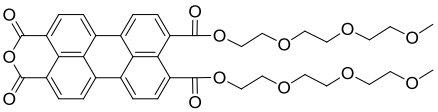	21%
PEA-2EG	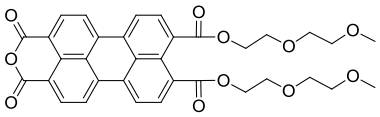	26%
PEA-(*Z*)-C10-3EG	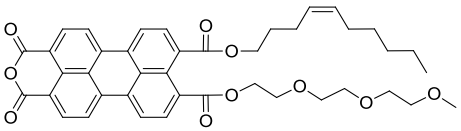	20%

Table 3.1 Summary of intramolecular cyclization yields for different PEAs

The new, mild procedure also allows the inclusion of isolated C=C bonds in the peripheral group, which is shown by the successful synthesis of PEA-di-(*Z*)-C10. It is interesting to observe that the solubility of PEA-di-(*Z*)-C10 in common organic solvents is much higher than its *n*-alkyl counterpart. Most likely this is because it is much more difficult for the flexible peripheral chains with a kinked chain structure originated from the *cis*-C=C bonds to pack efficiently in the solid phase. Note that C=C bonds are also vulnerable in a strongly acidic (and wet) environment.

The even more powerful testimony to the mildness of new procedure is the successful synthesis of PEA-BZ-D10, containing an ester group in the peripheral chain. An ester linkage is generally considered to be even more labile than an ether or a C=C and can be cleaved in either a basic or an acidic environment. However, the labile ester groups easily survived the new mild one-pot procedure as they only need to experience a weakly basic (step 2) and a weakly acidic environment (step 3) at a mild temperature (~ 60 °C), as shown in **Scheme 3.4**. Apparently, PEA-BZ-D10 cannot be prepared by original procedure as it will cleave the ester groups in the peripheral chains.

The successful synthesis of these PEAs confirmed that acidification/cyclization of triester is indeed a viable approach toward PEAs. Although so far all the perylene triesters carry three identical flexible chains, a perylene triester carries two kinds of flexible chains on one side of the perylene ring should also cyclize into the corresponding PEA upon protonation, which would result in the formation of an unsymmetrically substituted PEA. Besides the intermolecular

interactions that dictate the self-assembly of symmetrically substituted PEA, the intermolecular interaction between two types of peripheral chains could add one more dimension to the self-assembly of unsymmetrically substituted PEAs. For instance, if two chemically incompatible flexible peripheral chains are installed on one PEA molecule, the self-assembly of the PEA is expected to be under the influence of the micro-phase segregation between two flexible chains, which adds one handle for one to control the hierarchical structure of PEAs.

The preparation of the first such PEA is outlined in **Scheme 3.6**. The expected micro-phase segregation between the hydrophilic OEG chains and the hydrophobic (*Z*)-4-decenyl chains may become the new variable in the self-assembly of the PEA and potentially lead to the formation of new phases. In the first step, triethylene glycol monomethyl ether was allowed to nucleophilically attack the carbonyl carbon of the anhydride group of PDA in the presence of 1,8-Diazabicycloundec-7-ene (DBU). Each of such a nucleophilic attack generate one ester linkage plus a highly stable carboxylate ion, which ensures that only one triethylene glycol monomethyl ether chain is attached to one side of the perylene ring, even in the presence a large excess of alcohol. In the second step, the other type of flexible chains, (*Z)*-4-decenyl was introduced in the form of a tosylate. To encourage the formation of the perylene triester, only one molar equivalent was used (based on PDA). After the acidification/cyclization step, the first unsymmetrically substituted PEA was indeed obtained at an isolated yield of 20%.

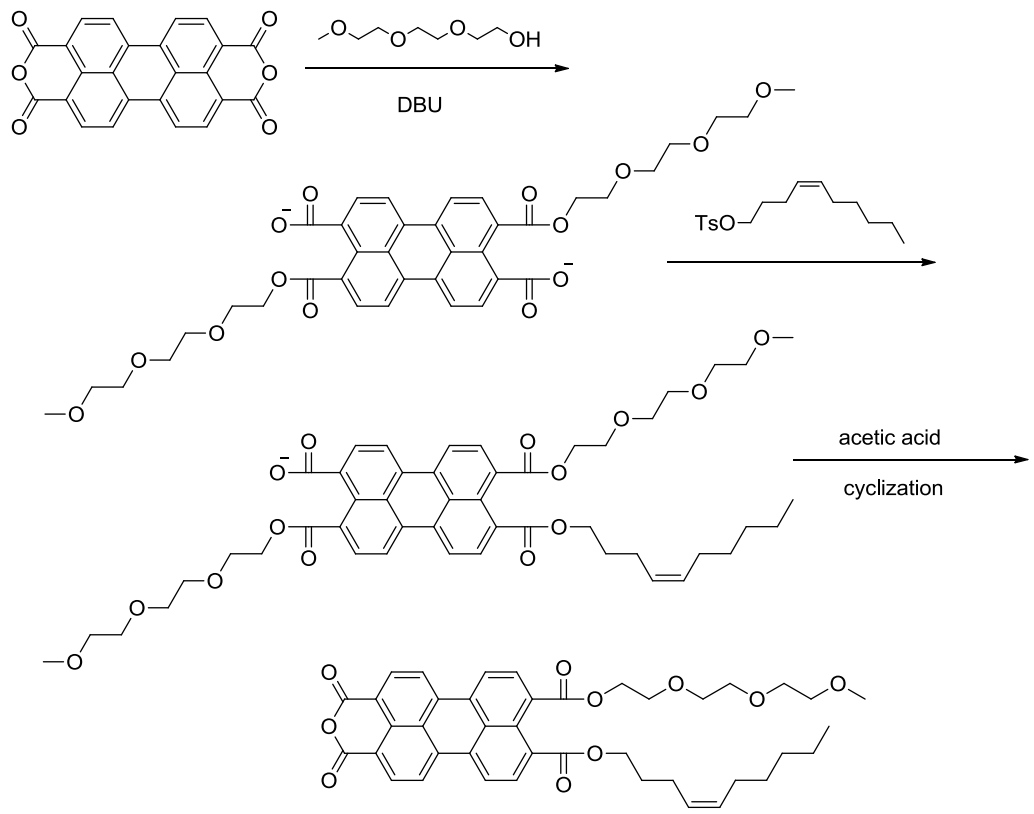

Scheme 3.6 Synthesis of PEA-(*Z*)-C10-3EG via intramolecular cyclization

As far as intermolecular interaction is concerned, PEA-(*Z*)-C10-3EG can be considered as a triphilic molecule, with the rigid perylene core, the flexible and hydrophilic OEG chain and the flexible but hydrophobic (*Z*)-4-decenyl chain as the three molecular components that tend to associate with same kind of molecular components but avoid different ones. In addition to its own potentially interesting self-assembly behaviors, the availability of PEA-(*Z*)-C10-3EG enabled us to prepare the first tetraphilic perylene derivative PEI X. The additional molecular component is a perfluorinated alkyl chain. Due to the so-called "fluorophobic" effect, perfluorinated alkyl chains tend to segregate from the rigid perylene cores, the hydrophilic OEG and hydrophobic (*Z*)-4-decenyl chains. Its preparation is shown in **Scheme 3.7** with the isolated overall yield higher than 80%. Note that the compound is chiral and optically

pure, which may lead to helical perylene π-stacks with a preferred handedness. The optical activity stems from the use of optically pure L-alanine in the first step.

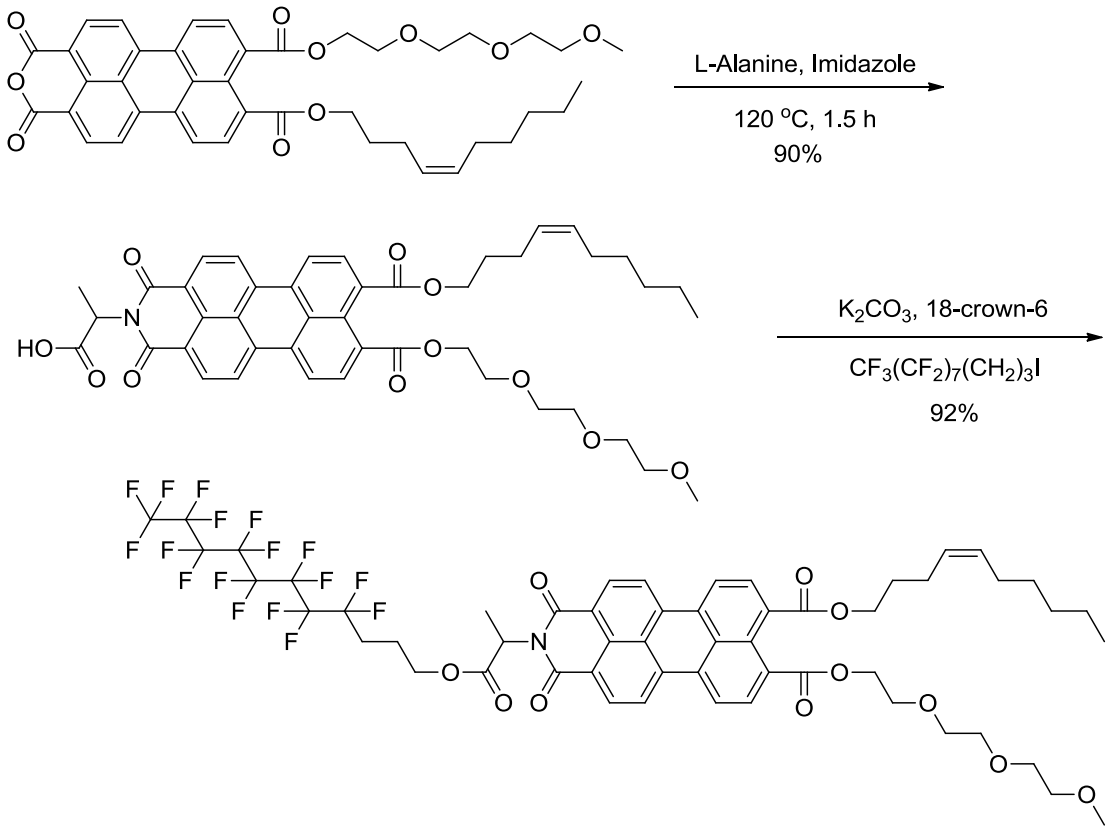

Scheme 3.7 Synthesis of asymmetric PEI X

The self-assembly of PEI X in its neat phase has been explored using DSC, PLM and XRD. As shown in **Figure 3.1**, the DSC traces revealed that PEI X only exhibits two phases in the studied temperature range.

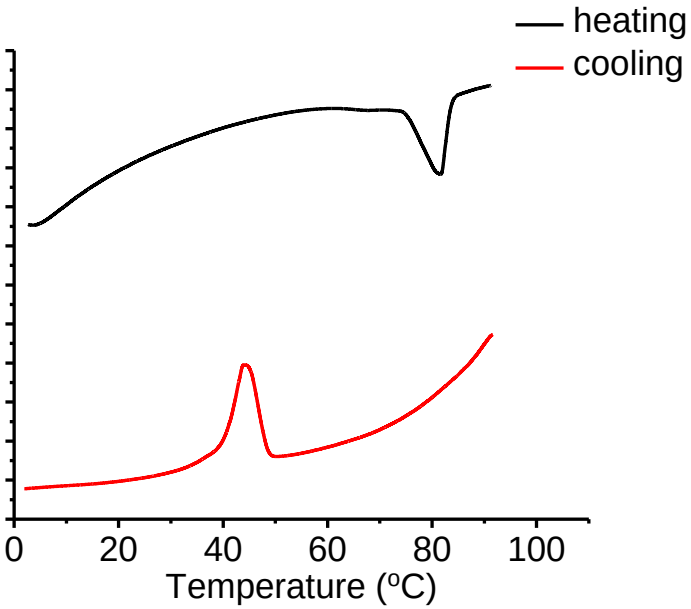

Figure 3.1 DSC result of PEI X

PLM observations confirmed that the endothermic peak at 82 °C during heating can be attributed to the isotropization process. At RT, PEI X is a red solid that can be deformed fairly easily by mechanical shearing, leading to a molecular oriented specimen, as indicated by PLM and XRD results. The 2D XRD pattern of a shear-aligned PEI X specimen at RT is depicted in Figure 3.2.

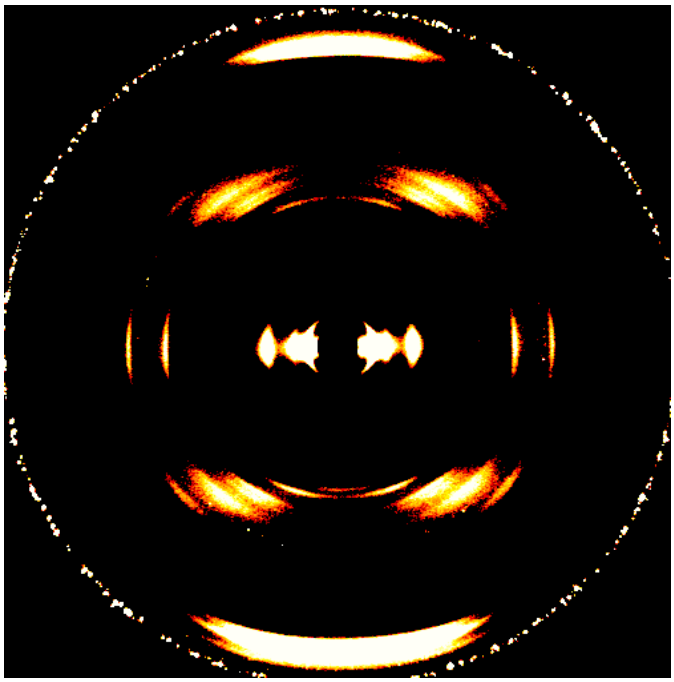

Figure 3.2 2D wide-angle XRD pattern of PEI X

The strongest diffraction on the meridian at q = 1.81 $Å^{-1}$ (d = 0.347 nm) confirms that rigid perylene cores are indeed phase-separated from flexible peripheral chains, forming tightly packed π-stacks. Crystallographically, this diffraction can be indexed as (002) diffraction. The equator diffractions originate from the 2D packing of perylene π-stacks (columns). They can be fitted into an oblique lattice with a = 4.468 nm, b= 6.343 nm, γ= 113.8 °. Since the (002) diffraction is on the meridian, a=b = 90 °. The presence of lines of (hk1) diffractions confirmed the existence of 3D long-range positional order instead of 1D or 2D order. Thus the RT phase of PEI X is a genuine crystalline phase with 3D long-range positional order instead of a liquid crystalline phase. The fact that (002) diffraction arises from π-stacking of perylene rings also implies that there are a periodicity of two stacked perylene cores along the stacking axis. The most probable packing mode is two crystallographically non-equivalent perylene molecules are cofacially stacked along the c-axis. Each perylene core rotates a certain angle with respect to its neighboring molecules in the same stack, around its plan normal.

An interesting finding is that in order to yield a reasonable calculated density, there must be three perylene π-stacks in each monoclinic unit cell (calculated density = 1.358 g/cm^3; experimental density = 1.36 g/cm^3). If no microphase segregation among incompatible flexible peripheral chains, there should be only one perylene π-stack in each unit cell (as shown in **Figure 3.3**). Thus the fact that there are three π-stacks in each unit cell suggests that microphase segregation is directing the

self-assembly of PEI X. As shown in **Figure 3.4**, each hexagon could be considered to consist of two face-to-face stacked PEI X molecules. Each color represents a type of peripheral chains in PEI X. For instance, red color represents the perfluorinated alkyl chain; green color represents the OEG chain and blue color is assigned to (*Z*)-4-decenyl chain. Due to the mutual incompatibility, in the process of self-assembly, three molecular components tended to associate with same kind of molecular components but avoid different ones, which leads to a multi-stack columnar crystalline structure. Since each PEI X molecule has three mutual-avoiding chains, a three-π-stack-per-unit cell model was proposed with an excellent agreement with the experimental diffraction and density results.

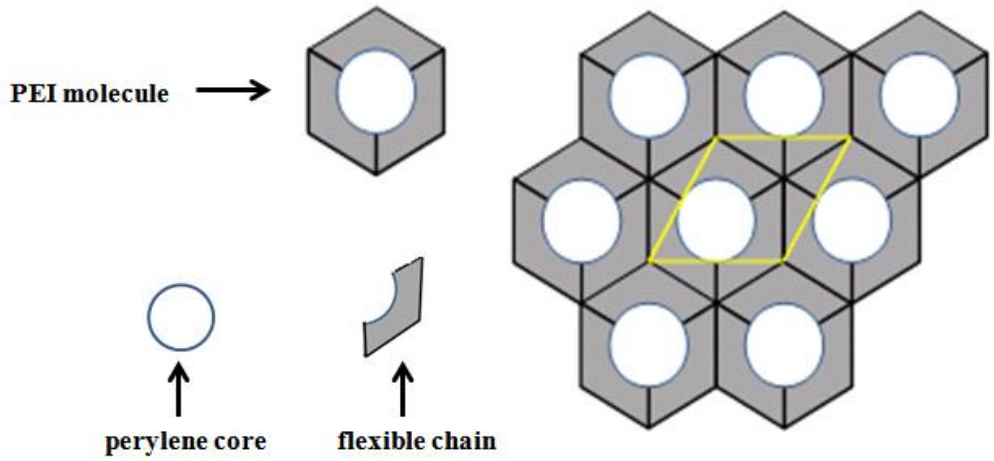

Figure 3.3 PEI X's single stack packing mode

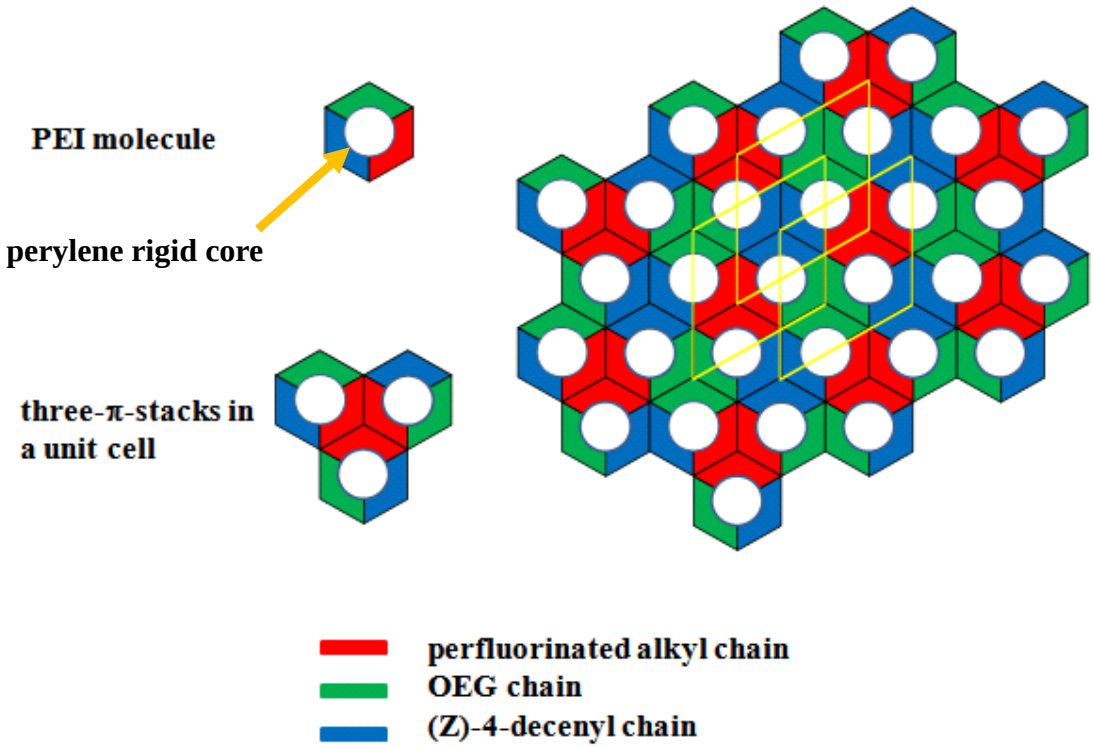

Figure 3.4 PEI X's multi-stack packing mode

In conclusion, we have designed a novel synthesis strategy and successfully synthesized a series of PEAs which contain labile functional groups. This intramolecular cyclization method can accommodate a wide range of functional groups and give a reasonable yield. Furthermore, some PEAs can serve as the versatile intermediate for the synthesis of novel unsymmetrically substituted PEIs. More importantly, due to their unique molecular structures, PEAs themselves can give valuable structure characteristics and phase behaviors. The structure details will be discussed thoroughly in Chapter 5.

3.3 Experimental section

Synthesis of halides, tosylates, PEAs and PEIs

2-decyltetradecyl 4-methylbenzenesulfonate (1)

A 50 mL round-bottomed flask was charged with 3.55 g (10 mmol) 2-decyltetradecan-1-ol, 2.52 g (25 mmol) triethylamine, 0.14 g (1.5 mmol) trimetylamine hydrochloride and 12 mL dichloromethane before being cooled to 0 °C in ice bath. Subsequently 2.86 g (15 mmol) 4-toluenesulfonyl chloride dissolved in 10 ml dichloromethane was added to the solution dropwise in 20 minutes. The solution was stirred for 2 hours at 0 °C. Then 4.9 g (50 mmol) phosphoric acid dissolved in 25 ml deionized water (pre-cooled to near 0 °C) was added to the mixture. The product was extracted using dichloromethane. Further purification was achieved by column chromatography over silica gel using 2/1 (v/v) hexane/chloroform as the eluent to afford **1** 4.82 g (95%) as a white solid.

methyl 3,5-bis(decyloxy)benzoate (2)

A 100 mL Schlenk flask was charged with 8.4 g (50 mmol) methyl 3, 5-dihydroxybenzoate, 10.35 g (75 mmol) potassium carbonate, 2.64 g (10 mmol) 18-crown-6, 24.3 g (110 mmol) 1-bromodecane and 45 ml dimethylformamide. The mixture was purged with argon for 15 minutes before being heated at 60 °C for 6 hours. Then the mixture was poured into 200 ml deionized water. The light yellow solid was collected by suction filtration and dried in vacuum at 75 °C. The crude product was purified by recrystallization using acetone to afford **2** 18.4 g (82%) as a white solid.

3,5-bis(decyloxy)benzoic acid (3)

A 50 mL Schlenk flask was charged 2.5 g (5.6 mmol) **2**, 3.12 g (56 mmol) potassium hydroxide, 3 ml deionized water, 6 ml isopropanol and 20ml

tetrahydrofuran. The solution was purged with nitrogen for 15 minutes and then refluxed at 80 °C for 6 hours. After evaporation of solvents, the light yellow solid was suspended in 50ml deionized water and acidified with hydrochloric acid until PH= 2. The product was extracted using chloroform to afford **3** 2.3 g (95%) as a light yellow solid.

4-bromobutyl-3,5-bis(decyloxy) benzoate (4)

A 50 mL round bottom flask was charged 1.7 g (3.9 mmol) **3**, 0.5 g (3.9 mmol) potassium carbonate, 0.1 g (0.4 mmol) 18- crown-6 and 10ml DMSO. The suspension was stirred at 60 °C for 20 minutes and became a clear yellow solution. Subsequently 6.8 g (8 eq) 1,4-dibromobutane was added. The solution was purged with nitrogen for 15 minutes, sealed well and stirred at 60 °C for 12 hours. Then the mixture was poured into 50 ml deionized water, the crude product was extracted using chloroform and purified by column chromatography with 2/1 (v/v) hexane/chloroform as the eluent to afford **4** 1.46 g (66%) as a colorless liquid.

3,5-bis(dexyloxy) phenyl methanol (5)

3 g **2** was dissolved in 15ml dry THF and cooled in ice bath. 1.2 equivalent lithium aluminum hydride was suspended in 15 ml dry THF and dropwise added to the benzoate-THF solution at 0 °C in 30 minutes. The mixture was stirred at room temperature for 3 hours. 3 ml water was carefully added to quench the reaction. The 3, 5-bis(dexyloxy) phenyl methanol (colorless liquid) was extracted by dichloromethane and dried by molecular sieve. The yield is 2.31 g (82%).

1-(chloromethyl)-3,5-bis(decyloxy) benzene (6)

2 g **5** and 3 equivalent tributylamine were dissolved in 5 ml dry THF, the mixture was cooled in ice bath for 10 minutes. Then 3 equivalent sulfonyl chloride dissolved in 2 ml dry THF was dropwise added to the solution. The mixture was stirred in ice bath for 2 hours and slowly warmed to room temperature and stirred for 8 more hours. Subsequently 15 ml water was added into the mixture and the crude product was extracted by dichloromethane and purified by column chromatography with 1/1 (v/v) hexane/chloroform as the eluent to afford **6** 1.88 g (90%) as a colorless liquid.

2-(2-methoxyethoxy)ethyl 4-methylbenzenesulfonate (7)

A 500 ml round bottom flask was charged 38.4 g (0.32 mol) 2-(2-methoxyethoxy) ethanol and 80 ml THF before being cooled to 0 °C in ice bath. The solution was mixed with 80 ml pre-cooled NaOH-water solution (5.8 mol/L) and stirred in ice bath for 20 minutes. Subsequently 80 ml TsCl-THF solution (3.75 mol/L) was dropped in the mixture for 2 hours. During dropping, the mixture's temperature was kept at 0~5 °C. The solution was stirred for an additional 2 hours at 0~5 °C, and then poured into 1 L ice water. The crude product was extracted with dichloromethane. Upon evaporation of solvent, the oily product was dried with anhydrous sodium sulfate to afford **7** 65.7 g (75%) as a colorless oily liquid.

2-(2-(2-methoxyethoxy)ethoxy)ethyl 4-methylbenzenesulfonate (8)

A 500 ml round bottom flask was charged 52.5 g (0.32 mol) 2-(2-(2-methoxyethoxy)ethoxy)ethanol and 80 ml THF before being cooled to 0 °C in ice bath. The solution was mixed with 80 ml pre-cooled NaOH-water solution (5.8

mol/L) and stirred in ice bath for 20 minutes. Subsequently 80ml TsCl-THF solution (3.75 mol/L) was dropped in the mixture for 2 hours. During dropping, the mixture's temperature was kept at 0~5 °C. The solution was stirred for an additional 2 hours at 0~5 °C, and then poured into 1 L ice water. The crude product was extracted with dichloromethane. Upon evaporation of solvent, the oily product was dried with anhydrous sodium sulfate to afford **8** 75.3 g (74%) as a colorless oily liquid.

(Z)-dec-4-en-1-yl 4-methylbenzenesulfonate (9)

A 50 ml round-bottomed flask was charged with 1.56 g (10 mmol) (Z)-dec-4-en-1-ol, 2.52 g (25 mmol) triethylamine, 0.14 g (1.5 mmol) trimetylamine hydrochloride and 12 mL dichloromethane before being cooled to 0 °C in ice bath. Subsequently 2.86 g (15 mmol) 4-toluenesulfonyl chloride dissolved in 10 ml dichloromethane was added to the solution dropwise in 20 minutes. The solution was stirred for 2 hours at 0 °C. Then 4.9 g (50 mmol) phosphoric acid dissolved in 25 ml deionized water (pre-cooled to near 0 °C) was added to the mixture. The product was extracted using dichloromethane. Further purification was achieved by column chromatography over silica gel using 2/1 (v/v) hexane/chloroform as the eluent to afford **9** 2.85 g (92%) as a colorless liquid.

perylene-3,4-anhydride-9,10-di-(2-decyltetradecyloxycarbonyl) (PEA-10/14)

A 25 ml round bottom flask was charged 350 mg (0.9 mmol) 3, 4, 9, 10-perylenetetracarobxyldianhydride, 1.68 g (3.6 mmol) tetrabutylammonium hydroxide (55% aqueous solution) and 5 ml DMSO. The mixture was stirred at 60 °C for 20 minutes. Subsequently 1.36 g (2.7 mmol) **1** dissolved in 4 ml acetone was

added to the mixture. The solution was purged with nitrogen for 10 minutes, sealed well and stirred at 50 °C for 72 hours. Then 0.2 g (3.6 mmol) acetic acid was added into the mixture. The solution was stirred for 4 hours at 60 °C and then poured in 100 ml methanol, the crude solid product was collected by suction filtration and purified by column chromatography with chloroform as the eluent to afford 242 mg product (25%) as a red solid.

^{1}H NMR ($CDCl_3$, 600 MHz): δ (ppm) = 8.62 (d, J= 7.98 Hz, 2H, Ar), 8.48 (t, 4H, Ar), 8.10 (d, J= 7.98 Hz, 2H, Ar), 4.26 (d, J= 6 Hz, 4H, -OC**H$_2$**CH), 1.83 (m, 2H, C**H**), 1.46 – 1.19 (m, 80 H, C**H$_2$**), 0.85 (m, 12 H, C**H$_3$**). ^{13}C NMR ($CDCl_3$, 75 MHz): δ (ppm) = 168.1 (ester C=O), 167.9 (ester C=O) 160.2 (anhydride C=O), 137.1 (Ar), 133.45 (Ar), 132.71 (Ar), 131.72 (Ar), 131.3 (Ar), 130.32 (Ar), 129.08 (Ar), 126.15 (Ar), 123.35 (Ar), 121.96 (Ar), 117.88 (Ar), 68.7 (O**C**H$_2$), 61.8 (O**C**H$_2$), 37.31 (**C**H), 31.93 (**C**H$_2$), 31.30 (**C**H$_2$), 29.98 (**C**H$_2$), 29.64 (**C**H$_2$), 29.62 (**C**H$_2$), 29.31 (**C**H$_2$), 26.69 (**C**H$_2$), 22.70 (**C**H$_2$), 14.13 (**C**H$_3$). HRMS $(M+e)^-$: calcd for $C_{72}H_{106}NO_7$ 1083.7967; found 1083.7886. (maldi) with benzopyrene as matrix.

perylene-3,4-anhydride-9,10-di-(4-((3,5-bis(decyloxy)benzoyl)oxy)butyloxycarbonyl) (PEA-4-BZ-D10)

A 25 ml round bottom flask was charged 160 mg (0.41 mmol) 3, 4, 9, 10-perylenetetracarobxyldianhydride, 0.77 g (1.64 mmol) tetrabutylammonium hydroxide (55% aqueous solution) and 3 ml DMSO. The mixture was stirred at 60 °C for 20 minutes. Subsequently 0.69 g (1.22 mmol) **4** dissolved in 2 ml acetone was added to the mixture. The solution was purged with nitrogen for 10 minutes, sealed

well and stirred at 50 °C for 24 hours. Then 0.1 g (1.6 mmol) acetic acid was added into the mixture. The solution was stirred for 4 hours at 60 °C and then poured in 100 ml methanol, the crude solid product was collected by suction filtration and purified by column chromatography with 2/1 (v/v) chloroform/hexane as the eluent to afford 146 mg product (26%) as a red solid.

^{1}H NMR ($CDCl_3$, 600 MHz): δ (ppm) = 8.62 (d, J = 8.04 Hz, 2H, Ar), 8.46 (d, J = 8.12 Hz, 2H, Ar), 8.49 (d, J = 7.986 Hz, 2H, Ar), 8.09 (d, J = 7.96 Hz, 2H, Ar), 7.12 (d, J = 2.51 Hz, 4H, Ar), 6.60 (t, J = 4.64 Hz ,2H, Ar**)**, 4.42 (t, J = 11.56 Hz, 4H, $CO_2C\mathbf{H_2}$), 4.38 (t, J = 11.18 Hz, 4H, $C\mathbf{H_2}$ CO_2), 3.73 (t, J= 12.85Hz, 4H, $OC\mathbf{H_2}CH_2$), 0.87 (t, J = 14.12 Hz, 6H, $C\mathbf{H_3}$), ^{13}C NMR ($CDCl_3$, 75 MHz): δ (ppm) = 168.8 (ester C=O), 166.456 (ester C=O), 160.14 (anhydride C=O), 134.6 (Ar), 132.1 (Ar), 131.166 (Ar), 130.3 (Ar), 129.6 (Ar), 129.2 (Ar), 128.7 (Ar), 127.6 (Ar), 126.5 (Ar), 122.1 (Ar), 119.87 (Ar), 107.655 (Ar), 105.566 (Ar), 77.069 ($O\mathbf{C}H_2CH_2$), 68.285 ($O\mathbf{C}H_2CH_2$), 64.603 ($O\mathbf{C}H_2CH_2$), 31.893($\mathbf{C}H_2$), 29.569 ($\mathbf{C}H_2$), 29.558 ($\mathbf{C}H_2$), 29.387 ($\mathbf{C}H_2$), 29.197 ($\mathbf{C}H_2$), 26.018 ($\mathbf{C}H_2$), 25.571 ($\mathbf{C}H_2$), 25.460 ($\mathbf{C}H_2$), 22.678 ($\mathbf{C}H_2$), 14.118 ($\mathbf{C}H_3$). HRMS $(M+Na)^+$: calcd for $C_{84}H_{116}O_{12}$ 1316.8467; found 1316.8468.

perylene-3,4-anhydride-9,10-di-(2-(2-methoxyethoxy)ethyloxycarbonyl) (PEA-2EG)

A 25 ml round bottom flask was charged 393 mg (1 mmol) 3, 4, 9, 10-perylenetetracarobxyldianhydride, 1.89 g (4mmol) tetrabutylammonium hydroxide (55% aqueous solution) and 6 ml DMSO. The mixture was stirred at 60 °C for 20

minutes. Subsequently 0.822 g (3 mmol) **7** was added to the mixture. The solution was purged with nitrogen for 10 minutes, sealed well and stirred at 60 °C for 36 hours. Then 0.2 g (3.6 mmol) acetic acid was added into the mixture. The solution was stirred for 4 hours at 60 °C and then poured in 100 ml saturated potassium chloride aqueous solution, the crude solid product was collected by suction filtration and purified by column chromatography with 20/1 (v/v) chloroform/methanol as the eluent to afford 160 mg product (26%) as a red solid.

^{1}H NMR ($CDCl_3$, 600 MHz): δ (ppm) = 8.61 (d, J = 7.86 Hz, 2H, Ar), 8.46 (d, J = 8.77 Hz, 2H, Ar), 8.42 (d, J = 8.45 Hz, 2H, Ar), 8.13 (d, J = 7.81 Hz, 2H, Ar), 4.54 (t, J = 9.66 Hz, 4H, COOC**H$_2$**), 3.89 (t, J = 9.91 Hz ,4H, $COOCH_2CH_2O$**)**, 3.72 (m, J = 9.308 Hz, 4H, OC**H$_2$**), 3.56 (m, J = 9.32 Hz, 4H, C**H$_2$**O) ^{13}C NMR ($CDCl_3$, 75 MHz): δ (ppm) = 168.211 (ester C=O), 160.138 (anhydride C=O), 132.459 (Ar), 130.466 (Ar), 129.875 (Ar), 122.46 (Ar), 121.058 (Ar), 116.777 (Ar), 77.255 (OCH_2CH_2), 71.9 (OCH_2CH_2), 68.97 (OCH_2CH_2), 64.484(OCH_2CH_2), 59.007 (OCH_3). HRMS $(M+Na)^+$: calcd for $C_{34}H_{30}O_{11}$ 614.1788; found 614.1787.

perylene-3,4-anhydride-9,10-di-(2-(2-(2-methoxyethoxy)ethoxy)ethyloxycarbonyl) (PEA-3EG)

A 25 ml round bottom flask was charged 393 mg (1 mmol) 3, 4, 9, 10-perylenetetracarobxyldianhydride, 1.89 g (4mmol) tetrabutylammonium hydroxide (55% aqueous solution) and 6 ml DMSO. The mixture was stirred at 60 °C for 20 minutes. Subsequently 0.955 g (3 mmol) **8** was added to the mixture. The solution was purged with nitrogen for 10 minutes, sealed well and stirred at 60 °C for 72 hours.

Then 0.2 g (3.6 mmol) acetic acid was added into the mixture. The solution was stirred for 4 hours at 60 °C and then poured in 100 ml saturated potassium chloride aqueous solution, the crude solid product was collected by suction filtration and purified by column chromatography with 25/1 (v/v) chloroform/methanol as the eluent to afford 147 mg product (21%) as a red solid.

^{1}H NMR ($CDCl_3$, 600 MHz): δ (ppm) = 8.62 (d, J = 7.84 Hz, 2H, Ar), 8.45 (d, J = 8.82 Hz, 2H, Ar), 8.39 (d, J = 8.61 Hz, 2H, Ar), 8.11 (d, J = 7.96 Hz, 2H, Ar), 4.52 (t, J = 9.82 Hz, 4H, COOC**H$_2$**), 3.89 (t, J = 9.92 Hz ,4H, $COOCH_2C\mathbf{H_2}O$**)**, ^{13}C NMR ($CDCl_3$, 75 MHz): δ (ppm) = 168.011 (ester C=O), 160.122 (anhydride C=O), 135.456 (Ar), 133.016 (Ar), 131.875 (Ar), 123.46 (Ar), 121.007 (Ar), 117.72 (Ar), 77.249 ($O\mathbf{C}H_2CH_2$), 70.899 ($O\mathbf{C}H_2CH_2$), 70.562 ($O\mathbf{C}H_2CH_2$), 68.346($O\mathbf{C}H_2CH_2$), 64.671 ($O\mathbf{C}H_2CH_2$), 59.002 ($O\mathbf{C}H_3$). HRMS $(M+Na)^+$: calcd for $C_{38}H_{38}O_{13}$ 702.2312; found 702.2313.

perylene-3,4-anhydride-9,10-di-(3,5-bis(decyloxy)benzyloxycarbonyl) (PEA-BZ-D10)

A 25 ml round bottom flask was charged 320 mg (0.81 mmol) 3, 4, 9, 10-perylenetetracarobxyldianhydride, 1.54 g (3.24 mmol) tetrabutylammonium hydroxide (55% aqueous solution) and 5 ml DMSO. The mixture was stirred at 60 °C for 20 minutes. Subsequently 1.07 g (2.43 mmol) **6** dissolved in 4ml acetone was added to the mixture. The solution was purged with nitrogen for 10 minutes, sealed well and stirred at 50 °C for 24 hours. Then 0.19 g (3.24 mmol) acetic acid was added into the mixture. The solution was stirred for 4 hours at 60 °C and then poured in 100

ml methanol, the crude solid product was collected by suction filtration and purified by column chromatography with chloroform as the eluent to afford 206 mg product (21%) as a red solid.

^{1}H NMR ($CDCl_3$, 600 MHz): δ (ppm) = 8.58 (d, J = 7.998 Hz, 2H, Ar), 8.43 (d, J = 8.27 Hz, 2H, Ar), 8.40 (d, J = 7.863 Hz, 2H, Ar), 8.12 (d, J = 7.9 Hz, 2H, Ar), 6.59 (d, J = 2.164 Hz, 4H, Ar), 6.419 (t, J = 4.568 Hz ,2H, Ar**)**, 3.921 (t, J= 13.088Hz, 4H, OC**H$_2$**CH_2), 0.869 (t, J = 14.156 Hz, 6H, C**H$_3$**), ^{13}C NMR ($CDCl_3$, 75 MHz): δ (ppm) = 167.6 (ester C=O), 160.491 (anhydride C=O), 137.312 (Ar), 136.8 (Ar), 133.6 (Ar), 132.2 (Ar), 131.7 (Ar), 130.6 (Ar), 129.2 (Ar), 126 (Ar), 123.4 (Ar), 122.1 (Ar), 117.9 (Ar), 68.11 (COO**C**H_2), 31.89(**C**H_2), 29.599 (**C**H_2), 29.576 (**C**H_2), 29.431 (**C**H_2), 29.272 (**C**H_2), 26.066 (**C**H_2), 22.671 (**C**H_2), 14.103 (**C**H_3). HRMS $(M+Na)^+$: calcd for $C_{78}H_{102}O_{11}$ 1214.7422; found 1214.7414.

perylene-3,4-anhydride-9,10-di-((*Z*)-dec-4-en-1-yloxycarbonyl) (PEA-di-(*Z*)-C10)

A 25 ml round bottom flask was charged 393 mg (1 mmol) 3, 4, 9, 10-perylenetetracarobxyldianhydride, 1.89 g (4mmol) tetrabutylammonium hydroxide (55% aqueous solution) and 6 ml DMSO. The mixture was stirred at 60 °C for 20 minutes. Subsequently 0.93 g (3 mmol) **9** was added to the mixture. The solution was purged with nitrogen for 10 minutes, sealed well and stirred at 60 °C for 72 hours. Then 0.2 g (3.6 mmol) acetic acid was added into the mixture. The solution was stirred for 4 hours at 60 °C and then poured in 100 ml methanol, the crude solid product was collected by suction filtration and purified by column chromatography with 200/1 (v/v) chloroform/methanol as the eluent to afford 154 mg product (45%)

as a red solid.

^{1}H NMR ($CDCl_3$, 600 MHz): δ (ppm) = 8.63 (d, J = 8.04 Hz, 2H, Ar), 8.51 (d, J = 8.21 Hz, 2H, Ar), 8.49 (d, J = 8.02 Hz, 2H, Ar), 8.13 (d, J = 7.84 Hz, 2H, Ar) 5.42 (m, J = 55.83 Hz, 4H, -C**H**=C**H**-), 4.35 (t, J = 55.83 Hz ,4H, $CO_2C\mathbf{H_2}$**)**, 2.21 (q, J = 22.02 Hz, 4H, CO_2CH_2 $CH_2C\mathbf{H_2}$), 2.01 (q, J = 21.28 Hz, 4H, CH=CH $C\mathbf{H_2}(CH_2)_3CH_3$), 0.87 (t, J = 15.24 Hz, 6H, $C\mathbf{H_3}$), ^{13}C NMR ($CDCl_3$, 75 MHz): δ (ppm) = 167.817 (ester C=O), 159.87 (anhydride C=O), 133.47 (Ar), 131.017 (Ar), 130.688 (-CH=**C**H-), 129.458 (Ar), 128.012 (-**C**H=CH-), 128.789 (Ar), 128.320 (Ar), 122.99 (Ar), 122.125 (Ar), 121.87 (Ar), 64.979 (OCH_2CH_2), 31.663(CH_2), 29.056 (CH_2), 28.398 (CH_2), 27.36 (CH_2), 26.839 (CH_2), 23.649 (CH_2), 22.689 (CH_2), 14.132 (CH_3). HRMS $(M+H)^+$: calcd for $C_{44}H_4NaO_7$ 686.3234; found 686.3244.

perylene-3,4-anhydride-9-((Z)-dec-4-en-1-yloxycarbonyl)-10-(2-(2-(2-methoxyethoxy)ethoxy)ethyloxycarbonyl) (PEA-(*Z*)-C10-3EG)

A 25 mL round bottom flask was charged 0.59 g (1.5 mmol) 3, 4, 9, 10-perylenetetracarobxyldianhydride, 1.64 g (10 mmol) triethylene glycol monomethylether, 0.5 g (3.3 mmol) DBU and 8 ml DMSO. The suspension was stirred at 60 °C for 24 hours and became a dark red solution. Subsequently 465 mg (1.5 mmol) **9** was added. The solution was purged with nitrogen for 15 minutes, sealed well and stirred at 60 °C for 24 hours. Then 0.36 g (6 mmol) acetic acid was added into the mixture. The solution was stirred for 4 hours at 60 °C and then poured in 150 ml saturated potassium chloride aqueous solution, the crude solid product was collected by suction filtration and purified by column chromatography with 25/1 (v/v)

chloroform/acetone as the eluent to afford 208 mg product (20%) as a red solid.

^{1}H NMR ($CDCl_3$, 600 MHz): δ (ppm) = 8.66 (d, J = 8.16 Hz, 2H, Ar), 8.53 (d, J = 10.6 Hz, 1H, Ar), 8.50 (d, J = 11.96 Hz, 1H, Ar), 8.19 (d, J = 7.88 Hz, 2H, Ar), 8.14 (d, J = 7.88 Hz, 2H, Ar), 5.43 (m, J = 50.86 Hz, 2H, -C**H**=C**H**-),4.50 (t, J = 9.89 Hz, 2H, COOC**H$_2$**), 4.34 (t, J = 9.66 Hz, 2H, COOC**H$_2$**), 3.88 (t, J = 9.87 Hz ,2H, $COOCH_2C$**H$_2$**O**)**, 4.35 (t, J = 13.76 Hz ,2H, CO_2C**H$_2$)**, 2.21 (m, J = 23.41 Hz, 2H, CO_2CH_2 CH_2C**H$_2$**), 0.868 (t, J = 15.84 Hz, 3H, CHC**H$_3$**) ^{13}C NMR ($CDCl_3$, 75 MHz): δ (ppm) = 167.947.4 (ester C=O), 160.157 (anhydride C=O), 136.833 (Ar), 133.415 (Ar), 131.355 (Ar), 130.521 (-CH=**C**H-), 130.284 (Ar), 127.982 (-**C**H=CH-),123.248 (Ar), 121.967 (Ar), 117.863 (Ar), 77.221 (O**C**H_2CH_2), 70.646 (O**C**H_2CH_2), 70.565 (O**C**H_2CH_2), 68.913 (O**C**H_2CH_2), 65.44 (O**C**H_2CH_2), 59.029 (O**C**H_3), 31.541(**C**H_2), 29.335 (**C**H_2), 28.587 (**C**H_2), 27.23 (**C**H_2), 23.645 (**C**H_2), 22.559 (**C**H_2), 14.08 (**C**H_3). HRMS $(M+Na)^+$: calcd for $C_{41}H_{42}O_{10}$ 694.2778; found 694.2776.

***N*-(2-propanoicacid)-perylene-3,4-dicarboximide-9-((Z)-dec-4-en-1-yloxycarbonyl)-10-(2-(2-(2-methoxyethoxy)ethoxy)ethyloxycarbonyl)**

A 10 ml Schlenk flask was charged with 50 mg (0.075 mmol) **PEA-(*Z*)-C10-3EG**, 8 mg (0.09 mmol) L-Analine and 1g imidazole. The mixture was purged with argon for 15 minutes before being heated to 125 °C for 2 hours. The reaction was monitored by TLC. After 2 hours the mixture was cooled to 90 °C and then transferred into 20 ml saturated sodium sulfate aqueous solution. The red solution was acidified using phosphoric acid until PH=3. The red solid was collected

by suction filtration and dried in a vacuum at 75 °C. 40 mg (70%) product was obtained.

***N*-3-(perfluorooctyl)-propyl-(-2-propanoate)-perylene-3,4-dicarboximide-9-((Z)-dec-4-en-1-yloxycarbonyl)-10-(2-(2-(2-methoxyethoxy)ethoxy)ethyloxycarbonyl)**

A 25 ml round bottom flask was charged 23.3 mg (0.03 mmol) **N-(2-propanoicacid)-perylene-3,4-dicarboximide-9-((Z)-dec-4-en-1-yloxycarbonyl)-10-(2-(2-(2-methoxyethoxy)ethoxy)ethyloxycarbonyl)**, 3.9 mg (0.027 mmol) potassium carbonate, 3 mg (0.007 mmol) 18-crown-6 and 2 ml DMSO. The suspension was stirred at 60 °C for 20 minutes and became a clear red solution. Subsequently 29 mg (0.05 mmol) 3-(perfluorooctyl)-propyl iodide was added. The solution was purged with nitrogen for 15 minutes, sealed well and stirred at 60 °C for 1 hour. Then the mixture was poured into 50 ml saturated sodium sulfate aqueous solution, the crude product precipitated out and was collected using suction filtration and purified by column chromatography with 50/1 (v/v) chloroform/acetone as the eluent to afford 34 mg product (92%) as a dark red solid.

^{1}H NMR ($CDCl_3$, 600 MHz): δ (ppm) = 8.59 (d, J = 7.92 Hz, 2H, Ar), 8.46 (m, J = 18.96 Hz, 2H, Ar), 8.15 (d, J = 7.88 Hz, 2H, Ar), 8.11 (d, J = 7.88 Hz, 2H, Ar), 5.79 (m, J= 21.46, 1H, N-C**H**-CH_3), 5.44 (m, J = 51.83 Hz, 2H, -C**H**=C**H**-),4.39 (t, J = 9.82 Hz, 2H, COOC**H_2**), 3.88 (t, J = 9.87 Hz ,2H, $COOCH_2C$**H_2**O**)**, 4.35 (t, J = 13.76 Hz ,2H, CO_2C**H_2)**, 2.22 (q, J = 22.91 Hz, 2H, CO_2CH_2 CH_2C**H_2**), 0.858 (t, J = 16.24 Hz, 3H, CHC**H_3**) ^{13}C NMR ($CDCl_3$, 75 MHz): δ (ppm) = 170.95 (ester C=O), 168.1 (ester C=O), 162.842 (anhydride C=O), 135.736 (Ar), 131.898 (Ar), 131.656 (Ar),

131.321 (-CH=**C**H-), 127.989 (-**C**H=CH-),125.8 (Ar), 122.8 (**C**F_2), 121.537 (**C**F_2), 77.219 (O**C**H_2CH_2), 71.9 (O**C**H_2CH_2), 70.646 (O**C**H_2CH_2), 68.932(O**C**H_2CH_2), 65.299 (O**C**H_2CH_2), 58.995 (O**C**H_3), 58.977 (N**C**HCH_3), 64.667 (O**C**H_2CH_2), 31.521(**C**H_2), 29.324 (**C**H_2), 28.598 (**C**H_2), 27.208 (**C**H_2), 23.638 (**C**H_2), 22.533 (**C**H_2), 14.746 (**C**H_3). HRMS $(M+Na)^+$: calcd for $C_{55}H_{52}F_{17}NO_{11}$ 1225.3269; found 1225.3271.

CHAPTER 4. *TERT*-BUTYL SUBSTITUTED PERYLENE MONOHANHYDRIDE DIESTER: A PROMISING INTERMEDIATE FOR SYNTHESIS OF ASYMMETRICALLY SUBSTITUTED PERYLENE DIIMIDES

1.1 Introduction

Among the perylene carboxylic derivatives, PDI is most intensively investigated compound because of its unique characteristics. It has been widely used in photovoltaic devices [1], light-emitting diodes [2] and field-effect transistors. [3]Specifically, PDIs can serve as good candidates for *n*-type semiconductors because (1) they have relatively large electron affinities, which makes them powerful electron acceptors; (2) PDIs can assemble in π-stacks in the solid state which effectively enhances the intermolecular π-orbital overlap and facilitates charge transport; and (3) the π-π interactions can be tuned by changing the substituents on the imide nitrogen atoms, offering the opportunity to optimize charge carrier mobility by systematic structural variations.

Inspired by PDI's promising application potential and unique characteristics, intensive research effort has been attracted to PDI's molecule design and synthesis strategy. The synthesis of symmetrically substituted PDIs can usually be straightforwardly achieved via the direct condensation reaction between PDA and an appropriate primary amine. The reactions media can be water [4], benzene [5], quinoline [6, 7], or molten imidazole [8, 9], the most popular solvent for this type of reactions. Most of such reactions are of high yield. However, the synthesis of

unsymmetrically substituted PDIs is a challenge. A stepwise condensation of PDA with two different primary amines cannot afford unsymmetrically substituted PDI. This is because when one side of PDA is substituted and converted to imide group, the intermediate—perylene monoanhydride monoimide is generated. This intermediate's solubility is generally much higher than PDA. Once generated, the intermediate will immediately continue to react with amines and convert to PDI. In other words, the reaction of an excess amount of PDA with a primary amine will not produce one side substituted perylene monoimide monoanhydride as one might expected, instead the amine is completely converted to symmetrically substituted PDI and the excess of PDA remains unreacted. [10] In 1983, a synthesis route (shown in **Scheme 4.1**) was discovered by Troster. [11] First, the insoluble PDA was converted to the soluble tetra potassium salt in aqueous solution by adding a sufficient amount of potassium hydroxide. Second, the monoanhydride monopotassium salt was precipitated by a moderate acidification with an appropriate amount of acid (phosphoric acid, hydrochloride acid and acetic acid have been used) at 90 ~ 100 °C as this monopotassium salt is insoluble in any solvent even at high temperatures. Third, the monopotassium can be condensed with a primary amine offering perylene monoanhydride monoimides which can be subjected to the condensation with a different amine, resulting an unsymmetrical PDI. However, this procedure usually requires the first primary amine to be water soluble, which significantly limits the scope of the procedure.

An alternative synthesis method was reported by our group in 2009. [12] Using

PEA as the intermediate, the unsymmetrically substituted PDIs can be synthesized in three steps in high yield. Furthermore, the intermediate can even be used to prepare unsymmetrically substituted PTEs.

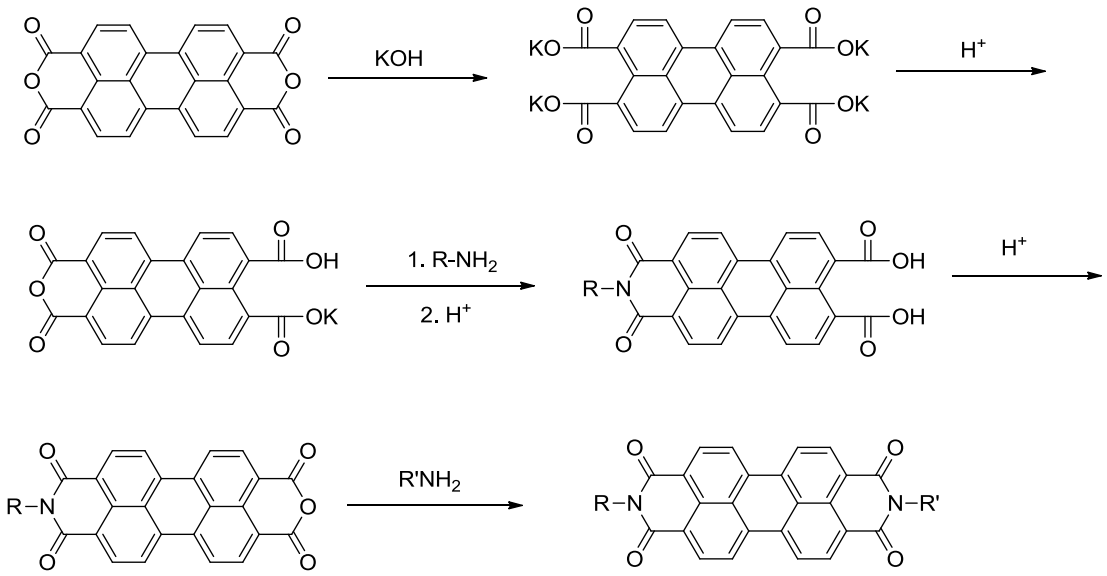

Scheme 4.1 Synthesis of unsymmetric PDI using Troster's method

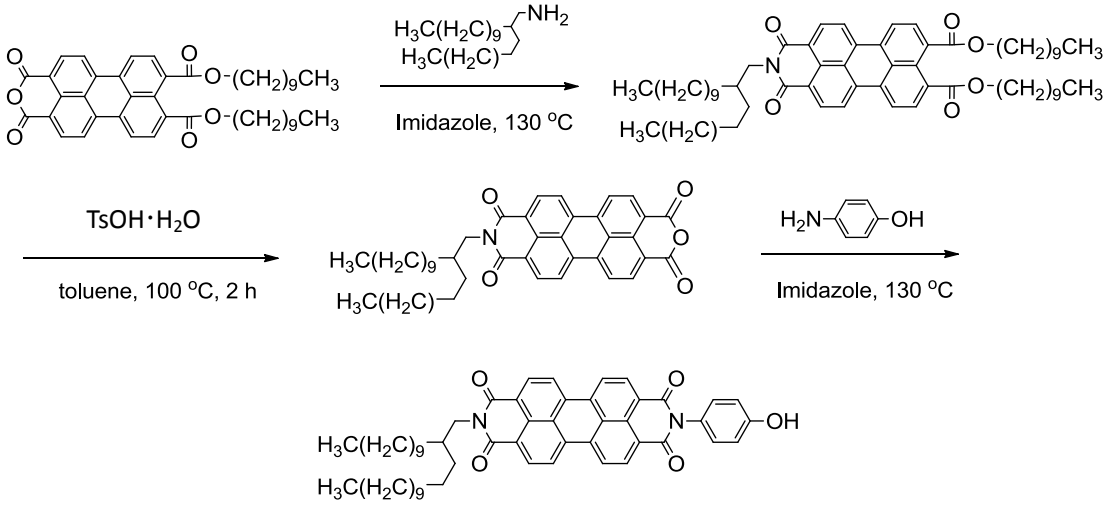

Scheme 4.2 Synthesis of unsymmetric PDI using PEA-diC10 as the intermediate

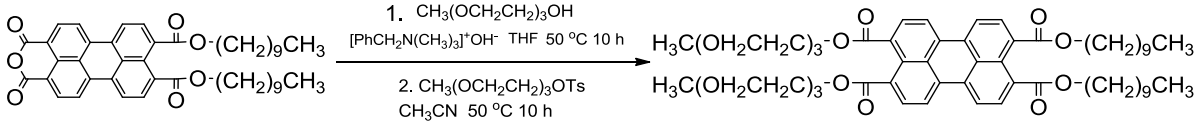

Scheme 4.3 Synthesis of unsymmetric PTE using PEA-diC10 as the intermediate

However, it is very challenging to prepare PDIs containing acid-sensitive

groups (such as esters, ether, etc.) via this method because the acid sensitive groups may not survive the strongly acidic cyclization process. Here we report the synthesis of a new PEA which can be employed as the intermediate to unsymmetrically substituted PDIs. The key feature here is that a much milder cyclization process will be involved so that the procedure will be compatible with labile functional groups. Since the condensation between an anhydride and a primary amine is usually of high yield, the key step in the synthesis of unsymmetrically substituted PDI from a PEA is the cyclization of the PEI (step 2 in **Scheme 4.2**), which converts the diester functionality to an anhydride group and readies the perylene derivative for the next condensation. The relatively drastic (strongly acidic, wet and high temperature) cyclization condition in **Scheme 4.2** which is necessary for the intended transformation to complete in a timely manner, is the major factor that limits its wide application to PDIs with labile functional groups. To broaden the range of applications of PEAs in the synthesis of unsymmetrically substituted PDIs, a milder reaction condition is desired for the generation of the needed anhydride group while keeping all functional groups at the other side of the perylene ring intact. It is well known that *tert*-butyl esters can be cleaved under a mild acidic condition that many labile functional groups can be preserved, which makes *tert*-butylation a widely-used procedure to protect a carboxylic group. Therefore a PEA carrying two *tert*-butyl groups at the ester side (perylene-3,4-anhydride-9,10-di-*tert*-butyloxycarbonyl) would be an excellent intermediate toward unsymmetrically substituted PDIs. However, the synthesis of such a compound has never been reported. In theory, such a compound

may be prepared by a partial cleavage/cyclization of tetra-*tert*-butyl perylene-3, 4, 9, 10-tetracarboxylate. The problem is, even the synthesis of this PTE has never been reported. We attempted to prepare the tetra-(*tert*-butyl) PTE by reacting *tert*-butyl bromide with tetra-butyl ammonium perylene tetracarboxylate. However, the desired tetraester was not detected.

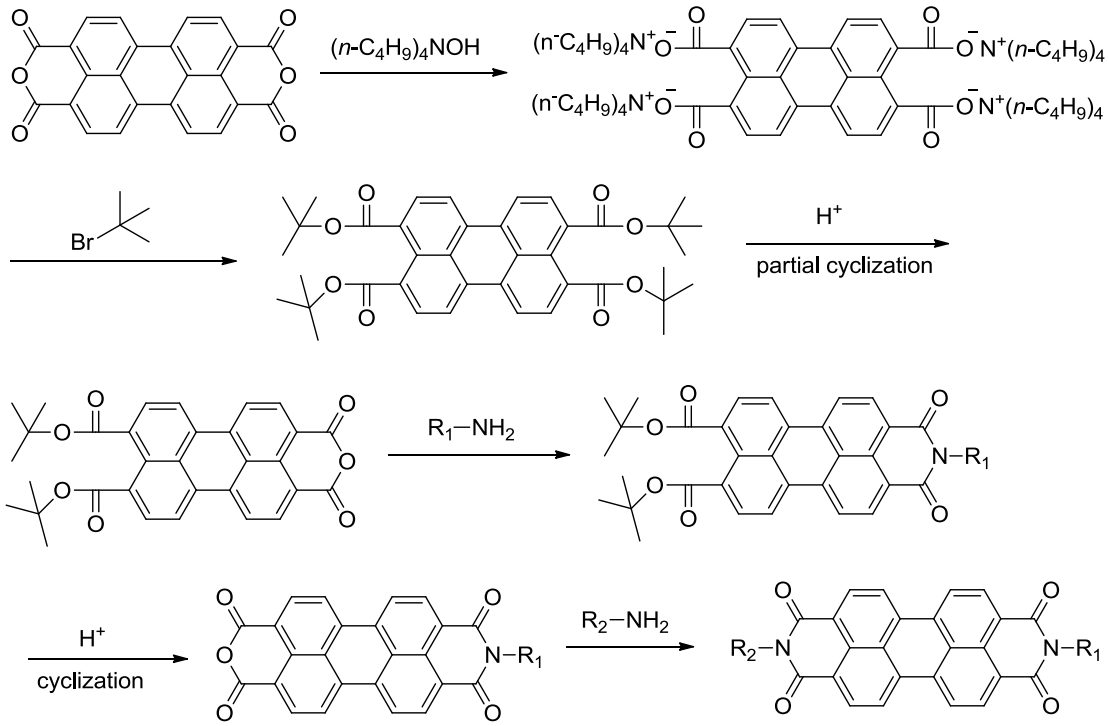

Scheme 4.4 Hypothetic unsymmetric PDI synthesis routine using di-*tert*-buytl-PEA as the intermediate

Fortunately, a mild anhydride-forming cyclization does not require having two *tert*-butyl groups at the ester side of the perylene ring. The results from the previous chapter has shown that once one of the two ester groups at one side of a perylene ring is cleaved, the intra-molecular cyclization of the monoester monocarboxylic acid into the anhydride group occurs rapidly. In other words, only one *tert*-butyl group is needed at the ester side of a perylene ring to enable a mild route toward

unsymmetrically substituted PDIs. For instance, the conversion of a PEI with a structure shown in **Scheme 4.5** to the corresponding monoimide monoanhydride is expected to occur at a much milder condition than step 2 in **Scheme 4.2**. This is because the *tert*-butyl group can be cleaved under a mild condition, resulting in the intermediate X with an *n*-alkyl ester and a carboxylic acid at the same side of the perylene ring. Under even a weakly acidic environment, intermediate X readily turns into the desired monoimide monoanhydride via an intramolecular reaction. Most importantly, the corresponding *tert*-butyl_PEAs, as shown in **Scheme 4.5**, appear to be synthetically accessible.

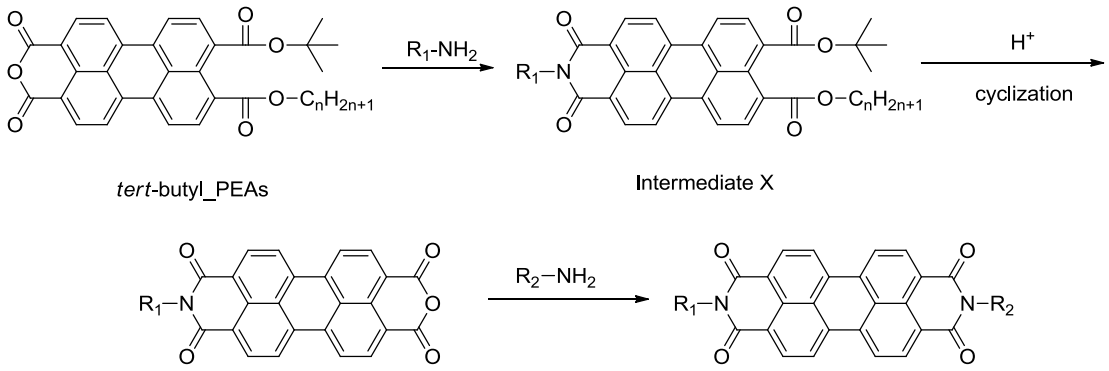

Scheme 4.5 Unsymmetric PDI synthesis routine using *tert*-buytl-PEA as the intermediate

4.2 Results and discussion

4.2.1 Synthesis of *tert*-butyl_PEAs

A logical approach toward *tert*-butyl_PEA is to partially cyclize the corresponding tetraester, PTE X. A facile procedure to prepare a PTE X would be the installation of the *tert*-butyl group first by nucleophilic attack to an anhydride carbonyl group, followed by a S_N2 reaction with an appropriate primary alkyl bromide.

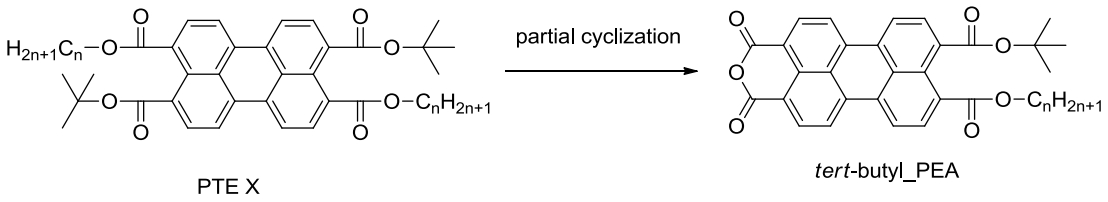

Scheme 4.6 Partial cyclization of PTE X

Our first attempt toward PTE is outlined in **Scheme 4.7**. In the first step *tert*-butanol was allowed to react with PDA in the presence of DBU, a strong organic base. The product would be a perylene diester dicarboxylate which can be alkylated by a primary alkyl bromide to afford the desired PTE in the second step. However, while many primary alcohols work well as a nucleophile to open the anhydride ring in the presence of a base such as DBU [13], our experimental results showed that the nucleophilicity of *tert*-butanol is too low, probably due to the large steric hindrance. Even after 10 days at 60 °C, the solution phase remained nearly colorless (indicating the formation of little perylene diester dicarboxylate) and nearly all PDA remain unreacted as a red solid.

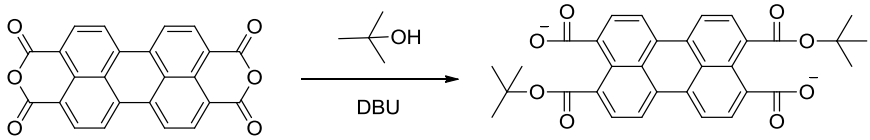

Scheme 4.7 Unsuccessful nucleophilic reaction using *tert*-butanol

To solve the low nucleophilicity problem, *tert*-butoxide was then used as the nucleophile. With much enhanced nucleophilicity, the nucleophilic cleavage of the anhydride ring as shown in Scheme 4.8 proceeded readily. With the progress of the reaction, PDA, a red solid, gradually dissolved in the reaction mixture, giving a dark red solution, signaling the formation of perylene diester dicarboxylate. Upon the completion of the first step, an appropriate *n*-alkyl bromide is added to the reaction

mixture to alkylate the perylene diester dicarboxylate. To our surprise, the addition of an *n*-alkyl bromide directly produced the target PEA instead of the predicted PTE, even with a large excess of *n*-alkyl bromide. While the mechanism by which the PEA forms directly is not complete clear to us, we speculate that it may involve the simultaneous (or tandem) S_N2 and E2 reactions between a perylene diester dicarboxylate and *n*-alkyl bromide molecules. This speculation is supported by the observation that PDA is nearly the sole side product in the reactions. To form PDA, the perylene diester dicarboxylate intermediate must be protonated and the β-hydrogen atoms are only sensible sources of protons in the reaction system. Although elimination products have been rarely observed with a carboxylate nucleophile due to its low basicity, the large steric hindrance of the *tert*-butyl ester group may reduce the nucleophilicity of the carboxylate at the same side of the perylene ring to a degree that the rate of elimination (by E2 mechanism) of the *n*-alkyl halide is fully comparable to the substitution reaction (by S_N2). The reaction yields are listed in **Table 4.1**.

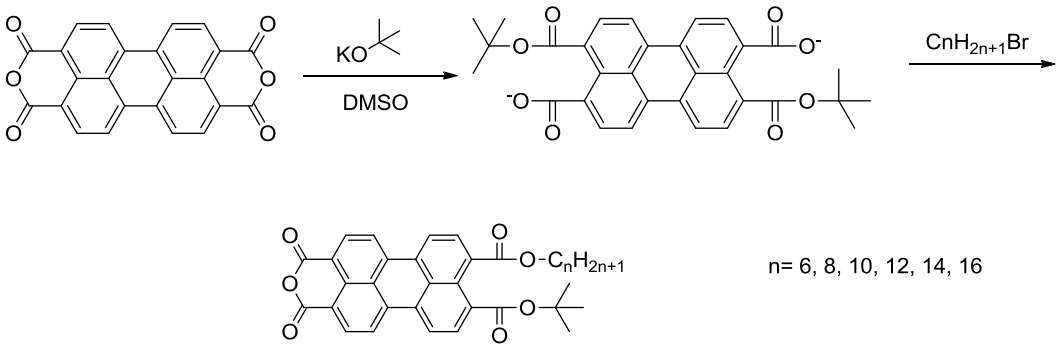

Scheme 4.8 Synthesis of *tert*-butyl-based PEAs

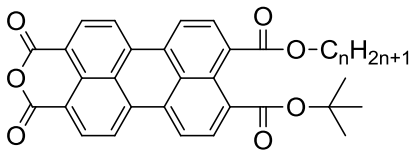

n	6	8	10	12	14	16
Yield	43%	40%	31%	20%	12%	9%

Table 4.1 Summary of reaction yields of Cn-*tert*-butyl PEAs

One of these PEAs has been chosen to test its potential as a starting material toward unsymmetrically substituted PDIs. Two factors were considered when such a choice was made. First, the preparation of such a PEA should be of a reasonable yield. On this regard, as shown in **Table 4.1**, C6-*tert*-butyl-PEA and C8-*tert*-butyl-PEA stand out. Second, the PEA should have good processability. The C6-*tert*-butyl-PEA's solubility at room temperature in chloroform is less than 3 mg/ml. While the C8-*tert*-butyl-PEA's solubility can reach 10 mg/ml. Based on these considerations, we choose C8-*tert*-butyl-PEA as the starting material to carry out further reactions.

4.2.2 Cyclization of C8_*tert*-butyl_PEA

Although it is well-known that *tert*-butyl ester group can be cleaved under a mild condition, it is still valuable for us to identify the mildest condition such a cleavage can complete when the PEA is used in the synthesis of a unsymmetrically substituted PDI. The milder condition the *tert*-butyl ester cleavage is, the more labile functional groups can be accommodated in the perylene derivative. It is expected that the reactivity of the *tert*-butyl group in C8-*tert*-butyl_PEA is similar to that of PEA in **Scheme 4.4**, we directly tested the cyclization conditions of C8-*tert*-butyl_PEA. The results are summarized in **Table 4.2**.

Acid	Solvent	Temperature (°C)	Reaction Time	Result
benzoic acid	toluene	100	4 hours	negative
2-chlorobenzoic acid	toluene	100	4 hours	negative
2-chlorobenzoic acid	1,2-dichlorobenzene	100	4 hours	negative
phosphoric acid	1,2-dichlorobenzene	100	4 hours	negative
Trifluoro-acetic acid	dichloromethane	25	2 hours	negative
sulfuric acid	Chloroform (aliquat 336 as the catalyst)	25	2 hours	positive
Phosphoric acid	Toluene (phosphoric acid-(2-ethyhexyl)-ester) as the catalyst	25	5 hours	positive
Sodium bisulfate	Chloroform (aliquat as the catalyst)	25	2 hours	positive

Table 4.2 Reaction condition tests for C8-*tert*-butyl-PEA cyclization

As shown in the table, due to the labile *tert*-butyl group, C8-*tert*-butyl-PEA indeed can be cyclized under a much milder condition than what is needed to cyclize an *n*-alkyl perylene tetraester. A much weaker acid (sodium bisulfate or phosphoric acid-(2-ethylhexyl)-ester, in a sharp contrast with $TsOH \cdot H_2O$) and lower temperature

(RT versus ~100 °C) would allow the survival of many more labile functional groups.

4.2.3. Test run of C8-*tert*-butyl-PEA as starting material for the synthesis of unsymmetrically substituted PDIs

To test the power of C8-*tert*-butyl-PEA as a starting material for the synthesis of unsymmetrically substituted PDIs, we have chosen the ester-containing amine **1** to condense with C8-*tert*-butyl-PEA. Amine **1** not only possesses a labile ester group, but also features a weak nucleophilicity due to the fact that the NH_2 group connects to a very long and branched secondary alkyl-based group. Our previous studies on this compound have indicated that in order for **1** to condense with PDA at a reasonable rate, the reaction temperature must be above 150 °C. In a sharp contrast, due to the much improved processability of C8-*tert*-butyl-PEA in the comparison with PDA, its condensation with **1** can proceed to completion at 135 °C in about 4 hours, as monitored by TLC.

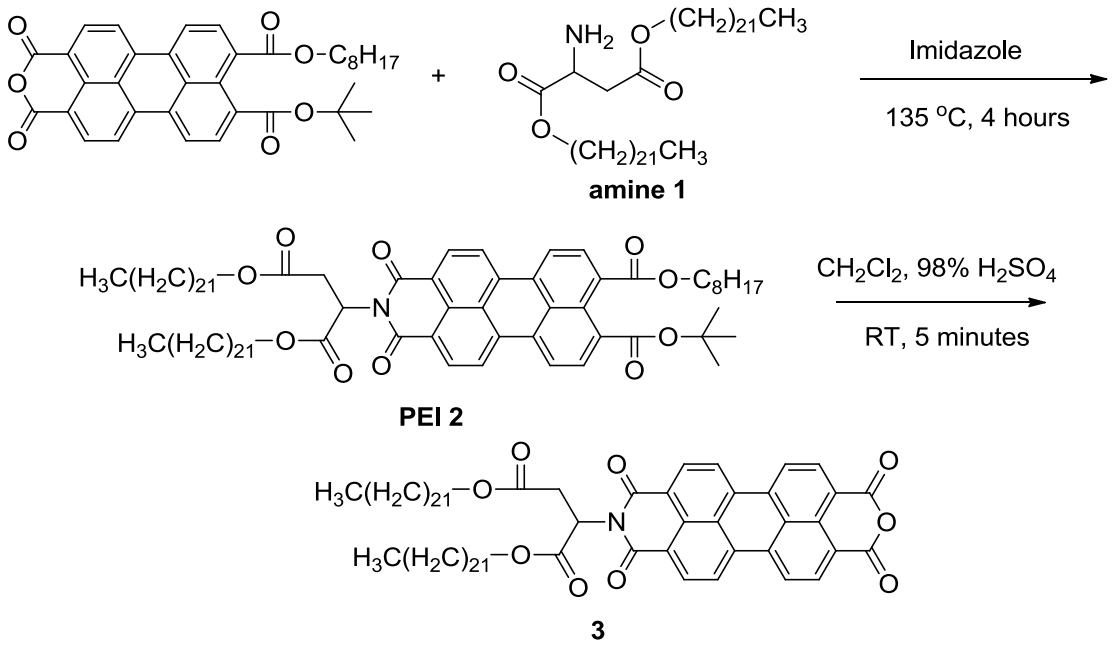

Scheme 4.9 Synthesis of perylene monoanhydride monoimide using C8-*tert*-butyl-PEA as the starting material

The first condensation reaction's yield can reach 80%. But the following cyclization reaction was troublesome. The *tert*-butyl PEA itself can be easily cyclized by sodium bisulfate at RT. However, the reactivity of PEI **3** is much lower than the original PEA, probably due to the attachment of the long, branched N-substituent, which significantly reduces the proton-*tert*-butyl ester collision probability. The PEI **2** can not even be cyclized by TsOH or phosphoric acid at 60 °C. Finally, we found 98% sulfuric acid was a proper reagent to cyclize PEI **2** at room temperature using dichloromethane as the solvent. [14] The reaction was fast (completes in several minutes) and ester groups survived. The yield was as high as 95%. The resulting monoanhydride monoimide **3** can be use to make unsymmetrically substituted PDIs through straightforward reactions.

In conclusion, we have designed and successfully synthesized a *tert*-butyl based PEA which has good solubility in most of the commonly used organic solvents. This compound can serve as the starting material for the synthesis of unsymmetrically substituted PEIs which could be further converted to unsymmetric PDIs. More importantly, compared to the former reported Di-C10_PEA, this PEA's cyclization condition is modest. So novel acid-sensitive groups containing PDIs can be made in high yield, which makes the PDI's molecular design and structure tuning more flexible.

4.3 Experimental section

Synthesis of *tert*-butyl based PEAs

Attempt to open the anhydride ring using the combination of *tert*-butanol and DBU

A 100 ml round bottom flask was charged 3.93 g (10 mmol) 3, 4, 9, 10-perylenetetracarboxyldianhydride, 3.8 g (25 mmol) DBU, 2.96 g (40 mmol) *tert*-butanol and 40 ml dry DMSO and sealed well. The mixture was stirred at 60 °C for 7 days, the vast majority of PDA remained as the red solid and solution was nearly colorless which indicates that the combination of the organic base, DBU, and *tert*-butanol failed to open the anhydride ring.

perylene-3,4-anhydride-9-(*tert*-butyloxycarbonyl)-10-(hexyloxycarbonyl)

A 100 ml round bottom flask was charged 3.93 g (10 mmol) 3, 4, 9, 10-perylenetetracarobxyldianhydride, 20.6 g (18 mmol) potassium *tert*-butoxide and 40 ml dry DMSO and sealed well. The mixture was stirred at 60 °C for 72 hours; subsequently 13.2 g 1-bromohexane (80 mmol) was added and the mixture was stirred for another 72 hours at 60 °C. Then the solution was poured into 150 ml methanol. The crude product was collected by suction filtration and purified by column chromatography with 100/1 (v/v) chloroform/acetone as the eluent to afford 2.36 g product (43%) as a red solid.

^{1}H NMR ($CDCl_3$, 600 MHz): δ (ppm) = 8.64 (d, J = 8.41 Hz, 2H, Ar), 8.52 (m, J = 11.46 Hz, 2H, Ar), 8.49 (m, J = 14.9 Hz, 2H, Ar), 8.11 (d, J = 2.29 Hz, 2H, Ar), 4.39 (t, J = 9.66 Hz, 2H, COOC**H$_2$**), 1.66 (s, 9H, C(C**H**$_3$)$_3$**)**, 0.89 (t, J=13.96 Hz, 3H, CH_2C**H**$_3$)

^{13}C NMR ($CDCl_3$, 75 MHz): δ (ppm) = 169.95 (ester C=O), 168.2 (ester C=O),

161.866 (anhydride C=O), 136.776 (Ar), 132.398 (Ar), 131.756 (Ar), 125.834 (Ar), 82.662 (O**C(**$CH_3)_3$), 73.92 (O**C**H_2CH_2), 29.558 (**C**H_2), 29.368(**C**H_2), 29.167 (**C**H_2), 28. 32 (OC**(C**$H_3)_3$), 14.087(**C**H_3).

perylene-3,4-anhydride-9-(*tert*-butyloxycarbonyl)-10-(octyloxycarbonyl)

A 100 ml round bottom flask was charged 11.8 g (30 mmol) 3, 4, 9, 10-perylenetetracarobxyldianhydride, 61.8 g (54 mmol) potassium *tert*-butoxide and 120 ml dry DMSO and sealed well. The mixture was stirred at 60 °C for 72 hours; subsequently 46.2 g 1-bromooctane (240 mmol) was added and the mixture was stirred for another 72 hours at 60 °C. Then the solution was poured into 400 ml methanol. The crude product was collected by suction filtration and purified by column chromatography with 100/1 (v/v) chloroform/acetone as the eluent to afford 6.9 g product (40%) as a red solid.

^{1}H NMR ($CDCl_3$, 600 MHz): δ (ppm) = 8.62 (d, J = 8.59 Hz, 2H, Ar), 8.51 (m, J = 11.32 Hz, 2H, Ar), 8.48 (m, J = 12.92 Hz, 2H, Ar), 8.10 (d, J = 2.31 Hz, 2H, Ar), 4.39 (t, J = 9.67 Hz, 2H, COOC**H$_2$**), 1.64 (s, 9H, C(C**H**$_3)_3$**)**, 0.88 (t, J=14.2 Hz, 3H, CH_2C**H**$_3$) ^{13}C NMR ($CDCl_3$, 75 MHz): δ (ppm) = 169.92 (ester C=O), 167.99 (ester C=O), 161.836 (anhydride C=O), 136.706 (Ar), 132.288 (Ar), 131.816 (Ar), 125.821 (Ar), 82.15 (O**C(**$CH_3)_3$), 74.06 (O**C**H_2CH_2), 29.658 (**C**H_2), 29.502(**C**H_2), 29.177 (**C**H_2), 28. 229 (OC**(C**$H_3)_3$), 14.077(**C**H_3).

perylene-3,4-anhydride-9-(*tert*-butyloxycarbonyl)-10-(decyloxycarbonyl)

A 100 mL round bottom flask was charged 3.93 g (10 mmol) 3, 4, 9,

10-perylenetetracarobxyldianhydride, 20.6 g (18 mmol) potassium *tert*-butoxide and 40 ml dry DMSO and sealed well. The mixture was stirred at 60 °C for 72 hours; subsequently 17.7 g 1-bromodecane (80 mmol) was added and the mixture was stirred for another 72 hours at 60 °C. Then the solution was poured into 150 ml methanol. The crude product was collected by suction filtration and purified by column chromatography with 100/1 (v/v) chloroform/acetone as the eluent to afford 1.89 g product (31%) as a red solid.

perylene-3,4-anhydride-9-(*tert*-butyloxycarbonyl)-10-(dodecyloxycarbonyl)

A 100 ml round bottom flask was charged 3.93 g (10 mmol) 3, 4, 9, 10-perylenetetracarobxyldianhydride, 20.6 g (18 mmol) potassium *tert*-butoxide and 40 ml dry DMSO and sealed well. The mixture was stirred at 60 °C for 72 hours; subsequently 19.9 g 1-bromododecane (80 mmol) was added and the mixture was stirred for another 72 hours at 60 °C. Then the solution was poured into 150 ml methanol. The crude product was collected by suction filtration and purified by column chromatography with 100/1 (v/v) chloroform/acetone as the eluent to afford 1.26 g product (20%) as a red solid.

perylene-3,4-anhydride-9-(*tert*-butyloxycarbonyl)-10-(tetradecyloxycarbonyl)

A 100 ml round bottom flask was charged 3.93 g (10 mmol) 3, 4, 9, 10-perylenetetracarobxyldianhydride, 20.6 g (18 mmol) potassium *tert*-butoxide and 40 ml dry DMSO and sealed well. The mixture was stirred at 60 °C for 72 hours; subsequently 22.1 g 1-bromotetradecane (80 mmol) was added and the mixture was

stirred for another 72 hours at 60 °C. Then the solution was poured into 150 ml methanol. The crude product was collected by suction filtration and purified by column chromatography with 100/1 (v/v) chloroform/acetone as the eluent to afford 0.79 g product (12%) as a red solid.

perylene-3,4-anhydride-9-(*tert*-butyloxycarbonyl)-10-(hexadecyloxycarbonyl) (6)

A 100 ml round bottom flask was charged 3.93 g (10 mmol) 3, 4, 9, 10-perylenetetracarobxyldianhydride, 20.6 g (18 mmol) potassium tert-butoxide and 40 ml dry DMSO and sealed well. The mixture was stirred at 60 °C for 72 hours; subsequently 24.4 g 1-bromododecane (80 mmol) was added and the mixture was stirred for another 72 hours at 60 °C. Then the solution was poured into 150 ml methanol. The crude product was collected by suction filtration and purified by column chromatography with 100/1 (v/v) chloroform/acetone as the eluent to afford 0.62 g product (9%) as a red solid.

Synthesis of PEI 2

Into a 25 ml Schlenk flask were charged **amine 1** 900 mg (1.2 mmol), **perylene-3,4-anhydride-9-(*tert*-butyl)-10-(octyl)** 578 mg (1 mmol), and imidazole (4 g). The mixture was purged with nitrogen for 15 minutes before the reaction. The mixture was heated at 135 °C with nitrogen purged on for 4 hours. Subsequently, the reaction mixture was cooled to 90 °C. Deionized water was then added to precipitate out the product. After the water solution was removed by suction filtration, the solid was dried at 50 °C in vacuum oven until constant weight.

Cyclization of PEI 2

131 mg **PEI 2** (0.1 mmol) was dissolved in 10 ml dichloromethane and stirred at RT for 10 minutes, then 0.3 mmol sulfuric acid (30 mg 98% sulfuric acid dissolved in 3 ml dichloromethane) was added to the mixture. The solution was stirred vigorously for 5 minutes at room temperature and the product precipitated out as red solid. The perylene monoimide monoanhydride product was obtained by suction filtration and purified by column chromatography with 100/2 (v/v) chloroform/acetone as the eluent. The yield was 106 mg (95%).

^{1}H NMR ($CDCl_3$, 600 MHz): δ (ppm) = 8.61 (d, J = 7.83 Hz, 2H, Ar), 8.44 (d, J = 8.81 Hz, 2H, Ar), 8.37 (d, J = 8.62 Hz, 2H, Ar), 8.11 (d, J = 7.94 Hz, 2H, Ar), 5.11 (t, J = 9.66 Hz, 1H, NC**H**CH_2), 3.11 (d, J = 9.92 Hz ,2H, NCHC**H_2)**

^{13}C NMR ($CDCl_3$, 75 MHz): δ (ppm) = 168.26 (ester C=O), 160.31 (anhydride C=O), 135.45 (Ar), 133.01 (Ar), 131.87 (Ar), 123.46 (Ar), 121.02 (Ar), 117.72 (Ar), 58.66 (N**C**HCH_2), 33.29 (NCH**C**H_2)

CHAPTER 5. BUNDLED-STACK DISCOTIC COLUMNAR LIQUID CRYSTALLINE PERYLENE MONOANHYDRIDE DIESTERS WITH A SINGLE STACKING MODE: PROMISING SEMICONDUCTORS WITH ENHANCED CHARGE TRANSPORT CHARACTERISTICS

5.1 Introduction

Discotic columnar liquid crystalline (DCLC) materials are receiving increasing attention in the search for high performance organic semiconducting materials which are technologically promising for photovoltaic devices. The tunable self-assembly of π-conjugated disc-shaped molecules into ordered supramolecular architectures is a subject of increasing research interest for the tailoring of their functionalities. Specifically, disk-shaped molecules with alkyl substituents can spontaneously self-assemble into columnar structures of face-to-face stacked rigid cores, and rigid conjugated discotic cores are micro-phase segregated from flexible peripheral chains. The coaxial mantle of peripheral chains forms a barrier to charge transport between columnar cores, leading to their designation as one-dimensional nanowires. [1, 2] DCLC materials' device performance might be enhanced by some decrease in the one-dimensionality of charge-transport, which could provide inter-stack bypasses at defects and grain/domain boundaries. [3] To this end, an inter-stack intra-column charge carrier migration concept was raised by Dr. Müllen et al in 2004. [1, 4] As shown in **Figure 5.1**, unlike the symmetrically substituted HBC1, HBC2's "wrapping" was partially stripped away. For each molecule, only three flexible chains were kept to ensure the solubility and phase-forming properties. With

this unique “unwrapped” structure, if HBC2 could self-assemble into the DCLC phase shown in **Figure 5.1**, the charge transport robustness can be substantially improved since each column has the potential to encompass a bundle of several conducting π-stacks with the stacking axes parallel to the column axis, so defects in a π-stack can be circumvented by moving to another π-stack in the same bundle to continue charge transport. This requires that there are no insulating moieties blocking intra-bundle inter-stack charge hopping. Such a bundled-stack DCLC (BSDCLC) phase is essentially a nanometer-sized version of insulated multi-strand conducting wires. However, no convincing structure characteristics of BSDCLC phase were identified in HBC2’s structure analysis.

To form a true BSDCLC phase, it is necessary to remove some flexible chains from a conventional DCLC molecule to expose the discotic mesogen to intra-column inter-stack mesogen-mesogen contact. In other words, the molecule should be intrinsically asymmetric so that the “unwrapped” part of conjugated discotic core π-stacks can bundle together forming the “head-to-head” column core while the bundle/column core is surrounded by peripheral flexible chains. On this regard, PEA should have the promising potential to form a BCDCLC phase. The lack of any peripheral substituents (even hydrogen atoms!) at the anhydride side of a PEA maximizes the probability of possible inter-stack charge carrier hopping. This, coupled with the strong π-stack formation tendency of the perylene ring, makes wedge-shaped PEA a suitable mesogen for a BSDCLC phase.

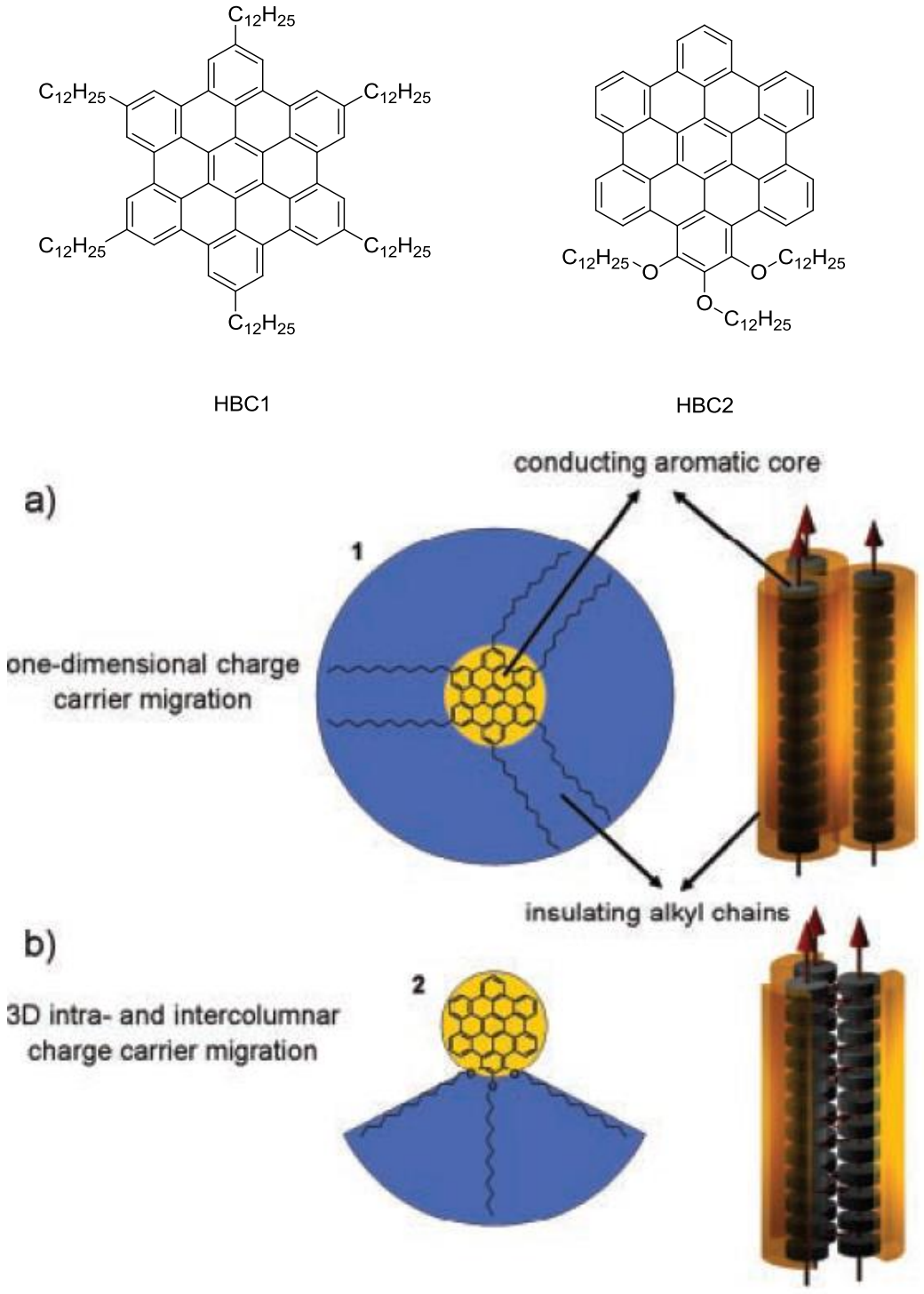

Figure 5.1 Schematic illustration of a) 1D charge carrier transport for symmetrically alkyl-substituted HBC1 and b) 3D intra-column charge carrier transport for asymmetrically substituted HBC2, where in addition the charges are allowed to perform inter-stack hopping. [1]

Keeping this in mind, the PEA-10/14 was designed and synthesized in our group in 2012. [5] The structure characterizations and simulation results revealed that it self-assembles into a unique composite BSDCLC phase at RT, which means the intra-column charge migration was realized for the first time. The charge transport advantage of the BSDCLC phase has been confirmed by its respectful charge carrier mobility. The sum of PEA-10/14's1D charge carrier mobility, as measured by pulse-radiolysis time resolved microwave conductivity technique (PR-TRMC), is $5.41x10^{-2}$ $cm^2V^{-1}s^{-1}$, fully comparable to those high mobility values by the same method reported for DCLC PDIs. [6-7] However, there are two drawbacks in the structure of the BSDCLC phase of PEA-10/14 as a charge transport material. First, two stacking modes are involved in the bundled-stack column structure. Based on the 2D XRD pattern, the density measurement and molecular modeling, the presence of packing discontinuities at three-stack/four-stack interfaces is proposed. The second disadvantage is the relatively large π-stack spacing (0.3606 nm), probably due to the steric hindrance of the sp^3 hybridized branching point in the long alkyl peripheral chains. A larger spacing is associated with a weaker intermolecular π-orbital coupling which tends to result in lower charge carrier mobility. [8]

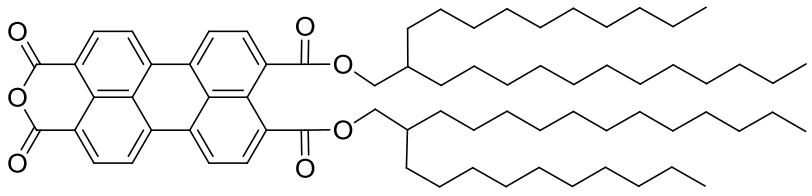

Scheme 5.1 Chemical structure of PEA-10/14

As an effort to overcome these drawbacks, especially the relative large π-stack spacing, the significant steric hindrance results from the sp^3-hybrided carbon at the

branching points will be eliminated first. Based on the simulation done on PEA-10/14, when packed in the four-stack structure, the *n*-alkyl chains suffer too few gauche dihedrals, resulting in an entropy penalty. Since the sp^3 carbon is fairly closed to the perylene core, the surface area of a bundled-stack column core is too small to accommodate eight chains with an entropically comfortable conformation. Conversely, when packed in the three-stack mode, the *n*-alkyl chains have to adopt a conformation with a relatively large number of gauche dihedrals, which comes with an enthalpy cost leading to a higher free energy. By combining three- and four-stack modes, *n*-alkyl chains are in a conformation with a free energy advantage that is more than enough to compensate for the energy cost from the packing discontinuities in the composite structure and makes it the most stable one.

5.2 BSDCLC PEA's molecular structure engineering via the tuning of alkyl substituents

To achieve a BSDCLC phase with a single stacking mode and tightly-stacked mesogens, the PEA-BZ-D10 is first designed and synthesized using the intramolecular cyclization which is discussed in Chapter 3. Instead of the sp^3 hybrid carbons, the sp^2 hybrid carbons serve as the branch-points in PEA-BZ-D10. Every branch-point carbon forms the planar structure with the three neighboring carbons, which can efficiently weaken the steric hindrance effect. In addition, for each PEA molecule, four *n*-decyl chains are indirectly attached to the perylene core through a carbon-oxygen single bond to ensure the compound's solution processability and phase-forming properties.

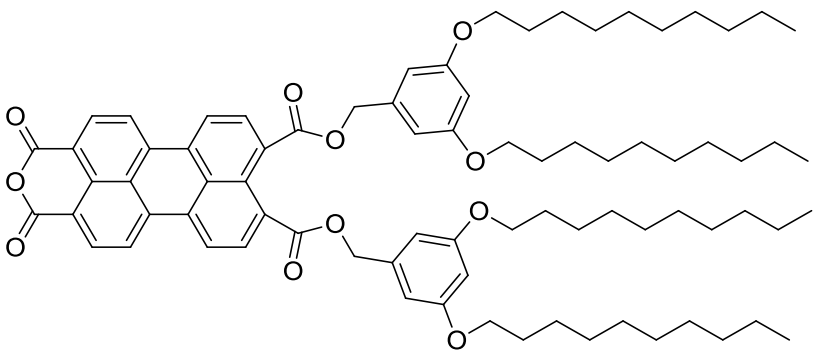

Scheme 5.2 Chemical structure of PEA-BZ-D10

DSC and PLM were first utilized to probe its phase transition behaviors. The DSC traces are shown in **Figure 5.2**. The endothermic peak with the onset at 185 °C during heating can be attributed to the isotropization process as confirmed by PLM results. And exothermic peak with onset at 174.7 °C hints the development of the phase from liquid. Based on the PLM observations, PEA II is a bright solid under polarized microscope at RT, during heating, the sample begins to turn dark at 111 °C and the whole sample becomes dark at 133 °C, indicating an optically isotropic state. However, at this point, the sample is not a liquid as it does not flow. The transition was confirmed by DSC results as a broad peak was observed around 111 °C-133 °C. As the heating continues, the sample starts entering the isotropic liquid state at 179 °C, and the transition complete at 185 °C.

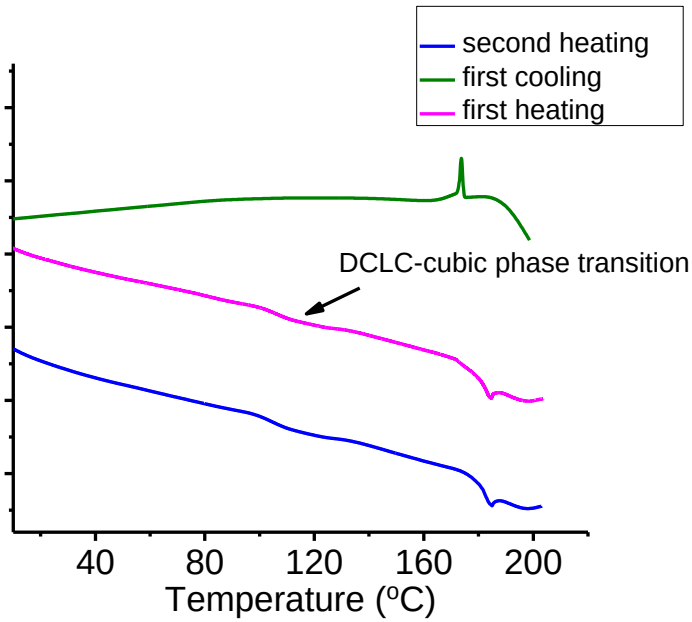

Figure 5.2 DSC data of PEA PEA-BZ-D10

Between 111 °C and 133 °C, PEA-BZ-D10 was in an optically isotropic and soft phase, probably a cubic phase. To test this assumption, PEA-BZ-D10's wide-angle and small-angle X-ray scattering (WAXS and SAXS) powder patterns were collected at 132 °C. As shown in **Figure 5.3**, the absence of any sharp diffraction peaks at wide-angle region indicates the lack of crystallinity while the sharp peaks in the small-angle region reveal the ordered nature of the phase. This ordered nature was confirmed by the 1D SAXS pattern shown in **Figure 5.4**. The fact that the phase is both optically isotropic (dark view in PLM) and ordered suggests that it is most likely a cubic LC phase.

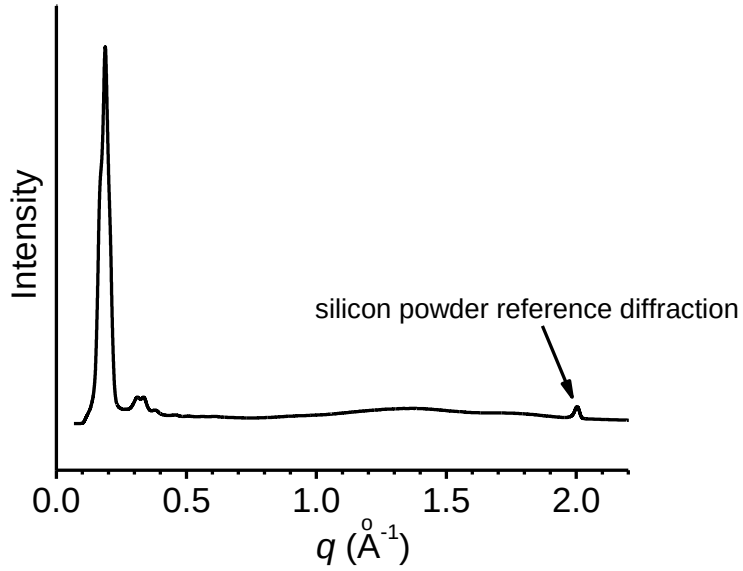

Figure 5.3 1D WAXS pattern of PEA PEA-BZ-D10 at 132 °C

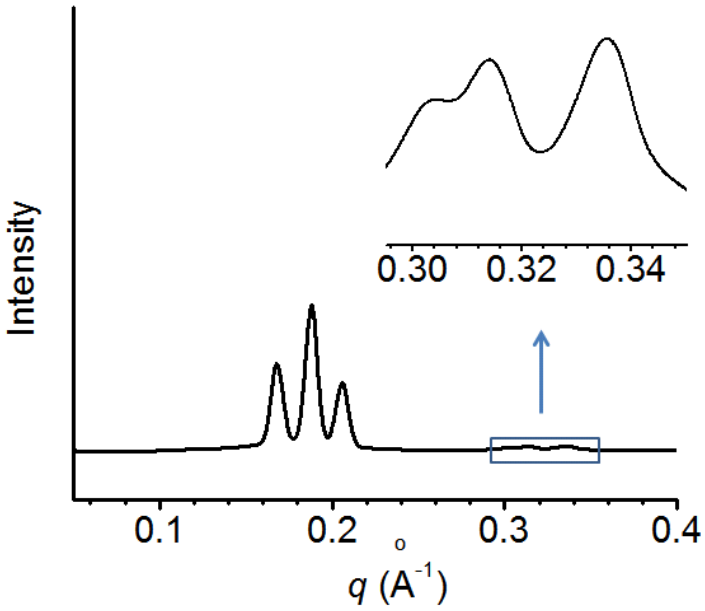

Figure 5.4 1D SAXS pattern of PEA PEA-BZ-D10 at 132 °C

Furthermore, PEA-BZ-D10's RT DCLC characteristics were investigated by collecting the RT 1D XRD pattern shown in **Figure 5.5**. The ordered nature of the LC phase's columnar packing is testified by the appearance of multiple sharp diffraction peaks at the small-angle region. In contrast, the alkyl chains are in a disorder,

liquid-like state, as indicated by the absence of sharp diffraction peaks between 1.3 and 1.7 $Å^{-1}$. The peak at 1.764 $Å^{-1}$ (d-spacing = 0.356 nm) can be attributed to π-stacked perylene units. The absence of any sharp diffraction peaks in quadrants excludes the possibility of a 3D long-range ordered crystalline phase. The q values of small-angle peaks (0.1488, 0.256, 0.292 and 0.392 $Å^{-1}$) fit the ratio of $1:\sqrt{3}:2:\sqrt{7}$ suggesting that the existence of a 2D hexagonal lattice. This, combining with the lack of 3D crystalline order, confirms that at RT PEA II is in a DCLC phase. The hexagonal inter-columnar distance (4.5 nm) is much larger than the PEA molecular size (~2 nm), indicating that multi-stack mode could be involved in the intra-column structure.

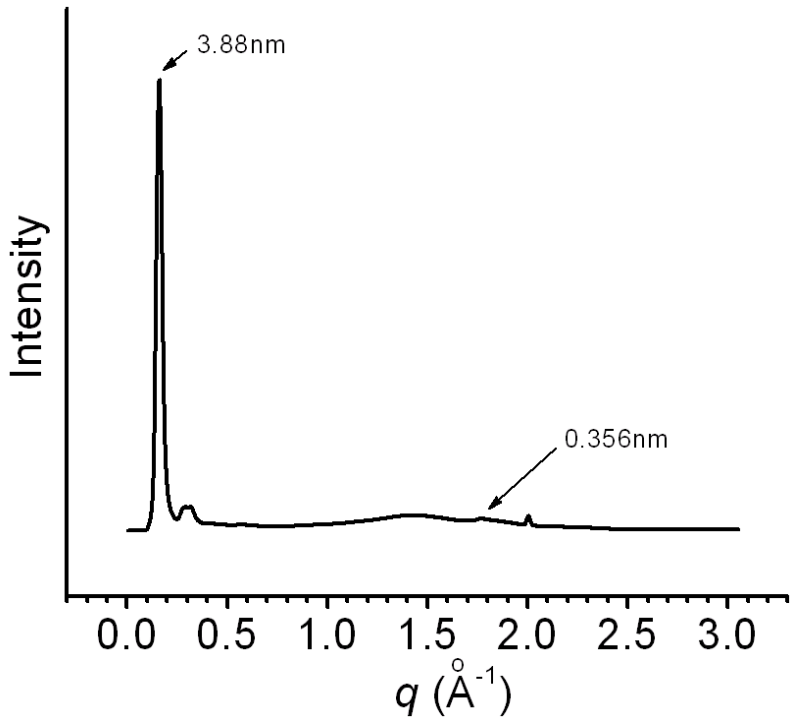

Figure 5.5 1D WAXS pattern of PEA-BZ-D10 at RT

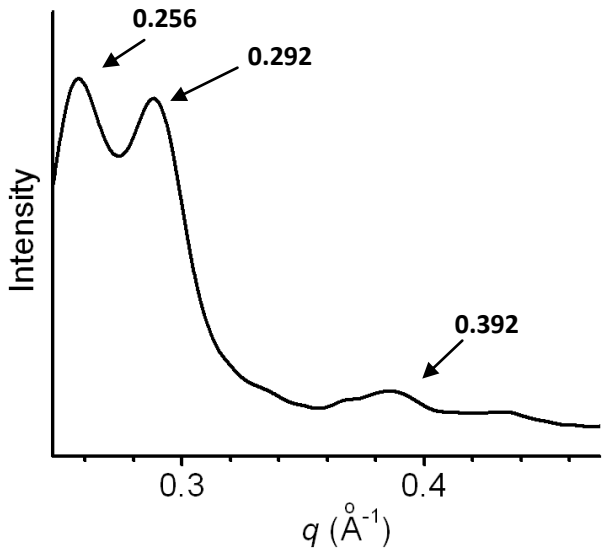

Figure 5.6 Partly enlarged 1D WAXS pattern of PEA-BZ-D10 (small angle part)

To extract more in-depth structural information, a 2D XRD pattern was collected on a well-aligned PEA-BZ-D10 which was readily prepared by mechanical shearing, thank to its RT DCLC nature. As displayed in **Figure 5.7**, the series of diffractions on the equator originate from supramolecular columns well-aligned along the shearing direction. The diffused halo with d ≈ 0.45 nm suggested that the alkyl chains don't have clear preferential orientation despite oriented columns, which is in agreement with their liquid-like character. The strongest diffraction on the meridian at d = 0.356 nm can be assigned to π-stacking order of perylene units. The fact that this diffraction does not split means that discotic mesogens are perpendicular to the column axis. Had only one perylene π-stack involved in each supramolecular column, the density calculated from given cell parameters would be 0.323 g/cm^3. However, the measured value is 1.22 g/cm^3. To match the experimental density value, about 3.78 π stacks in each column are needed. Such an intra-column structure should be responsible for the appearance of those diffused scatterings in yellow circles on the

meridian and in the quadrants, as shown in **Figure 5.7**.

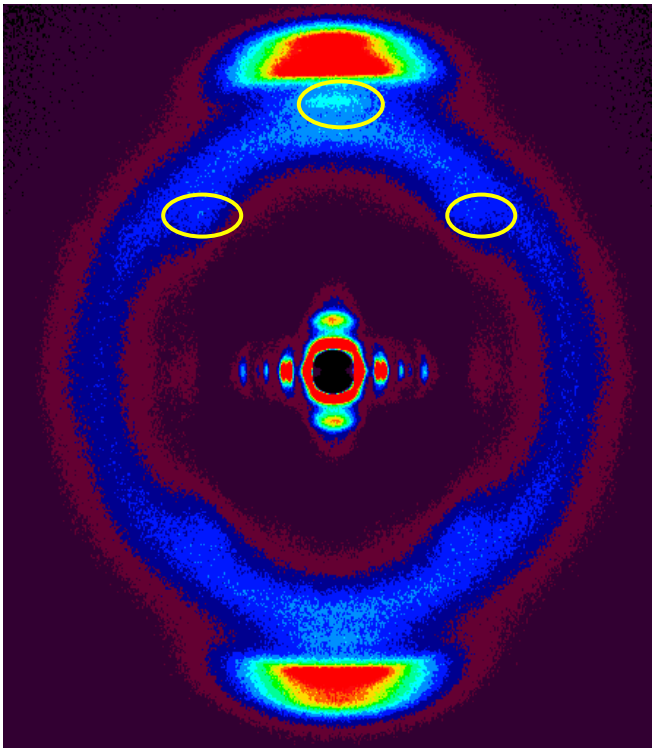

Figure 5.7 2D RT WAXS pattern of PEA-BZ-D10

The meridian diffraction pattern implies a structure with appreciable electron density variations in the unit cell along the column axis direction other than what arises from the regularly π-stacked perylene rings. Similar to PEA-10/14, the bundled-stack intra-column structure involving two π-stacking modes also applies to PEA-BZ-D10. The electron density variation results from the contrast between the three-stack and four-stack regions. Besides the involvement of two stacking modes, another drawback of PEA-BZ-D10's phase behavior is the poor stability of the LC phase. Even at RT, it crystallizes slowly. The crystallization can be speeded up considerably by annealing at a higher temperature. A nearly completely crystallized specimen can be obtained by heating a mechanically sheared sample quickly to 110 °C and then cool to RT. As shown in **Figure 5.8**, the large number of sharp

diffractions in the small angle region, especially those in the quadrants, underline a crystalline structure.

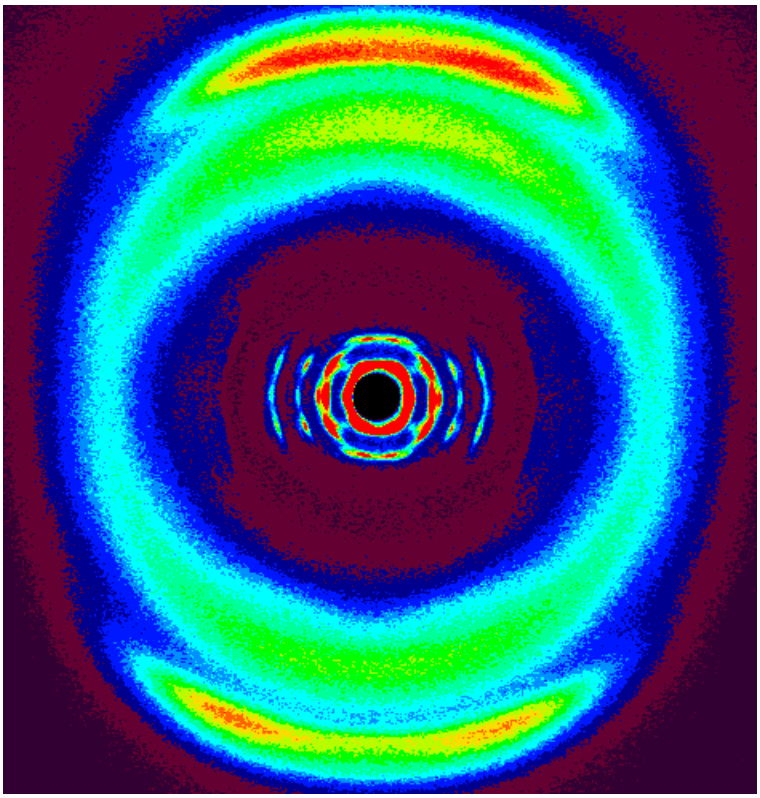

Figure 5.8 2D WAXS pattern of PEA-BZ-D10 after cooled from 110 °C

The structure analysis data have shown that, in PEA II, with the sp^3 branching-point is replaced by a branching unit only containing sp^2 carbon, a BSDCLC phase with somewhat smaller π-stack spacing is observed. However, the BSDCLC phase with single stack mode was still not achieved. We believe that the desire of soft *n*-alkyl chains to adapt the most comfortable conformation is one of the major driving forces behind the formation of the composite BSDCLC phase. Our early simulation work has shown that if only the intermolecular interaction of the rigid part is considered, the pure four-stack mode is the most enthalpically favored. The most likely reason for us to observe the composite BSDCLC phase instead of a simply four-stack BSDCLC phase is that if PEA-BZ-D10 molecules do pack in the

simple four-stack BSDCLC phase, the *n*-alkyl chains would pack too tightly so that they have to take a conformation with few gauche bonds, which results in an entropy penalty to the self-assembly system. The involvement of the three-stack mode together with the four-stack mode alleviated the entropy penalty.

From supramolecular engineering point of view, besides invoking a composite BSDCLC phase involving two stacking modes, another approach to relieve the possible entropy penalty which arises from the formation of the four-stack mode is to increase the surface area of the supramolecular column core which must be covered by *n*-alkyl chains. By doing so, the supramolecular columnar core surface area per *n*-alkyl chain will be increased so that each *n*-alkyl chain will have more room (cross-sectional area) to include a reasonable number of gauche bonds to reach its comfortable conformation. This can be done at the molecular level by inserting a spacer between the PEA core and the branching unit, which increases the distance between the inner end of each *n*-alkyl chain to the center of the supramolecular column (therefore the surface area of the supramolecular column core can be increased as well). It is very important to emphasize that, in this case, the involvement of two stacking modes might become unnecessary and probably yield a BSDCLC phase with the pure four-stack structure. To this end, we designed and synthesized PEA-2-BZ-D10.

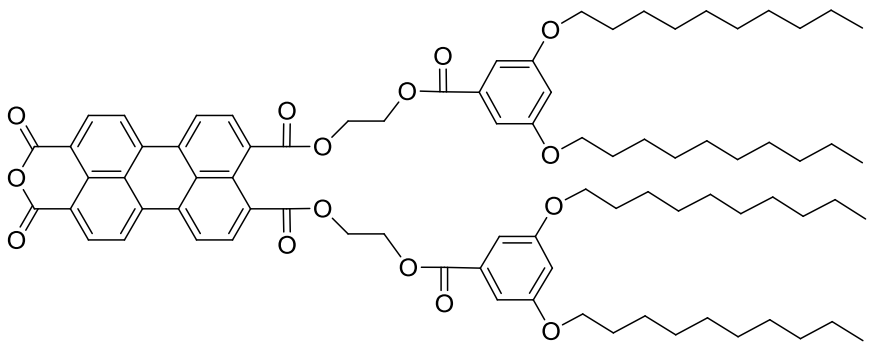

Scheme 5.3 Chemical structure of PEA-2-BZ-D10

In PEA-2-BZ-D10, the distance between the sp^2 branching-point and perylene core is increased by three bonds (one carbon-carbon and two carbon-oxygen bonds) than that in PEA-BZ-D10. Therefore there is a better chance that PEA-2-BZ-D10's peripheral *n*-alkyl chains would not suffer entropy penalty in the anticipated four-stack BSDCLC phase. To our surprise, neat PEA-2-BZ-D10 freshly cast from THF solution is a red liquid. However, a DCLC phase slowly develops at RT. The formation of the LC phase completes in about 48 hours at RT. The thermal behavior is similar to PEA-BZ-D10, which means that a cubic phase occurs between room temperature DCLC phase and the isotropization temperature. The red LC PEA-2-BZ-D10 is bright under PLM at RT, during heating, the sample begins to turn dark at 134 °C and the whole sample became dark at 145 °C. As the heating continued, the sample became isotropic liquid state at 188 °C. Unlike PEA-BZ-D10, no phase transition peaks can be clearly resolved in the PEA-2-BZ-D10's DSC traces.

To get in-depth phase transition and structure characteristics details, XRD patterns were collected under different conditions. First, the PEA-2-BZ-D10 sample was dissolved in THF to form a homogenous solution, then the majority of solvent was removed by nitrogen blow, the sample was further dried in vacuum oven for 1

hour at 50 °C to completely remove the residual solvent. The sample was stored in vacuum oven for another 48 hours at RT to develop the ordered DCLC phase. Then the temperature-varied small-angle XRD powder patterns were collected to monitor the PEA-2-BZ-D10's phase transition behavior. The temperature was raised at the rate of 6 °C per minute, and every data collection took 20 minutes.

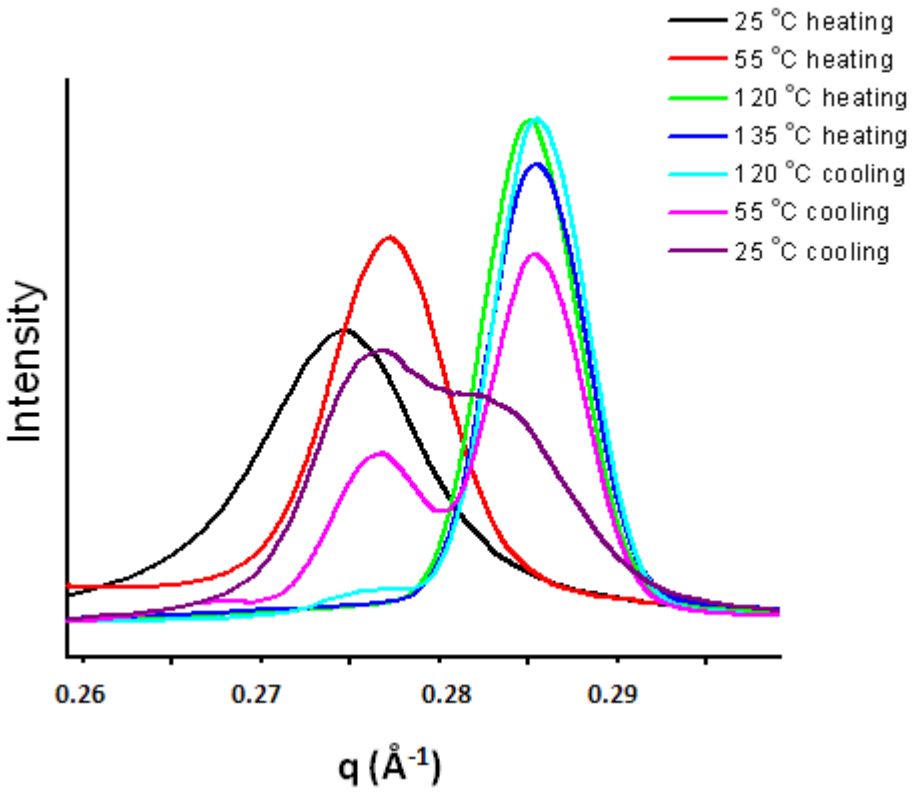

Figure 5.9 SAXS patterns of PEA-2-BZ-D10 at different temperatures

As shown in **Figure 5.9**, upon heating to 55 °C, crystallization was already clearly observed as an additional sharp diffraction visible at 0.278 $Å^{-1}$, and the small angle diffractions became sharper. At 120 °C, the sample completely crystallized and this phase transition process was not reversible. When cooled back to 25 °C, the diffraction pattern is obviously different from the original one.

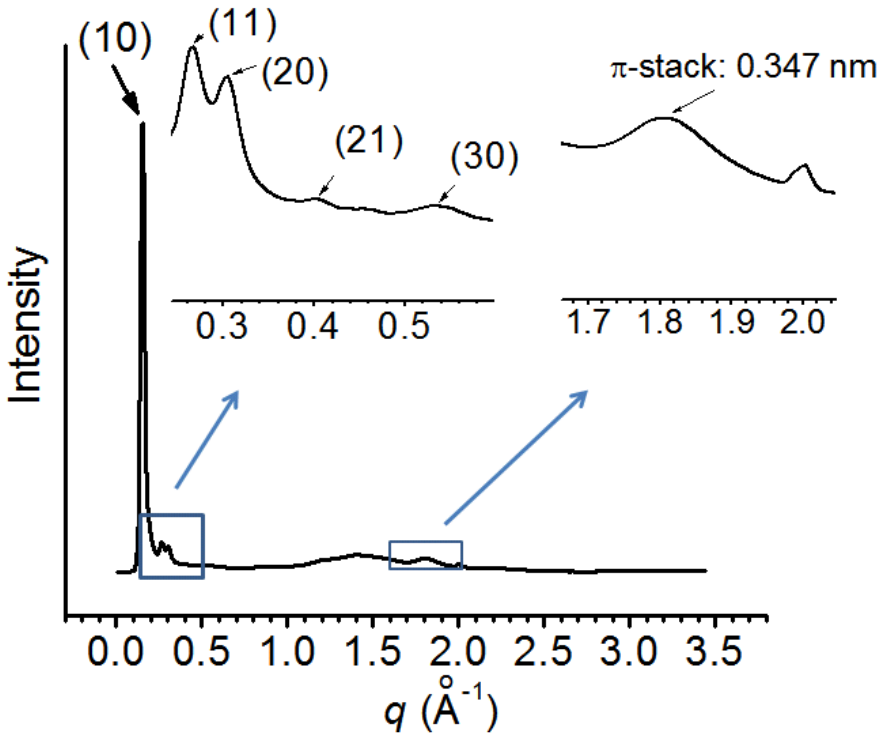

Figure 5.10 1D WAXS pattern of PEA-2-BZ-D10 at RT

More detailed structure information of PEA-2-BZ-D10 could be extracted from the 1D WAXS pattern shown in **Figure 5.10**. The multiple sharp diffraction peaks at the small-angle region are due to the long-range inter-column packing order. While the peripheral alkyl chains are in a disorder, liquid-like state, as indicated by the absence of sharp diffraction peaks between 1.3 and 1.7 $Å^{-1}$. Compared to that of PEA-BZ-D10, a somewhat tighter π-stacking (0.347 nm) is observed in PEA-2-BZ-D10. The absence of any sharp diffraction peaks other than those arising from 2D hexagonal lattice excludes the possibility of a 3D long-range ordered crystalline phase. The q values of small-angle peaks (0.153, 0.266, 0.305 and 0.401 $Å^{-1}$) fit the ratio of $1:\sqrt{3}:2:\sqrt{7}$ suggesting a highly ordered 2D hexagonal column packing. This, combining with the lack of 3D crystalline order, confirms that at RT PEA-2-BZ-D10 exhibits a DCLC phase. Furthermore, since the hexagonal

inter-columnar distance (4.1 nm) is much larger than the PEA molecular size (~2 nm), the multi-stack mode could be involved in PEA-2-BZ-D10's intra-column structure. To extract more in-depth structural information, a 2D WAXS pattern was collected on a well-aligned PEA-2-BZ-D10 which was readily prepared by mechanical shearing. As displayed in **Figure 5.11**, the series of diffractions on the equator originate from supramolecular columns well-aligned along the shearing direction. The diffused halo with d ≈ 0.45 nm suggested the alkyl chains' liquid-like character. The strongest diffraction on the meridian at d = 0.347 nm can be assigned to π-stacking order of perylene units. Had only one perylene π-stack involved in each supramolecular column, the density calculated from given cell parameters would be 0.325 g/cm^3. However, the measured value is 1.12 g/cm^3. To match the experimental density value, about 3.45 π stacks in each column are needed. This suggests that at RT, PEA-2-BZ-D10 may present BSDCLC phase involving two π-stacking modes (three-stack and four-stack). However, unlike PEA-10/14 and PEA-BZ-D10, diffused scatterings on the meridian and in the quadrants arising from electron density variations along the column axis are not observed in the 2D WAXS pattern of PEA-2-BZ-D10. This may be due to the relatively disordered nature of PEA-2-BZ-D10's intra-column structure. To the best of our knowledge, the pure BSDCLC phase with single stacking mode can not be obtained from PEA-2-BZ-D10.

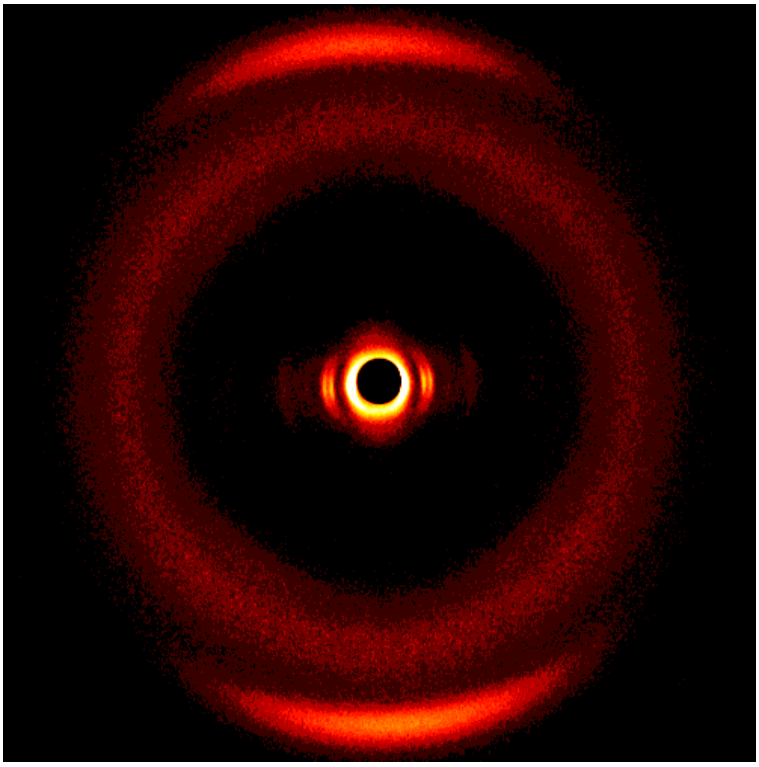

Figure 5.11 2D RT WAXS pattern of PEA-2-BZ-D10

With the insertion of a three-bond spacer, PEA-2-BZ-D10 self-assembles into a relatively disordered, composite BSDCLC phase, but with fairly tight π-stacks. Considering the spacer may not be long enough in PEA-2-BZ-D10, the PEA-4-BZ-D10 was designed. As shown in **Scheme 5.4**, compared to PEA-2-BZ-D10, the PEA-4-BZ-D10's sp^2 branch-point was further pulled away from the perylene core by two more carbons. The longer distance between the branch-point and perylene core may enable the formation of the simple four-stack structure without entropy penalty.

At RT, PEA-4-BZ-D10 presents a DCLC phase when freshly cast from THF solution. Similar to PEA-BZ-D10 and PEA-2-BZ-D10, a cubic phase appears between the RT DCLC phase and the isotropic liquid phase. The red liquid crystalline PEA-4-BZ-D10 is bright under PLM at RT, during heating, the sample turned dark at 198 °C, as the heating continues, the sample became isotropic liquid state at 246 °C.

No phase transition peaks can be clearly resolved in the PEA-4-BZ-D10's DSC traces.

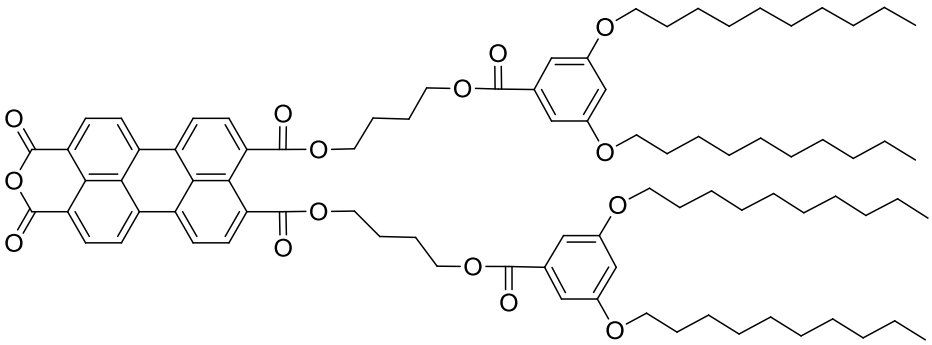

Scheme 5.4 Chemical structure of PEA-4-BZ-D10

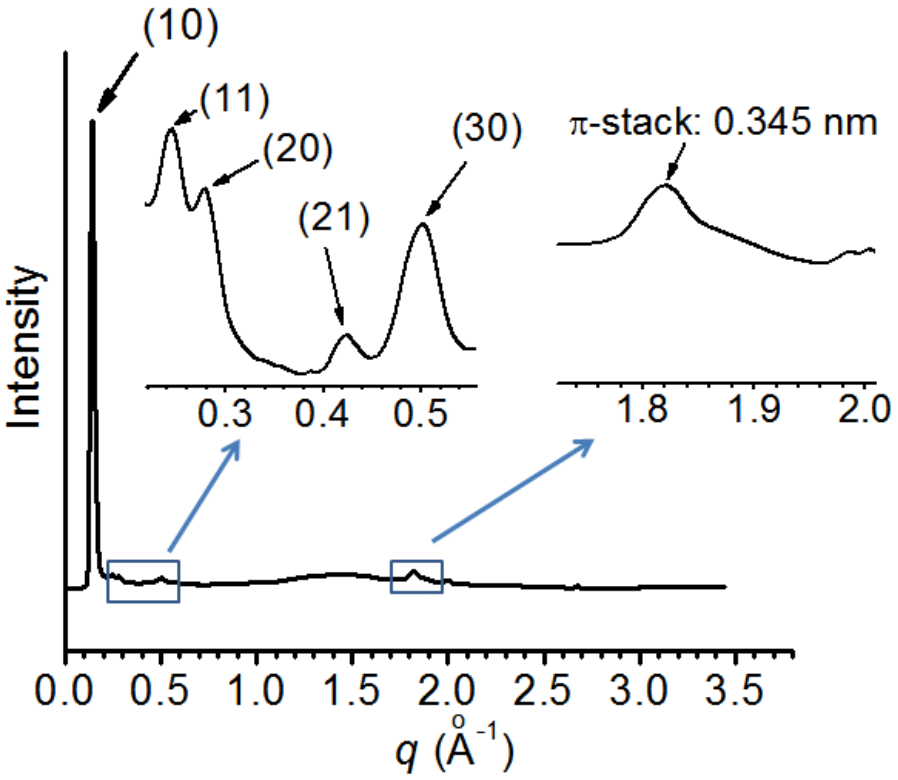

Figure 5.12 1D WAXS pattern of PEA-4-BZ-D10 at RT

Structural information of PEA-4-BZ-D10 could be extracted from the 1D WAXS pattern shown in **Figure 5.12**. The sharp diffraction peaks in the small-angle region and the absence of sharp diffraction peaks between 1.3 and 1.7 $Å^{-1}$ supports PEA-4-BZ-D10's LC characteristics. The somewhat sharp diffraction at 1.82 $Å^{-1}$ indicates that π-stacks are tight (inter-planar spacing: 0.345 nm). The q values of

small-angle peaks (0.1414--0.246--0.282--0.373 $Å^{-1}$) fit the ratio of 1:$\sqrt{3}$: 2:$\sqrt{7}$ suggesting that the column packing mode of PEA-4-BZ-D10 is a highly ordered symmetric hexagonal packing with an inter-column distance of 5.13 nm.

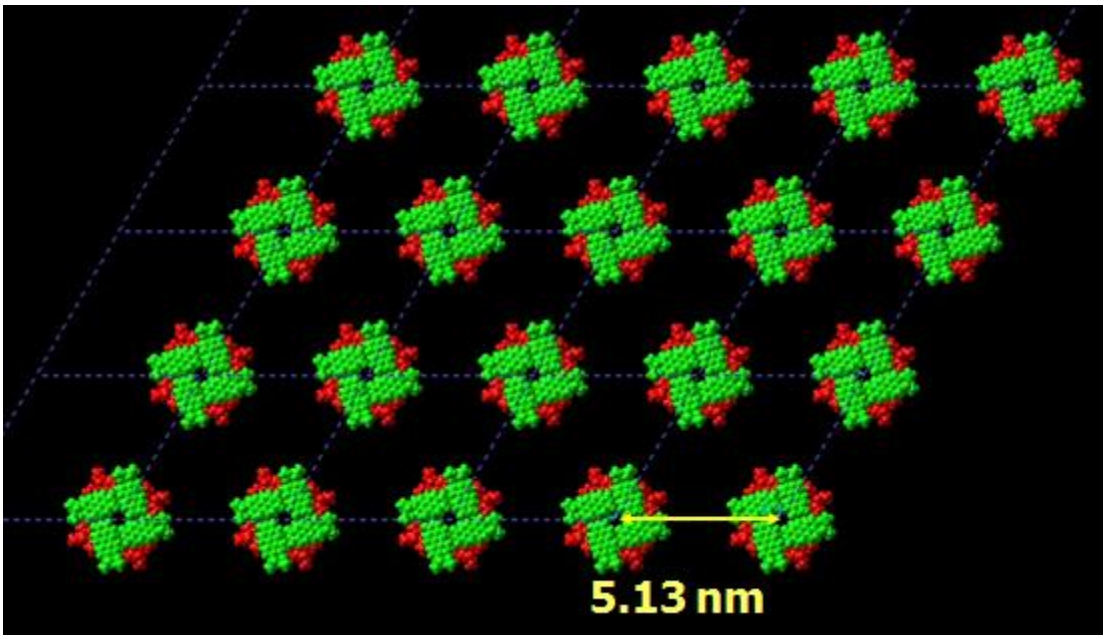

Figure 5.13 The column packing of PEA-4-BZ-D10

As shown in **Figure 5.13**, the hexagonal inter-columnar distance (5.13 nm) is much larger than the PEA molecular size (~2 nm), suggesting that a bundled-stack supramolecular column could be involved in PEA-4-BZ-D10's intra-column structure. A 2D WAXS pattern was collected on a well-aligned PEA-4-BZ-D10 by mechanical shearing to get more in-depth structure information.

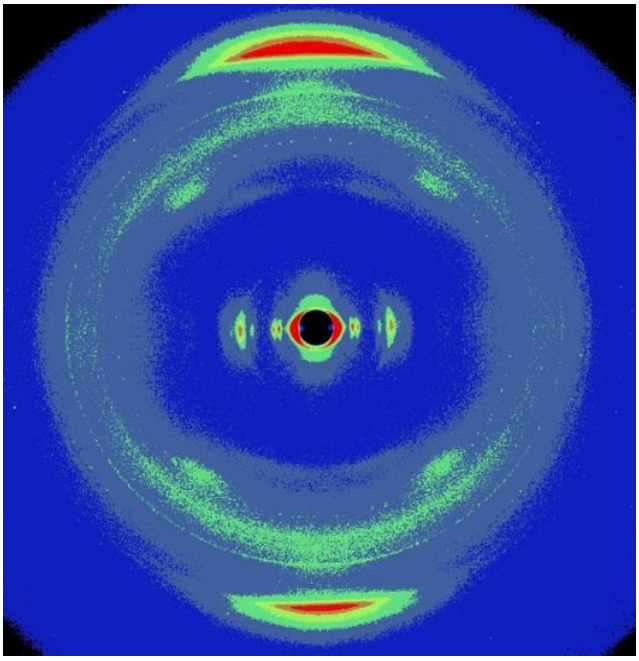

Figure 5.14 2D WAXS pattern of PEA-4-BZ-D10

As displayed in **Figure 5.14**, except the obvious π-stacking diffraction at d = 0.345 nm and diffused halo and quadrants which show the material's LC properties, there are no foreign meridian diffractions. This indicates that no electron density variations in the unit cell along the column axis direction exists other than what arises from the regularly π-stacked perylene rings. Had only one perylene π-stack involved in each supramolecular column, the density calculated from given cell parameters would be 0.293 g/cm^3. However, the measured density is 1.16 g/cm^3. To match the experimental density value, each supramolecular column should contain four π-stacks. Combined with the XRD analysis results and the density evidence, we can claim that a BSDCLC phase with pure four-stack mode is realized in PEA-4-BZ-D10 at RT.

The four-stack mode was simulated using Cerius 2. The simulated packing schemes are shown in **Figure 5.15**. It is worth mentioning that only the intermolecular interaction of the rigid part was considered during the simulation.

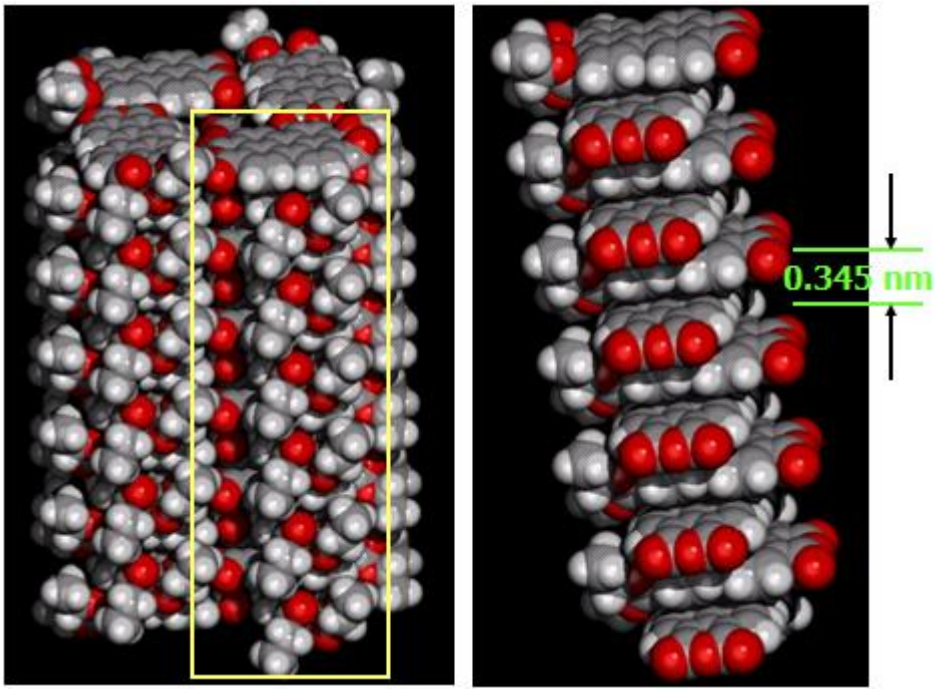

(a) **(b)**

Figure 5.15 Intra-column structure of PEA-4-BZ-D10 simulated using Cerius 2. (a) four-stack supra-column structure. (b) tight π-π stacking of perylene units in single stack.

As one can see from **Figure 5.15**, inside every stack, each mesogen rotates around its plane normal with respect to the neighboring mesogen in the same stack and the direction of rotation alternates along the stacking axis. Four stacks in the same column organize into a bundle with intra-bundle inter-stack mesogen-mesogen contacts facilitating charge hopping. The surface of columns is covered by flexible peripheral chains. The separation between adjacent perylene π-systems along the column axis direction is always 0.345 nm.

To further validate this intra-column pure four-stack mode, the simulated diffraction was generated from a single bundle and shown in **Figure 5.16**. The good agreement between experimental intra-column diffractions and the simulated pattern,

especially meridian and quadrant diffractions, strongly supports the proposed intra-column four-stack mode. The packing of mesogens is schematically represented in **Figure 5.17**.

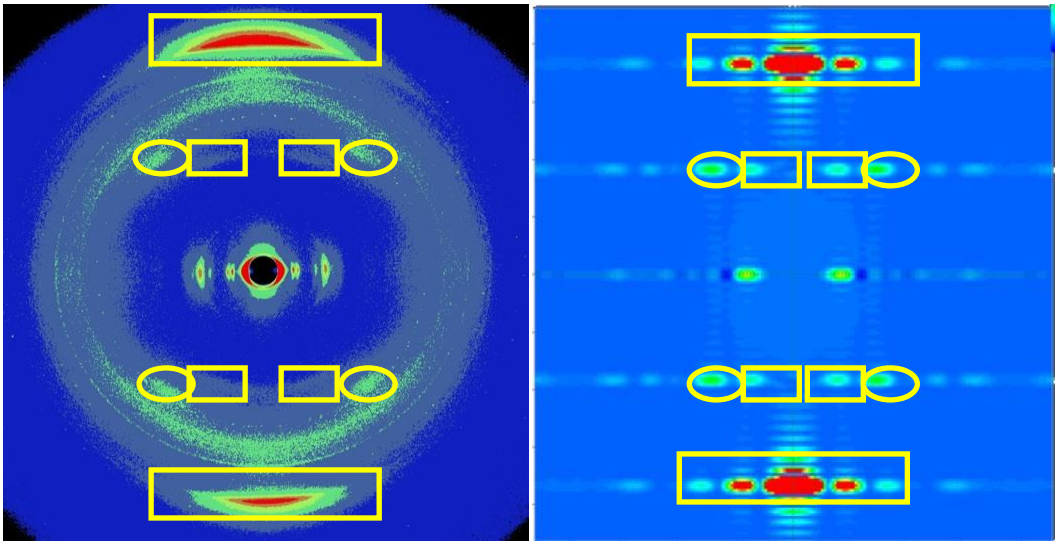

(a) **(b)**

Figure 5.16 (a) 2D WAXS pattern of a shear-oriented PEA-4-BZ-D10 (b) Simulated X-ray fiber pattern of PEA-4-BZ-D10 in the composite structure shown in Figure 5.15 (a). Intra-column diffractions in quadrants were circled.

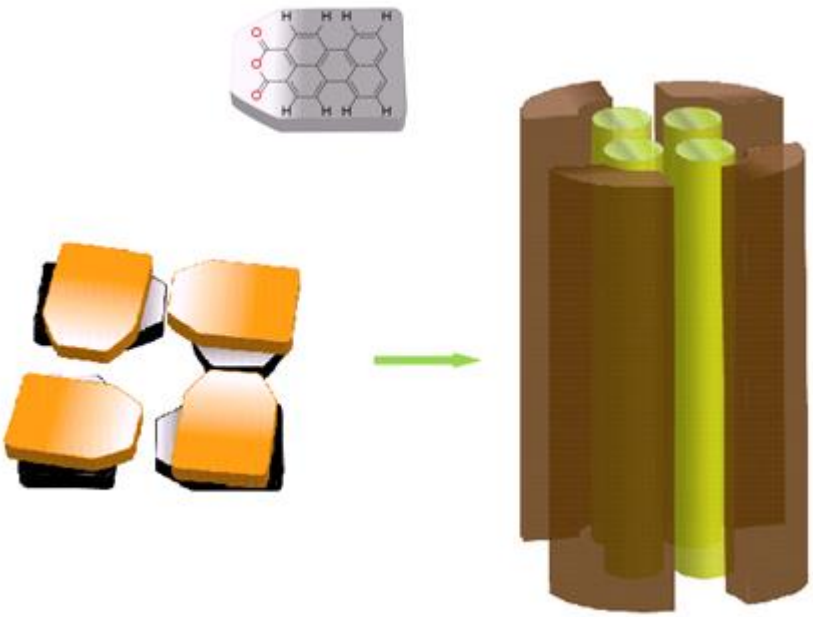

Figure 5.17 Schematic of PEA-4-BZ-D10's bundled-stack intra-column organization of mesogens.

For PEA-4-BZ-D10, the incorporation of the spacer effectively increased the distance between the inner end of each *n*-alkyl chain to the center of the supramolecular column. The column surface area was increased to a desirable degree that each *n*-alkyl chain has right room to take its comfortable conformation with a reasonable number of gauche bonds. Consequently, a simple four-stack intra-column organization was achieved in the BSDCLC phase of PEA-4-BZ-D10. In this case, packing discontinuities have been eliminated. This feature, combined with the small stack spacing (0.345 nm), makes the PEA-4-BZ-D10 a promising candidate for an organic semiconductor with respectable charge carrier mobility in its BSDCLC phase.

However, the PEA-4-BZ-D10 molecule achieves this single-stack mode BSDCLC phase with very low atom efficiency. To cover the four-stack supramolecular column surface, every PEA-4-BZ-D10 molecule needs 62 carbon atoms and 8 oxygen atoms in the flexible peripheral groups which make little contribution to charge transport other than the formation of the phase. In addition, the peripheral alkyl chain with complicated structure needs multiple steps to synthesize, which weakens the material's potential for large-scale industry application.

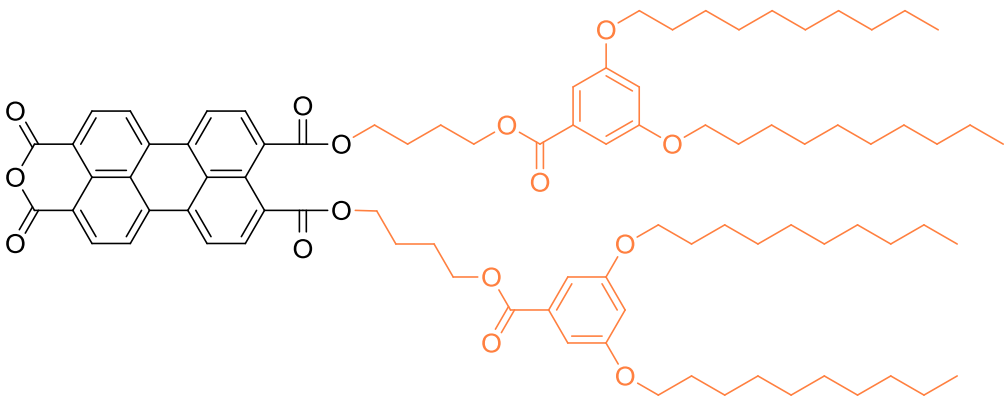

62 carbon atoms + 8 oxygen atoms

Scheme 5.5 Low atom efficiency of PEA-4-BZ-D10

To achieve higher atom efficiency without sacrificing BSDCLC feature, we need to apply an alternative supramolecular engineering strategy. As mentioned before, one approach to achieve the pure four-stack mode is to increase the surface area of the supramolecular column core since larger column surface area could relieve entropy penalty caused by the peripheral chains' tight packing. Alternatively, this entropy penalty could be relieved by decreasing the number of *n*-alkyl chains. Keeping this in mind, we designed and synthesized PEA-10/14-C2.

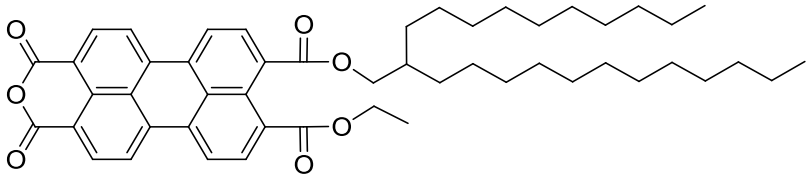

Scheme 5.6 Chemical structure of PEA-10/14-C2

As displayed in **Scheme 5.6**, the PEA-10/14-C2 molecule was designed by replacing one of the branched alkyl chains of PEA-10/14 with an ethyl group. With only one sp^3 branching point in each molecule, the steric hindrance will be effectively weakened to ensure the tight π-stacking. And the branched alkyl chain can ensure the compound's solution processability and phase-forming properties. Compared to

former PEAs, PEA-10/14-C2 has the smallest number of long *n*-alkyl chains, which could also effectively minimize the possibility of experiencing entropy penalty.

At RT, PEA-10/14-C2 presents a DCLC phase when freshly cast from THF solution. The red LC is bright under PLM at RT, and its clearing point is over 300 °C, which is beyond the compound's decomposition temperature. The RT 1D WAXS pattern (**Figure 5.18**) clearly shows PEA-10/14-C2's LC characteristics. And the peak at 1.82 $Å^{-1}$ (d-spacing = 0.345 nm) can be attributed to tightly π-stacked perylene units. The small-angle diffractions were indexed as (10), (11), (20) and (21), and the d-space sequence was close to a hexagonal column packing with inter-column distance of 3.98 nm, which was smaller compared to that of PEA-4-BZ-D10 due to the reduced number of long *n*-alkyl chains. The LC nature is confirmed by the liquid-like *n*-alkyl chains as there are no sharp peaks between 1.3-1.7 $Å^{-1}$.

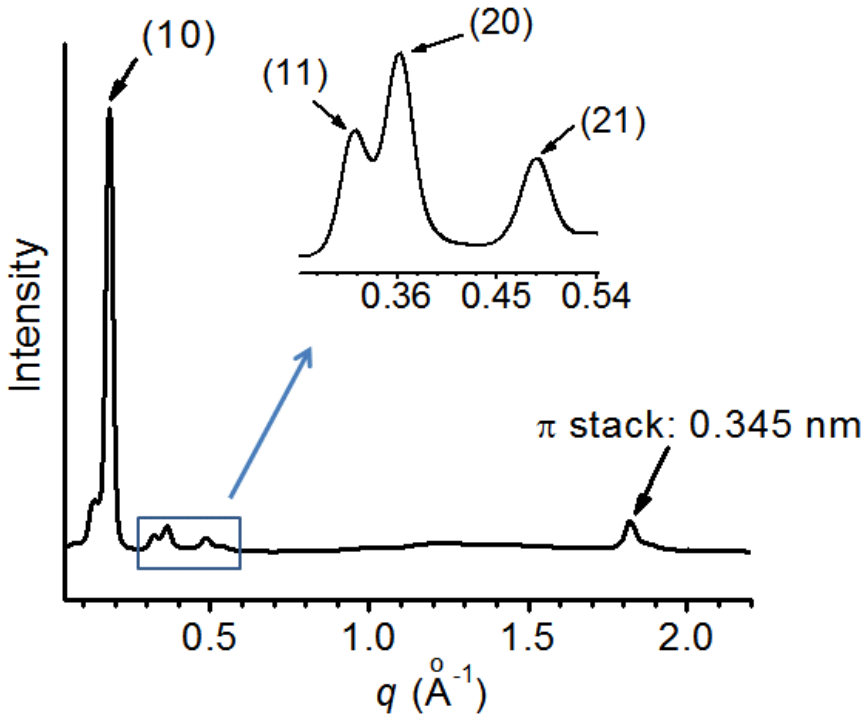

Figure 5.18 1D WAXS pattern of PEA-10/14-C2 at RT

2D WAXS data collected on a well-aligned PEA-10/14-C2 which was readily prepared by mechanical shearing is displayed in **Figure 5.19**. The series of diffractions on the equator originate from supramolecular columns well-aligned along the shearing direction. The diffused halo with d ≈ 0.45 nm suggested that the alkyl chains don't have clear preferential orientation despite oriented columns, which is in agreement with their liquid-like character. The strongest diffraction on the meridian at d = 0.345 nm represents π-stacking order of perylene units, and this is the only meridian diffraction. This indicates that there is no electron density variations in the unit cell along the column axis direction other than what arises from π-π stacking. The experimental density of PEA-10/14-C2 is 1.096 g/cm^3, and if each supramolecular column of PEA-10/14-C2 only consists of one π-stack, the theoretical density should be 0.272 g/cm^3. To match the experimental density, a pure four-stack mode should be adopted in PEA-10/14-C2's BSDCLC phase with the same intra-column/bundle structure. Furthermore, unlike PEA-4-BZ-D10's complicated phase transition behavior and low atom efficiency, PEA-10/14-C2 presents the BSDCLC phase in a broad temperature range with much higher atom efficiency. It could perfectly maintain the LC characteristics even after 1 hour's annealing at 90 °C. The after annealing sample's 2D WAXS pattern is presented in **Figure 5.20**.

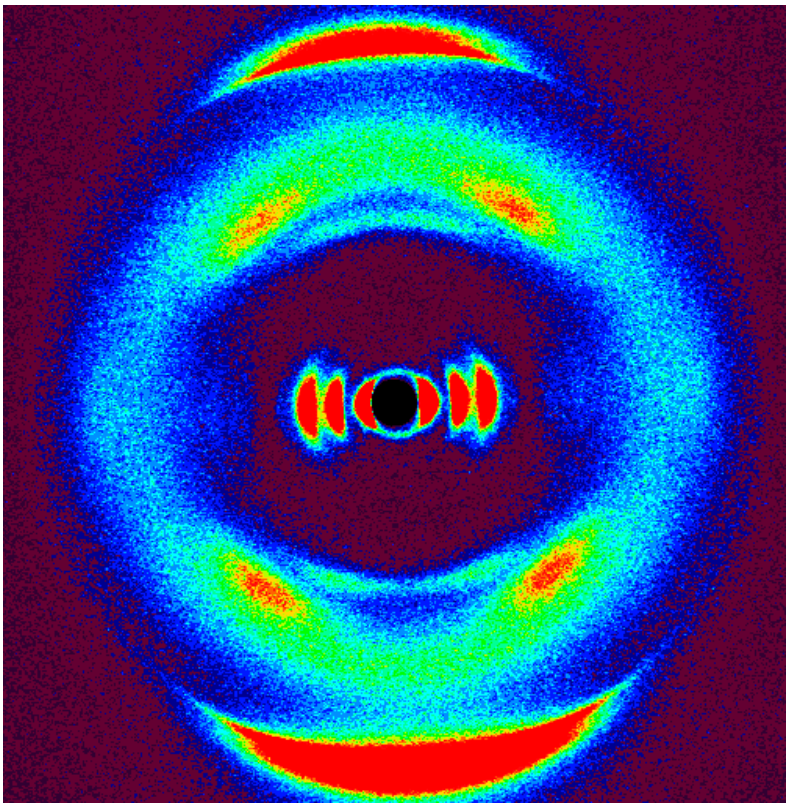

Figure 5.19 2D WAXS pattern of PEA-10/14-C2

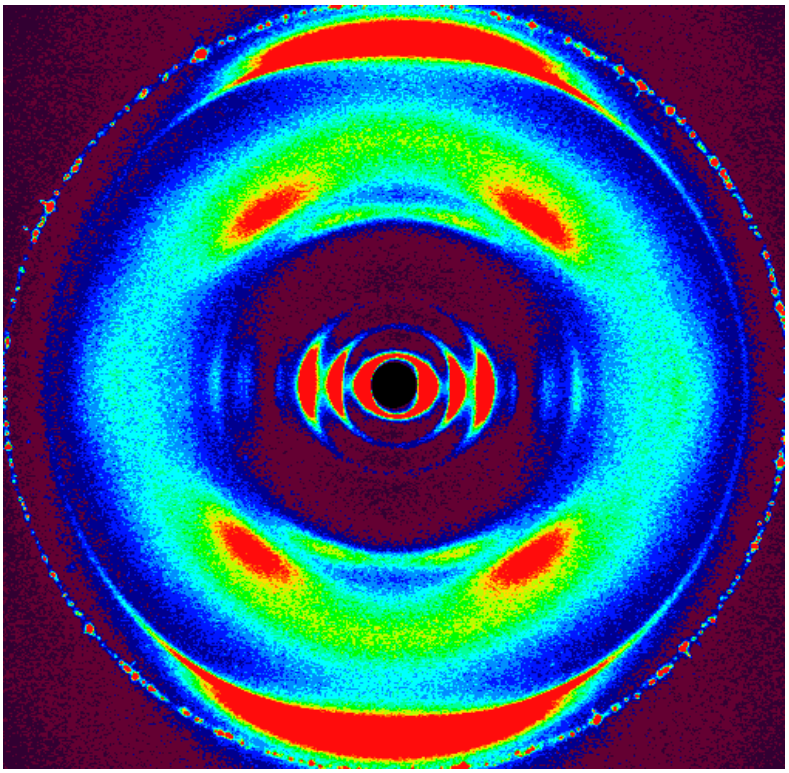

Figure 5.20 2D WAXS pattern of PEA-10/14-C2 after annealed at 90 °C for one hour

5.3 BSDCLC PEA's molecular structure engineering via the tuning of OEG substituents

Motivated by the results of PEA molecular structure engineering by tuning of alkyl chains and the position of branch-points, we present the following study aims to pursue the BSDCLC phase with single stacking mode using a different substituent: oligo ethylene glycol (OEG) chain. Compared to alkyl chains, OEG chains hold a high degree of rotational freedom at the oxygen branching site and the energy difference between so-called "anti" and "gauche" conformations is much smaller. When formed into BSDCLC phase, the peripheral OEG chains are more flexible to choose the most comfortable conformation to cover the supramolecular column core's surface. Keeping this in mind, we designed and synthesized a series of OEG substituted PEAs to investigate their structure properties and phase behavior.

As mentioned in Chapter 3, PEA-diC10 was synthesized using straightforward procedures in our group in 2009. It presents crystalline phase at RT and poor processability. The two *n*-decyl chains in each PEA molecule are not flexible and far from enough to provide the material's good processability and phase-forming properties. Thus, our first try is replacing PEA-diC10's *n*-decyl chain with triethylene glycol chain since their chain lengths are fairly close. Detailed structure characterization was applied to the resulted PEA to see whether it could present unique structure properties.

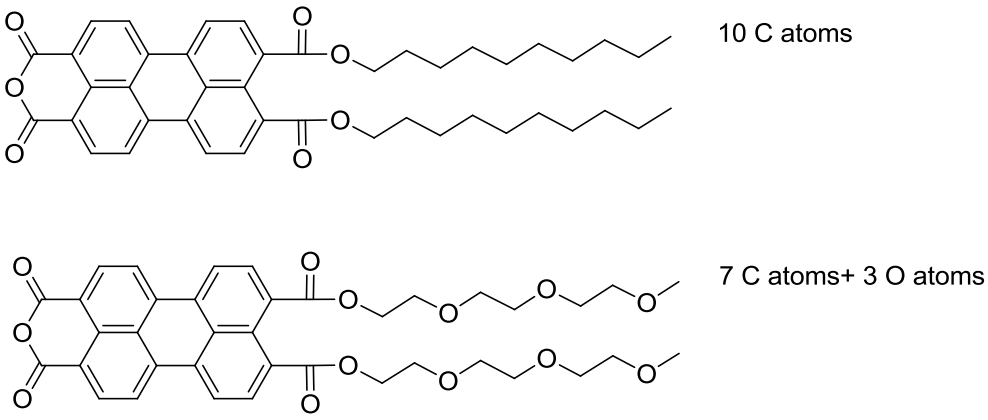

Scheme 5.7 Chemical structure comparison of PEA-3EG and PEA-diC10

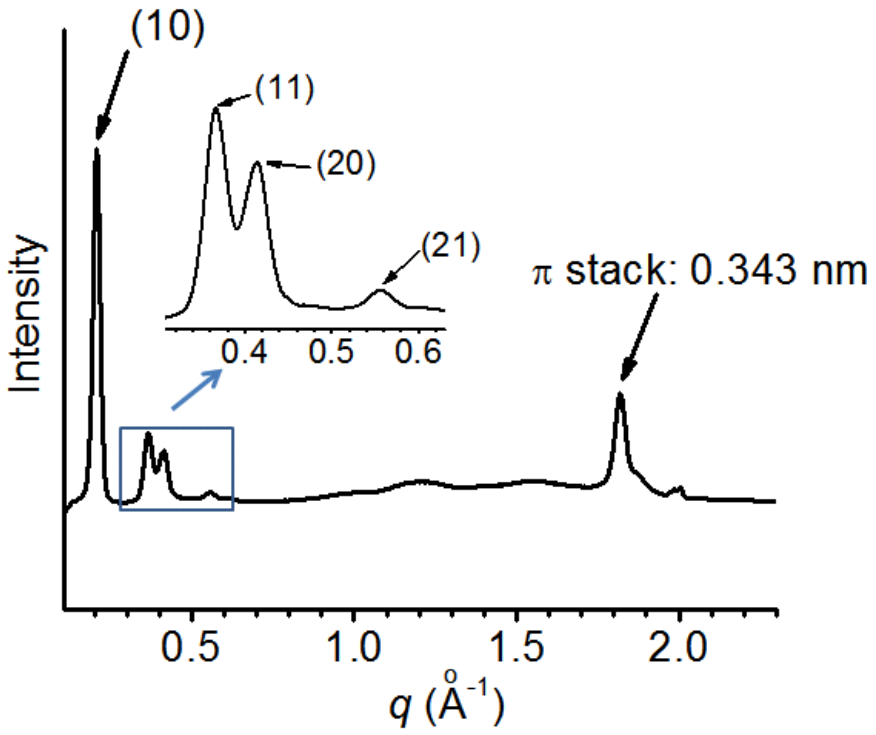

Figure 5.21 1D WAXS pattern of PEA-3EG at RT

Interestingly, PEA-3EG presents DCLC phase when freshly cast from THF solution. The red LC PEA-3EG is bright under PLM at RT and its clearing point is over 300 °C. As shown in **Figure 5.21**, The small-angle diffractions were indexed as (10), (11), (20) and (21) diffractions of a 2D hexagonal lattice with inter-column distance of 3.64 nm because of the sequence of peaks corresponding to a hexagonal

lattice sequence. More detailed intra-column information was obtained from the 2D WAXS pattern which is shown in **Figure 5.22**.

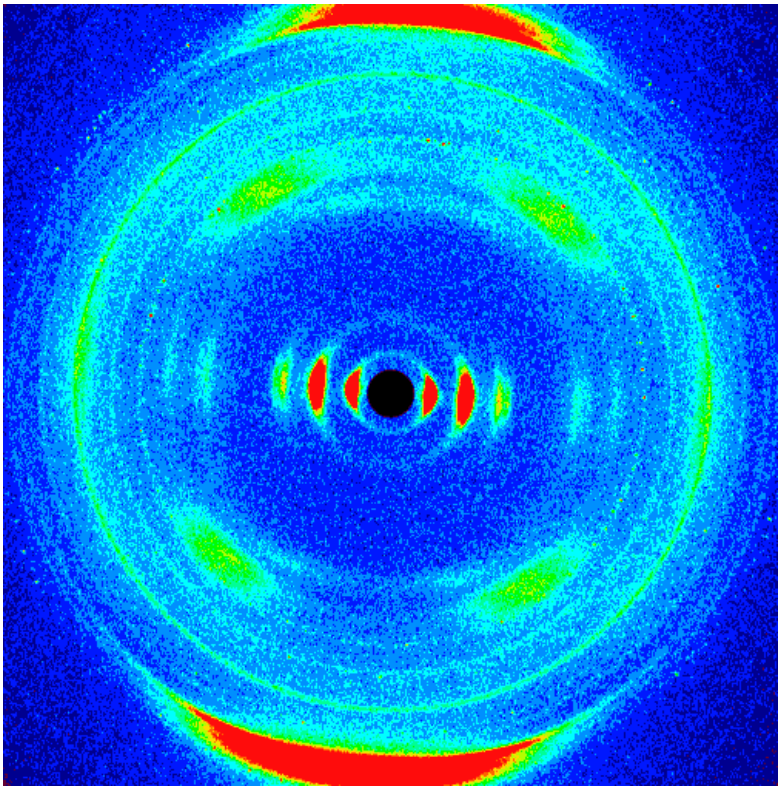

Figure 5.22 2D WAXS pattern of PEA-3EG at RT

The intra-column structure of PEA-3EG, which is presented by the diffused scatterings on the meridian and in the quadrants, is highly similar to those of PEA-4-BZ-D10 and PEA-10/14. And these experimental intra-column diffractions match the simulated pattern fairly well, which confirmed that PEA-3EG molecules self-assemble a BSDCLC phase with a single four-stack packing mode in its RT DCLC phase. Unfortunately, the density of PEA-3EG in RT DCLC phase could not be measured due to its good solubility in water and most of the commonly used organic solvents. In addition, PEA-3EG can not maintain the LC properties for long time, the crystallization happened even at RT. This feature can be detected in **Figure 5.23**. After 12 days at RT, the diffraction peaks between 1.3 and 1.7 $Å^{-1}$ became sharp; this

represents the appearance of a crystalline phase. Its long range column packing (seen from the peaks between 0.3 and 0.6 $Å^{-1}$) also deviated from highly ordered hexagonal column packing.

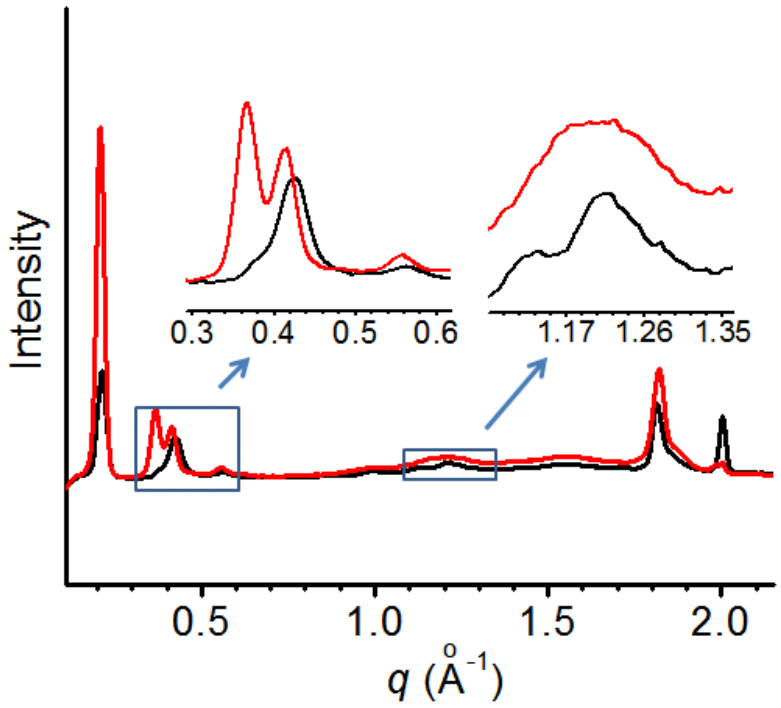

Figure 5.23 1D WAXS patterns of PEA-3EG at RT

: Right after cast from THF solution

: After 12 days

Besides the material's crystallization tendency, the high clearing point of PEA-3EG is a burden for in-depth physical properties investigation. Since the thermotropic behavior of DCLC materials is strongly dependent on the side chain length, the PEA series with longer OEG chains were synthesized. The chemical structures are presented in **Scheme 5.8**.

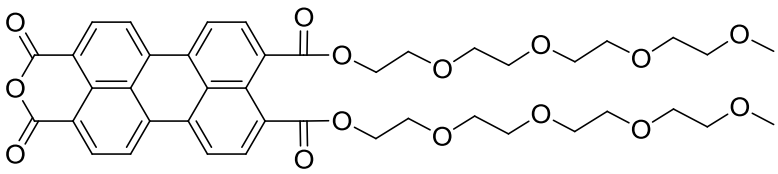

PEA-4EG

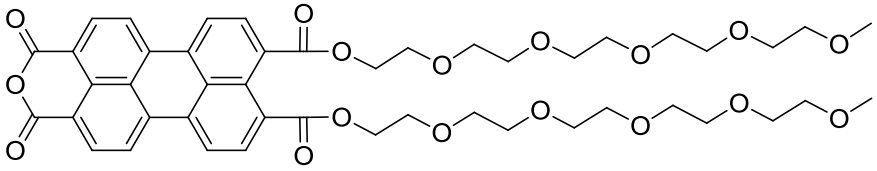

PEA-5EG

Scheme 5.8 The chemical structures of PEA-4EG and PEA-5EG

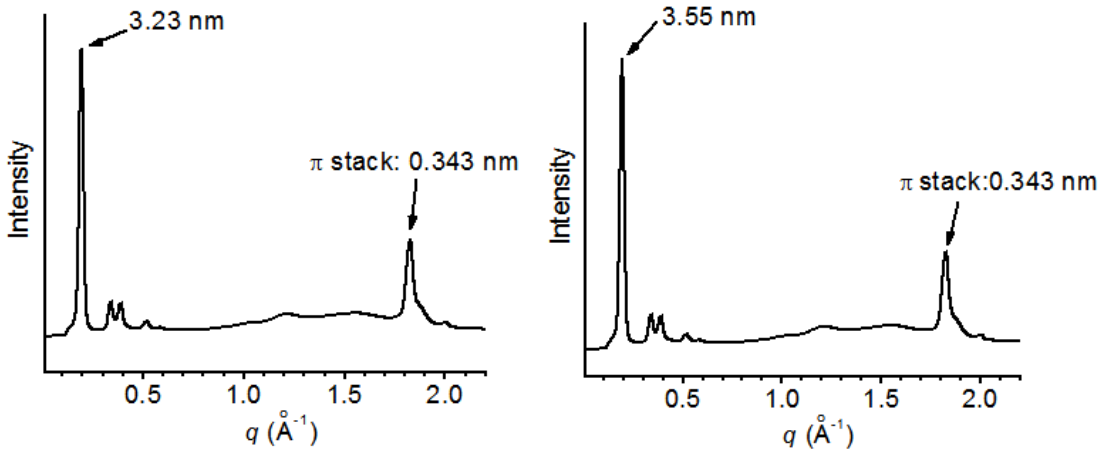

PEA-4EG PEA-5EG

Figure 5.24 1D WAXS patterns of PEA-4EG and PEA-5EG

Some interesting regularity was revealed by comparing 1D WAXS patterns of OEG substituted PEA series. Regardless of the OEG chain length, all the PEAs have the same π-π stacking space (0.343 nm). In terms of the long-range column packing, all the PEAs adopt the symmetric hexagonal packing mode. And the inter-column distance becomes large as the OEG chain length increases.

The intra-column structures of PEA VII and VIII are also highly similar. The

2D WAXS patterns are shown in **Figure 5.25**. We can see that in both of the patterns, the diffused scatterings on the meridian and in the quadrants are almost the same to those of PEA-4-BZ-D10, PEA-10/14 and PEA-3EG. And these experimental intra-column diffractions match the simulated pattern fairly well. So RT BSDCLC phase with pure four-stack mode could be proposed to PEA-4EG and PEA-5EG. And detailed comparison of 2D WAXS patterns between PEA-4-BZ-D10 and PEA-4EG are displayed in **Figure 5.26**. The high degree of similarity between the two WAXS patterns, especially the same meridian and quadrant diffractions, validates the proposed intra-column pure four-stack mode.

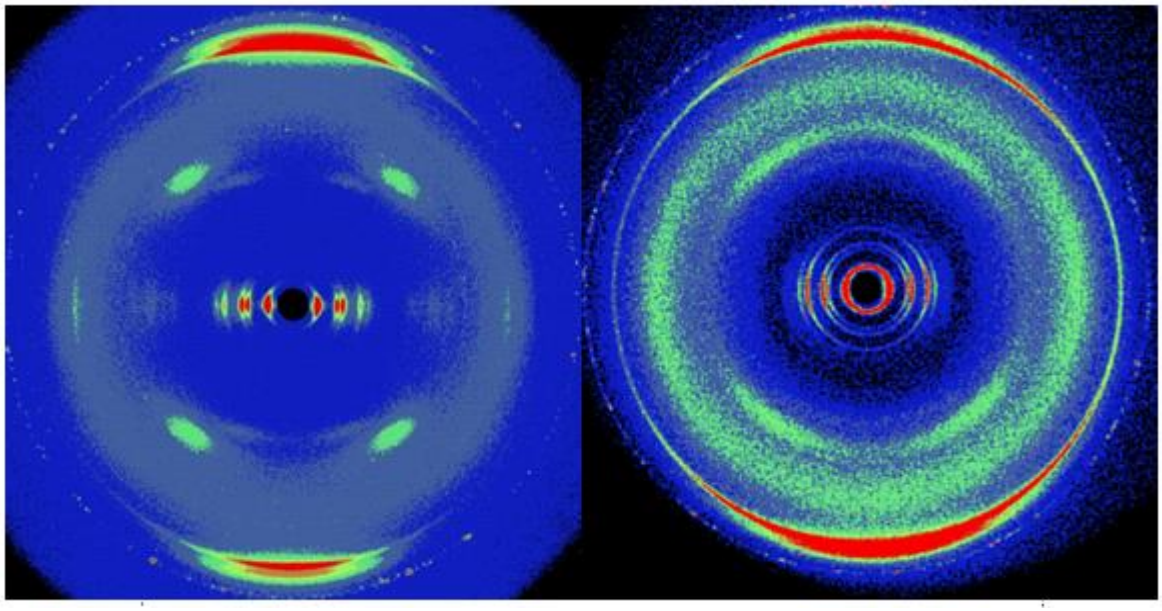

PEA-4EG (thin sample) PEA-5EG (thick sample)

Figure 5.25 2D WAXS patterns of PEA-4EG and PEA-5EG

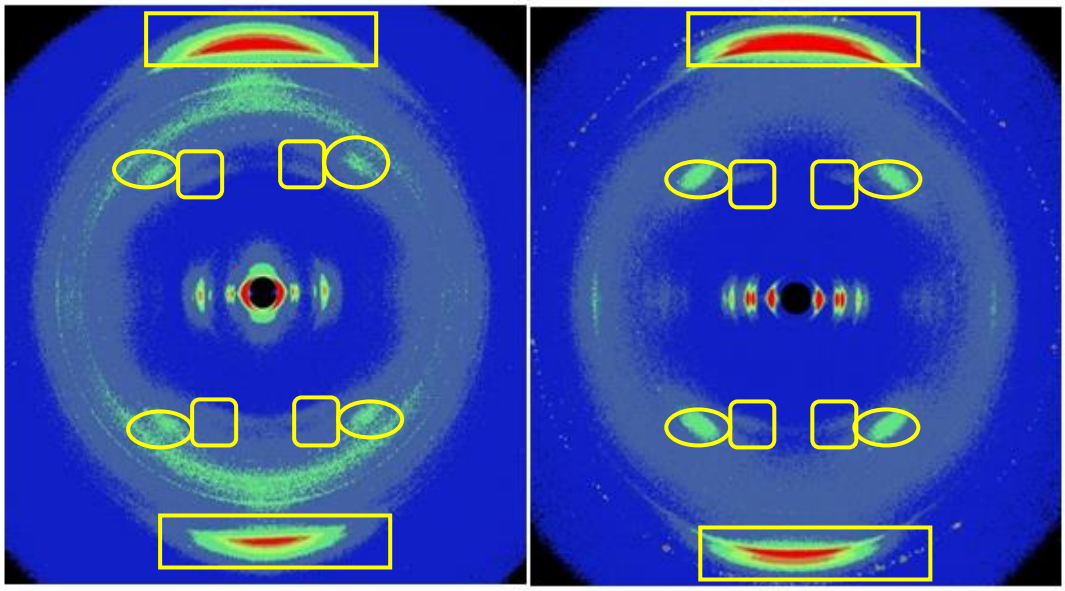

PEA-4-BZ-D10 PEA-4EG

Figure 5.26 Comparison of 2D WAXD patterns of PEA-4-BZ-D10 and PEA-4EG

Unlike PEA-3EG, the crystallization of PEA-4EG and PEA-5EG is very slow at RT. After processed out of THF solution, the samples showed no obvious crystallization even after 30 days. However, the clearing point of PEA-4EG is still above 300 °C. For PEA-5EG, its 294 °C clearing point is already beyond the decomposition temperature. It is worth noticing that the BSDCLC phase with non-detectable crystallinity was achieved by PEA-4EG with high atom efficiency. The comparison is presented in **Figure 5.27**.

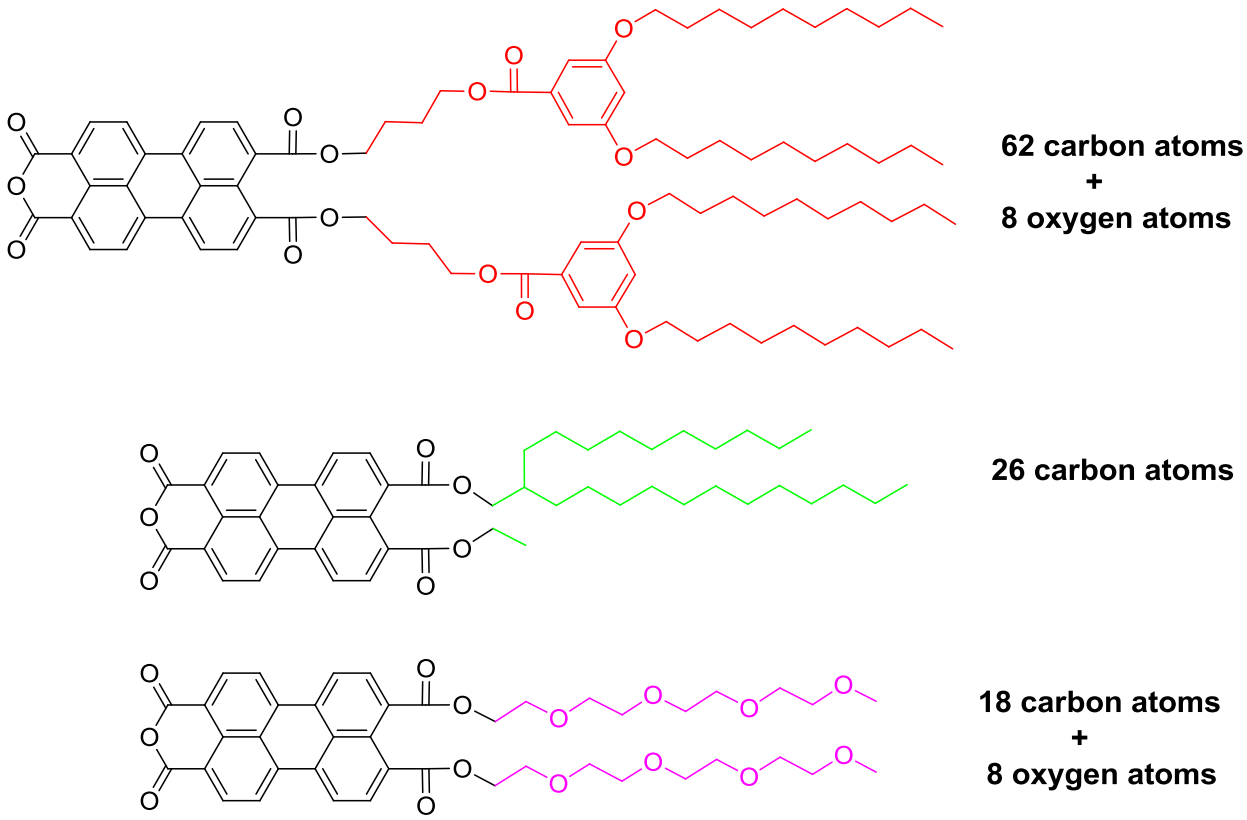

Figure 5.27 Atom efficiency comparisons of PEAs with BSDCLC phases

To achieve a systematic OEG-substituted PEA series and further investigate the short OEG chain's effect on the formation of PEA's BSDCLC phase, PEA-2EG and PEA-1EG was also synthesized and characterized.

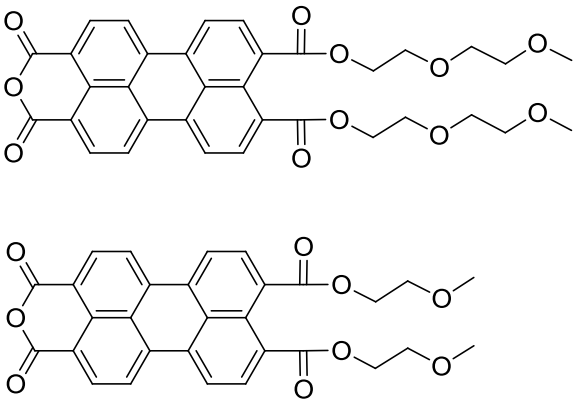

Scheme 5.9 Chemical structures of PEA-2EG and PEA-1EG

As expected, both of PEA-2EG and PEA-1EG showed high degree of crystallinity at RT owing to the short OEG chains. However, when freshly cast from

THF solution at RT, PEA-2EG still presented typical BSDCLC phase with pure four-stack mode. The 2D WAXS pattern of well-aligned sample is displayed in **Figure 5.29**.

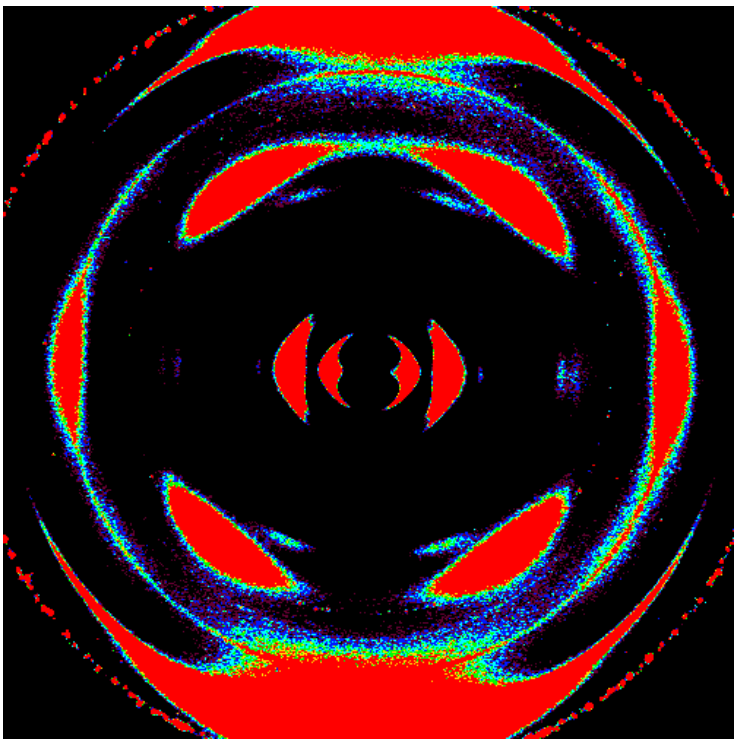

Figure 5.28 2D WAXS pattern of PEA-2EG at RT

However, PEA-2EG's BSDCLC phase can only be maintained for 12 hours at RT. The comparison of 1D WAXS patterns is presented in **Figure 5.29**. As seen from **Figure 5.29**, the diffraction peaks between 1.3 and 1.7 $Å^{-1}$ became sharp; this represents the nature of crystalline phase.

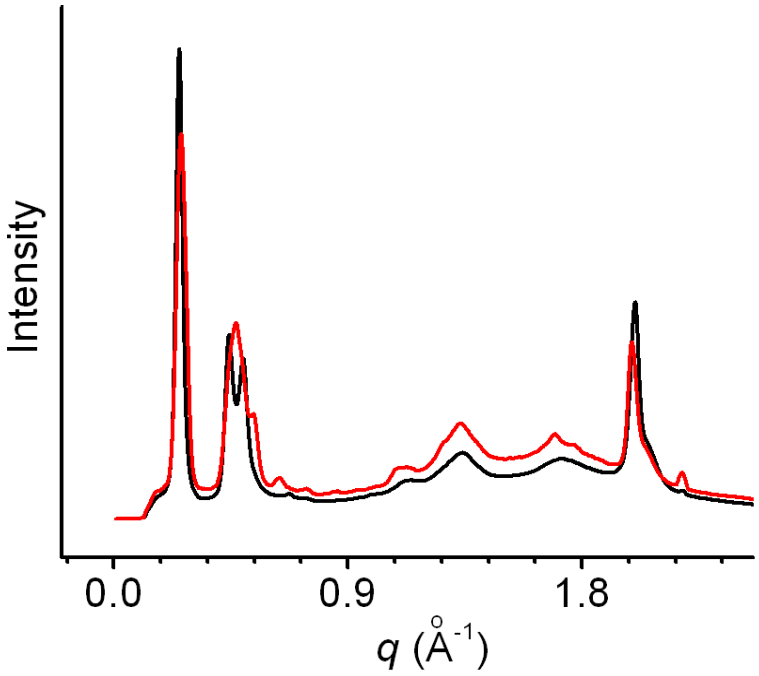

Figure 5.29 1D WAXS patterns of PEA-2EG at RT

: Right after cast from THF solution

: After 12 hours

PEA-1EG showed typical crystalline phase at RT, seen from the 1D WAXS pattern (**Figure 5.30**).

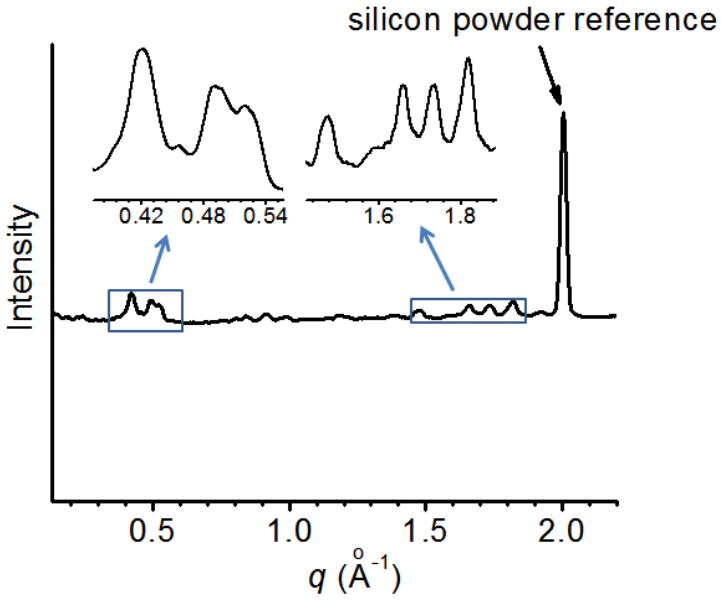

Figure 5.30 1D WAXS patterns of PEA-1EG at RT

It is worth mentioning that PEA-1EG does not present any long range column packing order at RT, the crystalline nature is confirmed by the sharp peaks between 1.3-1.7 $Å^{-1}$.

Finally, in a typical PEA-based BSDCLC phase, the polar heads (anhydride groups) point to the center of the supramolecular column and the column core surface is covered by peripheral flexible chains. Knowing that the desire of peripheral chains to adapt the most comfortable conformation is just one of the major driving forces behind the formation of the composite BSDCLC phase, we want to further investigate the anhydride group's role in the BSDCLC phase formation. To this end, the following three compounds were synthesized according to straightforward procedures. Unlike PEAs, there are no anhydrides groups in all the three compounds. All of them were sticky liquids at RT, and none of them showed any LC properties. This implies that dipole-dipole interaction resulting from anhydride group may play a key role in formation of BSDCLC phase.

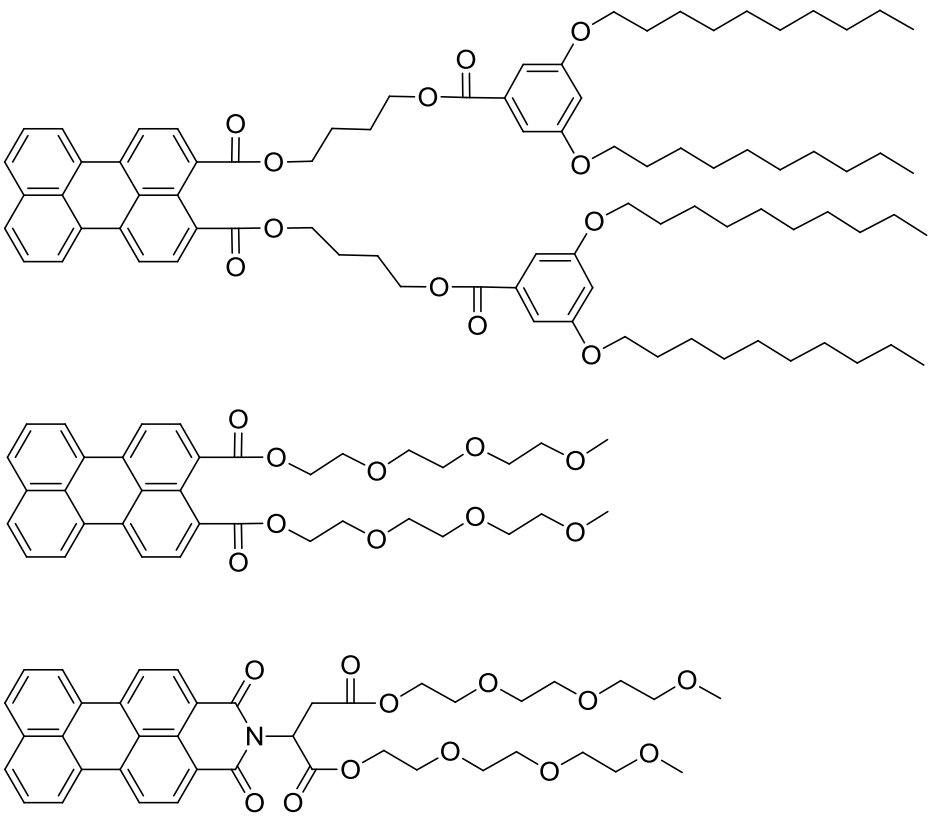

Scheme 5.10 Chemical structures of three asymmetric perylene compounds

5.4 Conclusion

To conclude, we have designed and synthesized a series of PEAs, via the systematic molecular engineering and structure tuning. Structure characterizations and simulation results revealed that PEA-4-BZ-D10, PEA-10/14-C2, PEA-2EG, PEA-3EG, PEA-4EG and PEA-5EG can self-assemble into the unique composite BSDCLC phase involving single stacking modes at RT. The combination of bundle-stack conducting channel, good solution processability, long-range order and tight π-π stacking make these LC materials potential active components in organic electronic devices. Charge carrier mobilities and performance of devices prepared from these PEAs are subject to future investigations. The application of the design principle to other DCLC mesogens may generate more BSDCLC materials with

improved charge transport characteristics. This study has provided a deeper insight into the molecule design and structure tuning of not only discotic columnar liquid crystal materials but also photovoltaic devices.

5.5 Experimental section

Detailed synthesis procedures of PEA-10/14, PEA-BZ-D10, PEA-4-BZ-D10, PEA-2EG and PEA-3EG are discussed in Chapter 3, PEA-10/14-C2 was synthesized by my labmate, Dr. Runkun Sun [9].

2-bromoethyl-3,5-bis(decyloxy) benzoate (I)

A 50 ml round bottom flask was charged 1.7 g (3.9 mmol) 3,5-bis(decyloxy)benzoic acid, 0.5 g (3.9 mmol) potassium carbonate, 0.1 g (0.4 mmol) 18- crown-6 and 10 ml DMSO. The suspension was stirred at 60 °C for 20 minutes and became a clear yellow solution. Subsequently 5.86 g (8 eq) 1,2-dibromoethane was added. The solution was purged with nitrogen for 15 minutes, sealed well and stirred at 60 °C for 12 hours. Then the mixture was poured into 50 ml deionized water, the crude product was extracted using chloroform and purified by column chromatography with 2/1 (v/v) hexane/chloroform as the eluent to afford **I** 0.53 g (26%) as a colorless liquid.

2-methoxyethyl 4-methylbenzenesulfonate (II)

A 500 ml round bottom flask was charged 38 g (0.5 mol) 2-methoxyethanol and 80 ml THF before being cooled to 0 °C in ice bath. The solution was mixed with 90 ml pre-cooled NaOH-aqueous solution (6 mol/L) and stirred in ice bath for 20 minutes. Subsequently 125 ml TsCl-THF solution (3.75 mol/L) was dropped in the

mixture for 2 hours. During dropping, the mixture's temperature was kept at 0~5 °C. The solution was stirred for an additional 2 hours at 0~5 °C, and then poured into 1 L ice water. The crude product was extracted with dichloromethane. Upon evaporation of solvent, the oily product was dried with anhydrous sodium sulfate to afford **II** 86.2 g (75%) as a colorless oily liquid.

2,5,8,11-tetraoxatridecan-13-yl 4-methylbenzenesulfonate (III)

A 100 ml round bottom flask was charged 5 g (24 mmol) 2,5,8,11-tetraoxatridecan-13-ol and 20 ml THF before being cooled to 0 °C in ice bath. The solution was mixed with 6.5 ml pre-cooled NaOH-water solution (5.8 mol/L) and stirred in ice bath for 20 minutes. Subsequently 9 ml TsCl-THF solution (3.75 mol/L) was dropped in the mixture for 2 hours. During dropping, the mixture's temperature was kept at 0~5 °C. The solution was stirred for an additional 2 hours at 0~5 °C, and then poured into 100 ml ice water. The crude product was extracted with dichloromethane. Upon evaporation of solvent, the oily product was dried with anhydrous sodium sulfate to afford **III** 7.14 g (82%) as a colorless oily liquid.

2,5,8,11,14-pentaoxahexadecan-16-yl 4-methylbenzenesulfonate (IV)

A 100 ml round bottom flask was charged 2.52 g (10 mmol) 2,5,8,11,14-pentaoxahexadecan-16-ol and 15 ml THF before being cooled to 0 °C in ice bath. The solution was mixed with 3 ml pre-cooled NaOH-water solution (5.8 mol/L) and stirred in ice bath for 20 minutes. Subsequently 2.5 ml TsCl-THF solution (3.75 mol/L) was dropped in the mixture for 2 hours. During dropping, the mixture's temperature was kept at 0~5 °C. The solution was stirred for an additional 2 hours at

0~5 °C, and then poured into 100 ml ice water. The crude product was extracted with dichloromethane. Upon evaporation of solvent, the oily product was dried with anhydrous sodium sulfate to afford **IV** 3.2 g (79%) as a colorless oily liquid.

perylene-3,4-anhydride-9,10-di-(2-((3,5-bis(decyloxy)benzoyl)oxy)ethyloxycarbonyl) (PEA-2-BZ-D10)

A 25 ml round bottom flask was charged 80 mg (0.2 mmol) 3, 4, 9, 10-perylenetetracarobxyldianhydride, 0.37 g (0.8 mmol) tetrabutylammonium hydroxide (55% aqueous solution) and 4 ml DMSO. The mixture was stirred at 60 °C for 20 minutes. Subsequently 0.33 g (0.61 mmol) **I** dissolved in 3 ml acetone was added to the mixture. The solution was purged with nitrogen for 10 minutes, sealed well and stirred at 50 °C for 24 hours. Then 0.048 g (0.8 mmol) acetic acid was added into the mixture. The solution was stirred for 4 hours at 60 °C and then poured in 50 ml methanol, the crude solid product was collected by suction filtration and purified by column chromatography with chloroform as the eluent to afford 66 mg product (25%) as a red solid.

^{1}H NMR ($CDCl_3$, 600 MHz): δ (ppm) = 8.59 (d, J = 7.808 Hz, 2H, Ar), 8.44 (d, J = 7.806 Hz, 2H, Ar), 8.42 (d, J = 8.347 Hz, 2H, Ar), 8.12 (d, J = 7.809 Hz, 2H, Ar), 7.12 (d, J = 2.35 Hz, 4H, Ar), 6.61 (t, J = 4.85 Hz ,2H, Ar**)**, 4.71 (t, J = 9.53 Hz, 4H, $CO_2C\mathbf{H_2}$), 4.67 (t, J = 9.52 Hz, 4H, $C\mathbf{H_2}\ CO_2$), 3.91 (t, J= 13.09Hz, 4H, $OC\mathbf{H_2}CH_2$), 0.856 (t, J = 14.397 Hz, 6H, $C\mathbf{H_3}$), ^{13}C NMR ($CDCl_3$, 75 MHz): δ (ppm) = 167.635 (ester C=O), 166.244 (ester C=O), 160.16 (anhydride C=O), 136.8 (Ar), 133.5 (Ar), 131.71 (Ar), 130.6 (Ar), 129.2 (Ar), 129 (Ar), 126.1 (Ar), 123.4 (Ar), 122.1 (Ar),

118.1 (Ar), 107.841 (Ar), 77.221 (O**C**H_2CH_2), 68.307 (O**C**H_2CH_2), 62.603 (O**C**H_2CH_2), 31.867(**C**H_2), 29.558 (**C**H_2), 29.539 (**C**H_2), 29.368 (**C**H_2), 29.301 (**C**H_2), 29.167 (**C**H_2),25.995 (**C**H_2), 22.652 (**C**H_2), 14.095 (**C**H_3). HRMS $(M+Na)^+$: calcd for $C_{82}H_{106}O_{15}$ 1330.7532; found 1330.7528.

perylene-3,4-anhydride-9,10-di-(2-2-(2-(2-methoxyethoxy)ethoxy)ethoxy)ethyloxycarbonyl (PEA-4EG)

A 25 ml round bottom flask was charged 196 mg (0.5 mmol) 3, 4, 9, 10-perylenetetracarobxyldianhydride, 0.945 g (2 mmol) tetrabutylammonium hydroxide (55% aqueous solution) and 4 ml DMSO. The mixture was stirred at 60 °C for 20 minutes. Subsequently 0.544 g (1.5 mmol) **III** was added to the mixture. The solution was purged with nitrogen for 10 minutes, sealed well and stirred at 60 °C for 72 hours. Then 0.12 g (2 mmol) acetic acid was added into the mixture. The solution was stirred for 4 hours at 60 °C and then poured in 50 ml saturated potassium chloride aqueous solution, the crude solid product was collected by suction filtration and purified by column chromatography with 25/1 (v/v) chloroform/methanol as the eluent to afford 59 mg product (15%) as a red solid.

^{1}H NMR ($CDCl_3$, 600 MHz): δ (ppm) = 8.59 (d, J = 8.38 Hz, 2H, Ar), 8.42 (d, J = 8.11 Hz, 2H, Ar), 8.39 (d, J = 8.01 Hz, 2H, Ar), 8.11 (d, J = 7.57 Hz, 2H, Ar), 4.51 (t, J = 9.36 Hz, 4H, COOC**H$_2$**), 3.88 (t, J = 10.06 Hz ,4H, $COOCH_2C$**H$_2$**O**)**, ^{13}C NMR ($CDCl_3$, 75 MHz): δ (ppm) = 167.858 (ester C=O), 160.366 (anhydride C=O), 135.56 (Ar), 133.986 (Ar), 131.811 (Ar), 125.46 (Ar), 122.943 (Ar), 117.276 (Ar), 77.251 (O**C**H_2CH_2), 70.754 (O**C**H_2CH_2), 70.646 (O**C**H_2CH_2), 68.886 (O**C**H_2CH_2), 64.411

(O**C**H_2CH_2), 59.875 (O**C**H_3).

perylene-3,4-anhydride-9,10-di-2-(2-(2-(2-(2-methoxyethoxy)ethoxy)ethoxy)ethoxy)ethyloxycarbonyl (PEA-5EG)

A 25 ml round bottom flask was charged 96 mg (0.246 mmol) 3, 4, 9, 10-perylenetetracarobxyldianhydride, 0.48 g (0.99 mmol) tetrabutylammonium hydroxide (55% aqueous solution) and 4 ml DMSO. The mixture was stirred at 60 °C for 20 minutes. Subsequently 300 mg (0.74 mmol) **IV** was added to the mixture. The solution was purged with nitrogen for 10 minutes, sealed well and stirred at 60 °C for 72 hours. Then 0.06 g (1 mmol) acetic acid was added into the mixture. The solution was stirred for 4 hours at 60 °C and then the solvents were removed by low pressure evaporation, the crude solid product was purified by column chromatography with 25/1 (v/v) chloroform/methanol as the eluent to afford 26 mg product (12%) as a red solid.

^{1}H NMR ($CDCl_3$, 600 MHz): δ (ppm) = 8.46 (d, J = 7.96 Hz, 2H, Ar), 8.25 (d, J = 4.78 Hz, 2H, Ar), 8.23 (d, J = 4.78 Hz, 2H, Ar), 8.02 (d, J = 7.96 Hz, 2H, Ar), 4.52 (t, J = 9.87 Hz, 4H, COOC**H$_2$**), 3.89 (t, J = 9.99 Hz ,4H, COOCH_2C**H$_2$**O**)**, ^{13}C NMR ($CDCl_3$, 75 MHz): δ (ppm) = 167.825 (ester C=O), 160.125 (anhydride C=O), 136.636 (Ar), 133.37 (Ar), 132.017 (Ar), 131.314 (Ar), 123.226 (Ar), 117.830 (Ar), 77.247 (O**C**H_2CH_2), 70.635 (O**C**H_2CH_2), 70.55 (O**C**H_2CH_2), 68.88 (O**C**H_2CH_2), 64.804 (O**C**H_2CH_2), 59.01 (O**C**H_3).

perylene-3,4-anhydride-9,10-di-(2-methoxyethoxycarbonyl) (PEA-1EG)

A 25 ml round bottom flask was charged 393 mg (1 mmol) 3, 4, 9,

10-perylenetetracarobxyldianhydride, 1.89 g (4 mmol) tetrabutylammonium hydroxide (55% aqueous solution) and 6 ml DMSO. The mixture was stirred at 60 °C for 20 minutes. Subsequently 0.69 g (3 mmol) **II** was added to the mixture. The solution was purged with nitrogen for 10 minutes, sealed well and stirred at 60 °C for 36 hours. Then 0.2 g (3.6 mmol) acetic acid was added into the mixture. The solution was stirred for 4 hours at 60 °C and then poured in 100 ml saturated potassium chloride aqueous solution, the crude solid product was collected by suction filtration and purified by column chromatography with 20/1 (v/v) chloroform/methanol as the eluent to afford 220 mg product (42%) as a red solid.

^{1}H NMR ($CDCl_3$, 600 MHz): δ (ppm) = 8.60 (d, J = 7.92 Hz, 2H, Ar), 8.45 (d, J = 8.69 Hz, 2H, Ar), 8.41 (d, J = 8.16 Hz, 2H, Ar), 8.12 (d, J = 7.86 Hz, 2H, Ar), 4.55 (t, J = 9.97 Hz, 4H, COOC**H$_2$**), 3.96 (t, J = 9.76 Hz ,4H, $COOCH_2C$**H$_2$**O**)**.

perylene-3,4-di-(4-((3,5-bis(decyloxy)benzoyl)oxy)butyloxycarbonyl)

A 25 ml round bottom flask was charged 60 mg (0.186 mmol) 3, 4-perylenedicarobxylanhydride, 0.18 g (0.373 mmol) tetrabutylammonium hydroxide (55% aqueous solution) and 3 ml DMSO. The mixture was stirred at RT for 1 hour. Subsequently 0.23 g (0.38 mmol) 4-bromobutyl-3,5-bis(decyloxy) benzoate dissolved in 2 ml acetone was added to the mixture. The solution was purged with nitrogen for 10 minutes, sealed well and stirred at RT for 12 hours. Then the solution was poured in 50 ml methanol, the crude product was collected by suction filtration and purified by column chromatography with 2/1 (v/v) chloroform/hexane as the eluent to afford 0.23 g product (96%) as a dark red sticky liquid.

^{1}H NMR ($CDCl_3$, 600 MHz): δ (ppm) = 7.41 (d, J = 7.33 Hz, 2H, Ar), 7.44 (d, J = 7.39 Hz, 2H, Ar), 7.92 (d, J = 7.88 Hz, 2H, Ar), 7.97 (d, J = 7.92 Hz, 2H, Ar), 8.16 (d, J = 8.02 Hz, 2H, Ar), 7.16 (d, J = 2.49 Hz, 4H, Ar), 6.63 (t, J = 4.56 Hz ,2H, Ar**)**, 4.46 (t, J = 11.39 Hz, 4H, $CO_2C\mathbf{H_2}$), 4.42 (t, J = 11.62 Hz, 4H, $C\mathbf{H_2}\ CO_2$), 3.61 (t, J= 12.72Hz, 4H, $OC\mathbf{H_2}CH_2$), 0.88 (t, J = 14.92 Hz, 6H, $C\mathbf{H_3}$), ^{13}C NMR ($CDCl_3$, 75 MHz): δ (ppm) = 168.2 (ester C=O), 166.6 (ester C=O), 134.5 (Ar), 132.2 (Ar), 131.6 (Ar), 130.2 (Ar), 128.6 (Ar), 127.2 (Ar), 125.4 (Ar),126.5 (Ar), 122.1 (Ar), 119.23 (Ar), 107.65 (Ar), 105.58 (Ar), 77.1 ($O\mathbf{C}H_2CH_2$), 68.72 ($O\mathbf{C}H_2CH_2$), 64.64 ($O\mathbf{C}H_2CH_2$), 31.91($\mathbf{C}H_2$), 29.72 ($\mathbf{C}H_2$), 29.65 ($\mathbf{C}H_2$), 29.41 ($\mathbf{C}H_2$), 29.21 ($\mathbf{C}H_2$), 26.07 ($\mathbf{C}H_2$), 25.59 ($\mathbf{C}H_2$), 25.46 ($\mathbf{C}H_2$), 22.68 ($\mathbf{C}H_2$), 14.12 ($\mathbf{C}H_3$).

perylene-3,4 -di-(2-(2-(2-methoxyethoxy)ethoxy)ethyloxycarbonyl)

A 25 ml round bottom flask was charged 60 mg (0.186 mmol) 3, 4-perylenedicarobxylanhydride, 0.18 g (0.373 mmol) tetrabutylammonium hydroxide (55% aqueous solution) and 3 ml DMSO. The mixture was stirred at RT for 1 hour. Subsequently 0.125 g (0.38 mmol) 2-(2-(2-methoxyethoxy)ethoxy)ethyl 4-methylbenzenesulfonate was added to the mixture. The solution was purged with nitrogen for 10 minutes, sealed well and stirred at RT for 12 hours. Then the solution was poured in 50 ml saturated potassium chloride aqueous solution, the crude solid product was collected by suction filtration and purified by column chromatography with 25/1 (v/v) chloroform/methanol as the eluent to afford 108 mg (92%) product as a dark red sticky liquid.

^{1}H NMR ($CDCl_3$, 600 MHz): δ (ppm) = 7.43 (d, J = 7.39 Hz, 2H, Ar), 7.47 (d,

J = 7.41 Hz, 2H, Ar), 7.91 (d, J = 7.89 Hz, 2H, Ar), 7.94 (d, J = 7.89 Hz, 2H, Ar), 8.15 (d, J = 8.03 Hz, 2H, Ar), 4.51 (t, J = 9.77 Hz, 4H, COOC**H$_2$**), 3.90 (t, J = 9.89 Hz ,4H, COOCH$_2$C**H$_2$O)**, ^{13}C NMR ($CDCl_3$, 75 MHz): δ (ppm) = 168.6 (ester C=O), 134.2 (Ar), 133.2 (Ar), 131.3 (Ar), 130.1 (Ar), 127.9 (Ar), 127.2 (Ar), 125.6 (Ar),124.5 (Ar), 77.2 (O**C**H$_2$CH$_2$), 70.9 (O**C**H$_2$CH$_2$), 70.7 (O**C**H$_2$CH$_2$), 68.5(O**C**H$_2$CH$_2$), 64.7 (O**C**H$_2$CH$_2$), 59.1 (O**C**H$_3$).

***N*-(2-succinicacid)-perylene-3,4-dicarboximide**

A 10 ml Schlenk flask was charged with 100 mg (0.31 mmol) 3, 4-perylenedicarobxylanhydride, 46 mg (0.33 mmol) 2-aminosuccinic acid and 1 g imidazole. The mixture was purged with argon for 15 minutes before being heated to 125 °C for 3 hours. Then the mixture was cooled to 90 °C and transferred into 50 ml deionized water. The red solution was acidified using phosphoric acid until PH=3. The red solid was collected by suction filtration and dried in a vacuum at 75 °C. 128 mg (95%) dark red solid product was obtained.

bis(2-(2-(2-methoxyethoxy)ethoxy)ethyl)-N-(2-succinicate)-perylene-3,4-dicarboximide

A 25 ml round bottom flask was charged 128 mg (0.29 mmol) N-(2-aminosuccinicacid)-perylene-3,4-dicarboximide, 0.28 g (0.59 mmol) tetrabutylammonium hydroxide (55% aqueous solution) and 3 ml DMSO. The mixture was stirred at RT for 20 minutes. Subsequently 0.17 g (0.6 mmol) 2-(2-(2-methoxyethoxy)ethoxy)ethyl 4-methylbenzenesulfonate was added to the mixture. The solution was purged with nitrogen for 10 minutes, sealed well and stirred

at RT for 12 hours. Then the solution was poured in 50 ml saturated potassium chloride aqueous solution, the crude solid product was collected by suction filtration and purified by column chromatography with 25/1 (v/v) chloroform/methanol as the eluent to afford 205 mg (94%) product as a dark red sticky liquid.

^{1}H NMR ($CDCl_3$, 600 MHz): δ (ppm) = 7.39 (d, J = 7.35 Hz, 2H, Ar), 7.42 (d, J = 7.36 Hz, 2H, Ar), 7.92 (d, J = 7.88 Hz, 2H, Ar), 7.97 (d, J = 7.87 Hz, 2H, Ar), 8.16 (d, J = 8.08 Hz, 2H, Ar), 5.08 (t, J= 9.61Hz, 1H, NC**H**CH_2), 4.52 (t, J = 9.81 Hz, 4H, COOC**H$_2$**), 3.88 (t, J = 9.81 Hz ,4H, $COOCH_2C$**H$_2$O)**,3.06 (d, J=6.88 Hz, 2H, NCHC**H$_2$**), ^{13}C NMR ($CDCl_3$, 75 MHz): δ (ppm) = 171.9 (ester C=O), 169.6 (ester C=O), 134.1 (Ar), 133.2 (Ar), 131.3 (Ar), 130.1 (Ar), 127.9 (Ar), 127.2 (Ar), 125.6 (Ar),124.5 (Ar), 77.2 (O**C**H_2CH_2), 70.9 (O**C**H_2CH_2), 70.7 (O**C**H_2CH_2), 68.5(O**C**H_2CH_2), 64.7 (O**C**H_2CH_2), 58.2 (N**C**HCH_2), 59.1 (O**C**H_3), 33.9 (NCH**C**H_2).

BIBLIOGRAPHY

CHAPTER 1

Part I

[1] Fenton, B. E.; Parker, J. M.; Wright, P. V. *Polymer*, **1973**, 14, 589.

[2] Wright, P. V. Br. *Polym. J.* **1975**, 7, 319.

[3] Qizhen Xiao, Xingzhu Wang,Wen Li, Zhaohui Li, Tianjing Zhang, Hailiang Zhang. *Journal of Membrane Science*, **2009**, 334, 117.

[4] H L Wang, H M Kao, M Digar et al. *Macromolecules*, **2001**, 34, 529.

[5] D.R. Sadoway . *Journal of Power Sources,* **2004**, 129, 1.

[6] Mitsuru Higa, Kazuaki Yaguchi, Ryousuke Kitani. *Electrochimica Acta,* **2010**, 55, 1380.

[7] R Hooper, L J Lyons, D A Moline et al. *Organometallics,* **1999**, 18, 3249.

[8] Yongku Kang, Namjung Cho, Kun-Ae Noh, Jeong soo Kim, Changjin Lee. *Journal of Power Sources,* **2005**, 146, 171.

[9] Yongku Kang, Kwangjo Cheong, Kun-Ae Noh, Changjin Lee, Do-Young Seung. *Journal of Power Sources,* **2003**, 119, 432.

[10] L. Charles Hardy and Duward F. Shiver, *J. Am. Chem. Soc*. **1986**, 108, 2887.

[11] Atsushi Nishimoto, Kunihiro Agehara, Noriyuki Furuya et al. *Macromolecules* **1999**, 32, 1541.

[12] Micah K. Stowe, Ping Liu, and Gregory L. Baker, *Chem. Mater*, **2005**, 17, 6555.

[13] Hanjun Zhang, Sunil Kulkarni, and Stephanie L. Wunder，*J. Phys. Chem. B*, **2007**, 111, 3583.

[14] Braja K. Mandal, Robert Filler, *Journal of Fluorine Chemistry,* **2005**, 126, 845.

[15] Zlatka Stoeva, Isabelle Martin-Litas, Peter G. Bruce et al. *J. Am. Chem. Soc.* **2003**, 125, 4619.

Part II

[1] S. Chandrasekhar, B. K. Sadashiva, K. A. Suresh, *Pramana*, **1977**, 9, 471.

[2] J. P. Straley, *Phys. Rev*. *A* **1974**, 10, 1881.

[3] M. O'Neill, S. M. Kelly, *Adv. Mate*r. **2003**, 15, 1135.

[4] N. R. Armstrong, B. Kippelen, D. F. O'Brien, S. M. Marder, J.-L. Bredas, *Proceedings—NCPV Program Review Meeting, Lakewood,* **2001**, 328.

[5] S. Kumar, *Curr. Sci.* **2002**, 82, 256.

[6] D. Hertel, C. D. Müllen, K. Meerholz, *Chem. Unserer Zeit*, **2005**, 39, 336.

[7] I. Seguy, P. Destruel, H. Bock, *Synth. Met*. **2000**, 111, 15.

[8] J. Kopitzke, J. H. Wendorff, *Chem. Unserer Zeit* **2000**, 34, 4.

[9] T. Kato, N. Mizoshita , K. Kishimoto , *Angew. Chem. Int. Ed*. **2006**, 45, 38.

[10] J. W. Goodby. et al, *Angew. Chem. Int. Ed*. **2008**, 47, 2754.

[11] W. Pisula, M. Zorn, J. Y. Chang, K. Müllen, R. Zentel, *Macromol. Rapid Commun*. **2009**, 30, 1179.

[12] M. O'Neill, S. M. Kelly, *Adv. Mater.* **2003**, 15, 1135.

[13] Y. Shimizu, K. Oikawa, K. I. Nakayama, D. Guillon, *J. Mater. Chem*. **2007**, 17, 4223

[14] M. Funahashi, *Polym. J.* **2009**, 41, 459.

[15] D. Philp, J. F. Stoddart , *Angew. Chem., Int. Ed*. **1996**, 35, 1155.

[16] Wojciech Pisula, Xinliang Feng, Klaus Müllen, *Adv. Mater.* **2010**, 22, 3634.

[17] Z. Chen, V. Stepanenko, V. Dehm, P. Prins, F. Wurthner, *Chem. Eur. J.* **2007**, 13, 436.

[18] D. Adam, P. Schuhmacher, J. Simmerer, L. Haussling, K. Siemensmeyer, K. H. Etzbach, H. Ringsdorf and D. Haarer, *Nature*, **1994**, 371,141.

[19] A. M. van de Craats, N. Stutzmann, O. Bunk, M. M. Nielsen, M.Watson, K. Müllen, H. D. Chanzy, H. Sirringhaus and R. H. Friend, *Adv.Mater.* **2003**, **15**, 495.

[20] L. Schmidt-Mende, A. Fechtenkötter, K. Müllen, E. Moons, R. H. Friend and J. D. MacKenzie, *Science*, **2001**,293, 1119.

[21] Y. Sagara, S. Yamane, T. Mutai, K. Araki, T. Kato, *Adv. Funct. Mater*. **2009**, 19, 1869.

[22] T. Ikeda, J. Mamiya , Y. Yu , *Angew. Chem.Int. Ed*. **2007**, 46, 506.

[23] S. Kutsumizu, M. Yamada , T. Yamaguchi, K. Tanaka, R. Akiyama , *J. Am. Chem. Soc*. **2003**, 125, 2858.

[24] M. I. Boamfa, M. W. Kim, J. C. Maan, T. Rasing, *Nature* **2003**, 421, 149.

[25] J. Piris, W. Pisula, A. Tracz, T. Pakula, K. Müllen J. M. Warman, *Liq. Cryst*. **2004**, 31, 993.

[26] Constanza Ruiz. et al, *J. Phys. Chem. Lett.* **2012**, 3, 1428.

[27] Channabasaveshwar V. Yelamaggad, Ammathnadu S. Achalkumar, D. S. Shankar Rao, and S. Krishna Prasad, *J. Org. Chem*. **2007**, 72, 8308.

[28] A. J. J. M. van Breemen, et al, *J. Am. Chem. Soc*. **2006**, 128, 2336.

[29] K. Hatsusaka, K. Ohta, I. Yamamoto, H. Shirai , *J. Mater. Chem*. **2001**, 11, 423

[30] S. Sergeyev, O. Debever, E. Pouzet , Y. H. Geerts, *J. Mater. Chem.* **2007**, 29, 3002.

[31] B. Tylleman, et al, *Chem. Mater*. **2009**, 21, 2789

[32] C. F. Vannostrum , S. J. Picken , A. J. Schouten , R. J. M. Nolte , *J. Am. Chem. Soc.* **1995,** *117,* 9957.

[33] G. R. J. Müller, C. Meiners, V. Enkelmann , Y. Geerts , K. Müllen, *J. Mater. Chem*. **1998**, 8, 61.

[34] K. Balakrishnan, A. Datar , T. Naddo, J. Huang , R. Oitker , M. Yen , J. Zhao , L. Zang , *J. Am. Chem. Soc.* **2006** , 128 , 7390.

[35] Shubin Yang, Robert E. Bachman, Xinliang Feng, and Klaus Müllen, *Acc. Chem. Res*. **2013**, 46, 116.

[36] Long Chen, Klaus Müllen. et al *J. Am. Chem. Soc*. **2012**, 134, 17869.

[37] J. S. Wu , W. Pisula , K. Müllen , *Chem. Rev.* **2007**, 107, 718 .

[38] Cornelus F. van Nostrum, Stephen J. Picken,' Arend-Jan Schouten and Roeland J. M. Nolte, *J. Am. Chem. Soc*. **1995**,117, 9957.

[39] Paul Smolenyak, Rebecca Peterson, Ken Nebesny, Michael To1rker, David F. O'Brien, Neal R. Armstrong. *J. Am. Chem. Soc.* **1999**, 121, 8628.

[40] Gabin Gbabode, Claire Amato, Claudine Buess-Herman, Vincent Lemaur, Sergey Sergeyev. *Chem. Mater*, **2009**, 21, 13.

[41] Anick M. van de Craats, John M. Warman, Andreas Fechtenkötter, Johann D. Brand, Martha A. Harbison, Klaus Müllen. *Adv. Mater.* **1999**, 11, 17.

[42] L. Schmidt-Mende, A. Fechtenkötter, K. Müllen, E. Moons, R. H. Friend, J. D. MacKenzie, *Science.* **2001**, 293, 1119.

[43] Sergeyev, S.; Pisula, W., Geerts, Y. H. *Chem. Soc. Rev.* **2007**, *36*, 1902.

[44] M. O'Neill, S. M. Kelly, *Adv .Mater.* **2003**, 15, 1135.

[45] Wurthner, F. *Chem. Commun.* **2004**, 1564 and the references therein.

[46] Zesheng An, Junsheng Yu, Seth R. Marder, *Adv. Mater*. **2005**, 17, 2580.

[47] Virgil Percec. et al, *J. Am. Chem. Soc*. **2011**, 133, 12197.

[48] X. Feng , W. Pisula , M. Takase , X. Dou , V. Enkelmann , M. Wagner , N. Ding K. Müllen , *Chem. Mater.* **2008,** *20,* 2872.

[49] V. Percec. et al, *Nature,* **2002**, 419, 384

[50] Virgil Percec. et al, *J. Am. Chem. Soc.*, **2004**, *126*, 6078.

[51] Kreouzis, T. et al. *J. Chem. Phys.* **2001**, 114, 1797.

[52] Shiyanovskaya, I., Singer, K. D. et al, *Phys. Rev. E*. **2002**, 65, 041715.

[53] Zhaohui Wang, Mark D. Watson, Jishan Wu and Klaus Müllen*, *Chem. Commun*. **2004**, 336.

CHAPTER 2

[1] Richard Hooper et al, *Macromolecules* **2001**, 34, 931.

[2] Micah K. Stowe, Ping Liu, and Gregory L. Baker, *Chem. Mater*, **2005**, 17, 6555.

[3] Hou X, Siow K.S. *Polymer* **2000**; 41:8689.

[4] Sarhan, A. A., Abdelaal, M. Y.; Ali, M. M. *Polymer* **1998**, 40, 233.

[5] Abdelaal, M. Y.; Kenawy, I. M. M.; Hafez, M. A. H. *J. Appl. Polym. Sci*. **2000**, 77, 3044.

[6] Sarhan, A. A.; El-Shehawy, A. A.; Abdelaal, M. Y. *React. Funct. Polym.* **2002**, 50, 139.

[7] Vogl, O. *Russian Pure Appl. Chem.* **1979**, 51, 2409.

[8] Gibson, H. W.; Bailey, F. C. *Macromolecules* **1976**, 9, 688.

[9] Han, X.; Shanks, G. R. A.; Pavel, D. *Macromol. Chem. Phys*. **2004**, 205, 743.

[10] T. Nishikubo, T. Iizawa, Y. Mizutani, M. Okawara, Makromol. *Chem. Rapid Commun*. **1982**, 3, 617.

[11] Perez M, Reina JA, Serra A, Ronda J. C. *Acta Polymerica* **1998**, 49,312.

[12] US Patent 4 268 450, **1981**, Energetic Hydroxy Terminated Azide Polymer, Frankel,M.B. and Flanagan, J.E.

[13] Raphae1l Riva, Ste´phanie Schmeits, Christine Je´roˆme, Robert Je´roˆme, Philippe Lecomte, *Macromolecules* **2007**, 40, 796.

[14] M. Pérez, J.A. Reina, A. Serra, J.C. Ronda, *Polymer*, **2000**, 41, 7331.

[15] Perez M, Reina JA, Serra A, Ronda J. C. *Polymer* **2000**, 41, 2349.

[16] Perez M, Reina JA, Serra A, Ronda J. C. *Polymer* **2001**, 42, 1.

[17] Bryan Parrish, Rebecca B. Breitenkamp, and Todd Emrick. *J. Am. Chem. Soc*. **2005**, 127, 7404.

[18] Mehmet S. Eroglu, Olcun Guven, *Journal of Applied Polymer Science*, **1996**, 60, 1361

[19] Rolf Chelmowski, *Langmuir* **2009**, 25, 11480.

[20] Zhishen Ge, Shiyong Liu, *J. Am. Chem. Soc.* **2009**, 131, 1628.

[21] Patric Jannasch, *Chem. Mater.* **2002**, 14, 166.

CHAPTER 3

[1] (a) Peumans, P.; Uchida, S.; Forrest, S. R. *Nature* **2003**, 158; (b) Hansel, H.; Zettl,

H.; Krausch, G.; Kisselev, R.; Thelakkat, M.; Schmidt, H. W. *Adv. Mater*. **2003**, 15, 2056.

[2] (a) Langhals, H.; Ismael, R.; Yürük, O. *Tetrahedron* **2000**, 56, 5435; (b) Langhals, H.; Karolin, J.; Johansson, L. B. Å. *J. Chem. Soc., Faraday Trans.* **1998**, 94, 2919.

[3] (a) Horowitz, G.; Kouki, F.; Spearman, P.; Fichou, D.; Nogues, C.; Pan, X.; Garnier, F. *Adv. Mater.* **1996**, 8, 242; (b) Malenfant, P. R. L.; Dimitrakopoulos, C. D.; Gelorme, J. D.; Kosbar, L. L.; Graham, T. O.; Curioni, A.; Andreoni, W. *Appl. Phys. Lett*. **2002**, 80, 2517.

[4] (a) Würthner, F. *Chem. Commun*. **2004**, 1564 and references cited therein; (b) Hoeben, F. J. M.; Jonkheijm, P.; Meijer, E. W.; Schenning, A. P. H. J. *Chem. Rev.* **2005**, 105, 1491; (c) Li, X. Q.; Stepanenko, V.; Chen, Z. J.; Prins, P.; Siebbeles, L. D. A.; Würthner, F. *Chem. Commun.* **2006**, 3871.

[5] (a) Yang, L.; Shi, M.; Wang, M.; Chen, H. *Tetrahedron* **2008**, 64, 5404; (b) Zhang, X. B.; Wu, Y. F.; Li, J. Z.; Li, F.; Li, M. *Dyes Pigments* **2008**, 76, 810.

[6] C. Xue, Runkun Sun, Shi Jin. *Tetrahedron Letters* **2009**, 50, 853.

[7] Dr. Runkun Sun’s dissertation thesis.

CHAPTER 4

[1] L. Schmidt-Mende, A. Fechtenkötter, K. Müllen, E. Moons, R. H. Friend, J. D. MacKenzie, *Science.* **2001**, *293*, 1119.

[2] C. Ego, D. Marsitzky, S. Becker, J. Zhang, A. C. Grimsdale, K. Müllen, J. D. Mackenzie, C. Silva, R. H. Friend, *J. Am. Chem. Soc.* **2003**, 125, 437.

[3] a) P. R. L. Malenfant, C. D. Dimitrakopoulos, J. D. Gelorme, L. L. Kosbar, T. O.

Graham, A. Curioni, W. Andreoni, *Appl. Phys. Lett.* **2002**, 80, 2517; b) R. J. Chesterfield, J. C. McKeen, C. R. Newman, C. D. Frisbie, *J. Appl. Phys.* **2004**, 95, 6396.

[4] Gopal Boobalan, Predhanekar Mohamed Imran, Samuthira Nagarajan, *Chinese Chemical Letters*, **2012**, 23, 149

[5] I. Lukic, H. Langhals, *Chem. Ber.*, **1983**, 116, 3524.

[6] BASF AG (Inv. F. Graser) D.O.S. 2139688 (Febr. 15, **1973**), D.O.S. 2210170 (Sept. 6, 1973) (Chem. Abstr., **1973**, 78, 137962v; Chem. Abstr., **1974**, 80, 49261h).

[7] A. Rademacher, S. Marklev, H. Langhals, *Chem. Ber.*, **1982**, 115, 2927.

[8] H. Langhals, *Chem.Ber.*, **1985**, 118, 4641.

[9] H. Langhals, D.O.S. 3703513 (Feb 5, 1987) (Chem. Abstr., **1988**, 109, P212376w).

[10] Y. Nagao, Y. Tanabe, T. Misono, N. Kaishi, 1979, 528 (Chem. Absrr., **1979**, 91, 38468a).

[11] H. Troster, *Dyes Pigm.*, **1983**, 4, 171 (Chem. Abstr., **1983**, 99, 39794f).

[12] C. Xue, Runkun Sun, Shi Jin. *Tetrahedron Letters*, **2009**, 50, 853.

CHAPTER 5

[1] Zhaohui Wang, Mark D. Watson, Jishan Wu and Klaus Müllen. *Chem. Commun.* **2004**, 336-337

[2] D. Adam, P. Schuhmacher, J. Simmerer, L. Haussling, K. Siemensmeyer, K. H. Etzbach, H. Ringsdorf and D. Haarer, *Nature*, **1994**, 371, 141.

[3] (a) A. M. van de Craats, N. Stutzmann, O. Bunk, M. M. Nielsen, M. Watson, K. Müllen, H. D. Chanzy, H. Sirringhaus and R. H. Friend, *Adv.Mater*, **2003**, 15, 495; (b) L. Schmidt-Mende, A. Fechtenkötter, K. Müllen, E. Moons, R. H. Friend and J. D. MacKenzie, *Science*, **2001**,293, 1119.

[4] Pisula, W.; Feng, X.; Müllen, K. *Adv. Mater*. **2010**, 22, 3634.

[5] Dr. Bin Wang's dissertation thesis, **2013,** Graduate Center, The City University of New York

[6] Dehm, V.; Chen, Z. J.; Baumeister, U.; Prins, P.; Siebbeles, L. D. A.; Würthner, F. *Org. Lett.* **2007**, 9, 1085.

[7] May, F.; Marcon, V.; Hansen, M. R.; Grozema, F.; Andrienko, D. *J. Mater. Chem.* **2011**, 21, 9538.

[8] Lemaur, V.; da Silva Filho, D. A.; Coropceanu, V.; Lehmann, M.; Geerts, Y.; Piris, J.; Debije, M. G.; van de Craats, A. M.; Senthilkumar, K.; Siebbeles, L. D. A.; Warman, J. M.; Brédas, J.-L.; Cornil, J. *J. Am. Chem. Soc.* **2004**, *126*, 3271.

[9] Dr. Runkun Sun's dissertation thesis, **2013**, Graduate Center, The City University of New York